LBL-11819
UC-91

Lawrence Berkeley Laboratory
UNIVERSITY OF CALIFORNIA, BERKELEY

EARTH SCIENCES DIVISION

AN INVESTIGATION OF DEWATERING FOR THE MODIFIED IN-SITU RETORTING PROCESS, PICEANCE CREEK BASIN, COLORADO

M. Mehran, T.N. Narasimhan, and J.P. Fox

October 1980

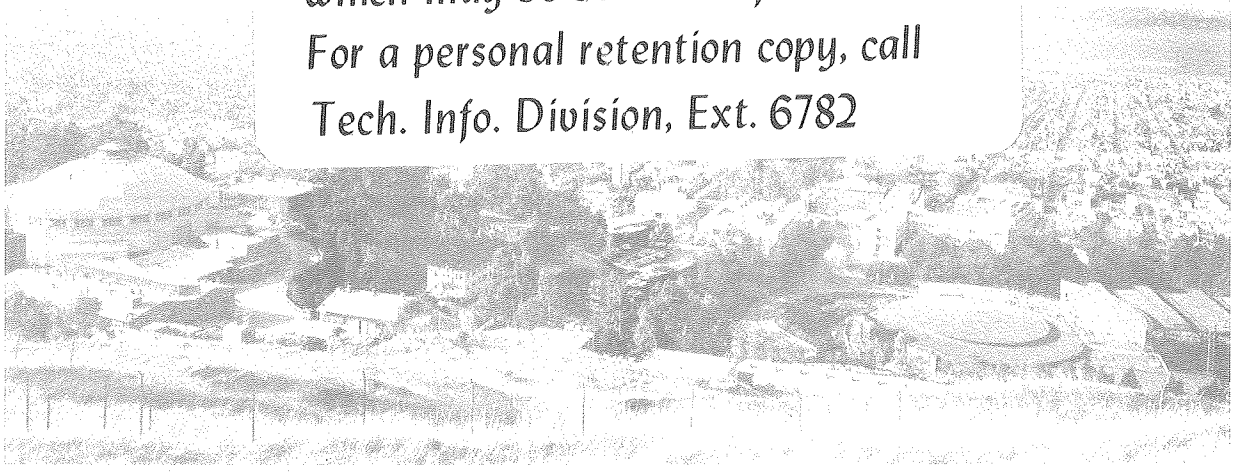

Prepared for the U.S. Department of Energy under Contract W-7405-ENG-48

DISCLAIMER

LBL-11819

AN INVESTIGATION OF DEWATERING FOR THE MODIFIED IN-SITU RETORTING PROCESS, PICEANCE CREEK BASIN, COLORADO

M. Mehran, T. N. Narasimhan, and J. P. Fox

Earth Sciences Division
Lawrence Berkeley Laboratory
University of California
Berkeley, CA 94720

October 1980

This work was funded by the Assistant Secretary for Environment, Office of Environmental Compliance and Overview, Environmental Control Technology Division and the Assistant Secretary for Fossil Energy, Office of Oil Shale, of the U. S. Department of Energy under Contract No. W-7405-ENG-48.

TABLE OF CONTENTS

ABSTRACT

The C-a and the C-b tracts in the Piceance Creek Basin are potential sites for the development of oil shale by the modified in-situ retorting (MIS) process. Proposed development plans for these tracts require the disturbance of over three billion m^3 (about six billion tons) of oil shale to a depth of about 400 m (1312 ft) or more below ground level. This disturbance will result in the modification of groundwater flows and fluid potentials and the alteration of the chemical and thermal regimes of native groundwaters. As a first step in evaluating the hydrogeologic consequences, the present study investigates the nature and impacts of dewatering and reinvasion that are likely to accompany the MIS process. Previous studies along these lines have been carried out by the U. S. Geological Survey and others (i.e., Tipton and Kalmbach, Inc. and Golder Associates).

The purpose of the present study is to extend these earlier investigations through more refined mathematical analysis. Physical phenomena not adequately covered in previous studies, particularly the desaturation process, are investigated. The present study also seeks to identify, through a parametric approach, the key variables that are required to characterize systems such as those at the C-a and C-b tracts. It is hoped that this study will eventually lead to the design of carefully controlled field experiments which will provide the critically required field data for long-term predictions.

In this study, the flow regions around the C-a and C-b tracts are idealized as a multilayered system of aquifers separated by aquitards. Within this system, the expanding mine is represented as a disc-shaped opening which grows with time. Water from the surrounding region drains

into the mine at atmospheric pressure. As the drainage takes place, the region above the mine will desaturate, accompanied by reduction in permeability. The materials making up the flow region may be isotropic or anisotropic. The layers are allowed to interact freely with each other. Although the fractured nature of the C-a and C-b tract systems are recognized, in the present work, they are treated as equivalent porous media.

In general, higher porosities, lower residual saturations, and higher hydraulic conductivites will tend to increase mine inflow rates. Depending on the magnitude of various parameters, the mine inflow rate after 60 years of dewatering at the C-b tract is expected to range from 0.48 to 0.90 m^3/sec (7600 to 14,200 gpm). At the C-a tract, the mine inflow rate after 30 years will vary from 0.15 to 1.38 m^3/sec (2300 to 21,800 gpm), depending upon the hydraulic conductivity of the lower aquifer. Although the results show an increase in total rate of inflow into the mine as the retorted region expands, the ratio of inflow to area gradually decreases with time. As a consequence, at the C-b tract, the flux into an individual retort may decrease from about 0.946×10^{-3} m^3/sec (15 gpm) in the first 10 years of dewatering to less than 0.126×10^{-3} m^3/sec (2 gpm) at the end of the project. The phreatic surface at the C-b tract at a distance of 3.5 km (2.1 mi) from the center of the retorted region (approximate location of Piceance Creek) could be lowered as much as 100 m (328 ft) after 60 years of dewatering. At the C-a tract, the maximum drawdown at a distance of 5 km (3.1 miles) from the center of the retorted region (approximate location of waters tributary to Yellow Creek) is expected to be about 31 m (100 ft) after 30 years of dewatering. The position of the phreatic surface relative to

the front of the excavated region is closely related to the thickness of the overburden above the mined region as well as the hydraulic properties of the medium.

Comparing the dewatering results of the present work with those of previous investigators (Tipton and Kalmbach, Inc., 1977; Golder Associates, 1977) indicates that, in general, our estimates of inflow rates into the mines and drawdowns of the phreatic surface are higher. This is primarily attributed to the inclusion of unsaturated flow in the present analysis.

The reinvasion process is complicated by: a) strong influence of the thermal regime, b) lack of knowledge of the state of saturation at the time of abandonment, and c) the hysteresis effect. The 200-year simulation results show that, initially, reinvasion takes place primarily in the retorted region because of its high porosity and hydraulic conductivity. During this period, the reinvasion into the upper aquifer appears to be an extremely slow process extending over centuries. It should be pointed out that because of uncertainties in the field data and the simplifying assumptions made in physical conceptualization of the system, the conclusions must be used and/or interpreted with considerable caution.

The nature of the desaturation process as well as the associated permeability variations have a significant effect on the dewatering and reinvasion processes. In-situ saturations might have a strong influence on the effectiveness of retort combustion, depending on the saturation characteristics of the oil shale as well as the inflow of water into individual retorts. Unfortunately, we have very limited knowledge on how to handle unsaturated flow on such a large scale.

The credibility of a predictive model is governed by its conceptual soundness which in turn depends on: a) realistic description of system geometry, b) generalization of material distribution, and c) understanding of the physical phenomena. It is therefore essential to bring together the expertise of field geologists, hydrologists, mining engineers, and computationalists to assemble a realistic conceptual model. A carefully planned workshop is recommended to initiate such an integrated effort.

INTRODUCTION

Oil shale deposits are widely distributed in every continent, and a majority of known oil shale resources (75-80%) is found in the United States. China and Canada have 11% and 7% of the estimated world reserves of oil shale, respectively. At present, oil shale is exploited in only three countries--the USSR where it is fed directly into a power station for generation of electricity, in China where oil production has been estimated at 6360 m^3/day (40,000 bbl/d) (Ranney, 1979), and in Brazil.

The Green River Formation of Colorado, Utah, and Wyoming is the largest and richest oil shale deposit in the world and is estimated to contain in excess of 600 billion barrels of high grade recoverable oil (Yen, 1976; Weeks et al., 1974). The recent energy crisis, increasing costs of crude petroleum, and high U. S. energy demand (33% of total world fossil fuel) may make shale oil a cost-effective source of crude oil if economically feasible and environmentally acceptable methods of recovery can be developed.

In the Piceance Creek Basin, oil shale is a dolomitic marlstone with about 86% mineral matter and 14% organic matter (Ranney, 1979). Oil can be extracted from oil shale either by mining and pyrolysis in above-ground retorts (ex-situ) or by pyrolysis in the shale formation itself (in-situ). In ex-situ processing, the shale is mined and then heated in above-ground vessels (retorts) to distill the oil. In a true in-situ (TIS) process, a deposit of oil shale is first fractured by explosives or other methods and then pyrolyzed underground. The shale oil is pumped to the surface through wells. Modified in-situ (MIS) retorting is perhaps a more advanced method in which a portion of the shale depo-

sit (about 20-40%) is mined out, and the rest is rubblized by explosives and retorted underground (Sass, 1980). The mined portion can either be retorted on the surface or disposed of as waste.

All of these processes require the removal of water (dewatering) to prevent interference with mining operations (pit development, shaft sinking, development of horizontal drifts) and underground combustion. The amount of water that must be removed depends on site geohydrology. The water pumped to the surface could be used beneficially in surface facilities, disposed of as waste, or reinjected back into the ground. The total water use in an MIS shale oil process is estimated to be about 0.27 to 1.07 m^3 (71 to 278 gal) per barrel of oil (Golder Associates, 1977; Fox, 1981).

Commercial-scale development of the MIS process is presently underway at federal lease tract C-b. The work on federal lease tract C-a is still in the modular development phase. It is roughly estimated that during the projected 60-year life of operation at the C-b tract, over 2.2 billion m^3 (about 4.4 billion tons) of material will be disturbed underground over an area of approximately 2023 hectares (5000 acres). Similarly, it is estimated that during the projected 30-year life of operation at the C-a tract, 1.25 billion m^3 (about 2.5 billion tons) of material will be disturbed underground over an area of about 1000 hectares (2470 acres). This disturbance, coupled with dewatering, could profoundly alter the groundwater regime and will affect the surface waters of the surrounding area. On retort abandonment, water will reinvade the area, leaching organic and inorganic materials from the spent shale into surrounding aquifers and eventually into surface waters. The environmental impacts of dewatering will include mining and depletion of

groundwater supplies, reduced stream flows, increased salinity in surface water bodies, and contamination of the total hydrologic system by organic and inorganic pollutants leached from spent shale. These impacts could affect irrigation, drinking water supplies, recreation, and aquatic biota of the area. The economic losses from decreased flows and increased salinity could reach 25 million dollars per year for a 2 million bbl/d industry (Sladek et al., 1980). In a recent review of water quality effects of in-situ oil shale development, Fox (1979) concluded that groundwater disruption (dewatering and reinvasion) will have gradual but long-term economic and environmental consequences.

The forecast of long-term hydrogeologic effects of MIS retorting is a problem of considerable complexity. The quantities that need consideration include: a) physical aspects of various dewatering options, b) water table profiles and fluid fluxes, c) initial conditions at the time of retort abandonment, d) two-phase flow behavior at the initiation of reinvasion, e) subsidence due to fluid withdrawal, f) chemistry of rock-water interactions, and g) chemical transport of contaminants during dewatering and reinvasion.

PURPOSE OF STUDY

The central theme of the present study is to investigate some of the possible hydrogeologic consequences of the proposed oil-shale developments at the C-a and C-b tracts. We will focus on dewatering and post-abandonment reinvasion, incorporating certain physical phenomena that have been neglected in earlier preliminary studies.

The role of hydrogeology in MIS oil shale development is unique in the sense that the actual production operations involve disturbance of

natural conditions on an unprecedented scale. It has been estimated that pumping rates of 1 m^3/s (15,850 gpm) from depths of 300-500 m (980-1640 ft) below ground surface and mining and hoisting on the order of 40 million kg/day (40,000 tons/day) of material are likely to be involved (Sass, 1980). Failure to properly assess the implications and long-term consequences of such a proposal could adversely affect the economics of the proposed operations.

PREVIOUS WORK

The first water resources reconnaissance of the Piceance Creek Basin was initiated by the United States Geological Survey (USGS) in cooperation with the Colorado Water Conservation Board in 1964. Reports by Coffin et al. (1968, 1971) describe this work. These investigations were the basis for further groundwater studies initiated in 1972 by the USGS in cooperation with the Colorado Department of Natural Resources. That study was completed by Weeks et al. (1974) and resulted in a preliminary groundwater model for the Piceance Basin. Since then, several other groundwater modeling efforts have been directed toward the Piceance Creek Basin in general and the C-a and C-b tracts in particular. The approach and the assumptions of these models (Table 1) and their significant findings are discussed below in chronological order.

Weeks et al. (1974)

Weeks et al. (1974) conceptualized the entire basin as a three-layer system with two horizontal aquifers separated by an aquitard. The Mahogany Zone, rich in kerogen content, was included within the aquitard. In this system, the flow was assumed to be horizontal in the

Table 1. Important features of various modeling activities in Piceance Creek Basin.

Study	Model	Solution Approach	Flow Regime	No. of Layers	Geometry	Interactions Between Layers	Mining Method Simulated
Weeks et al. (1974)	Quasi 3-D	Numeric	Saturated	3	Fixed	Only vertical leakage between aquifers	Room-and-Pillar
Tipton and Kalmbach (1977)	2-D	Analytic	Saturated	2	Expanding	No	TIS
Golder Associates (1977)	2-D	Analytic-Numeric	Saturated[a]	3	Expanding	No	MIS
Banks et al. (1978)	3-D	Numeric	Saturated	4	Fixed	Yes	Open-Pit
Robson and Saulnier (1980)	3-D	Numeric	Saturated	5	Fixed	Yes	MIS
Lawrence Berkeley Laboratory (1980)	2-D Axi-symmetric	Numeric	Saturated-Unsaturated	Variable	Expanding	Yes	MIS

[a]Flow from caved material in the unsaturated state is calculated from drainable porosity.

aquifers and vertical in the relatively low-permeability aquitard. The aquifers were assumed to be heterogeneous with transmissivities varying from place to place. The model considered different hydraulic heads within the upper and lower aquifers, leading to cross-flow between the aquifers. Finally, recharge due to precipitation in different parts of the basin was considered. Using this conceptualization, they first computed the steady-state potential distribution followed by the effect of mine emplacement on the existing groundwater regime.

They essentially used the quasi three-dimensional confined flow model of Bredehoeft and Pinder (1970). The upper and lower aquifers were treated as areal, two-dimensional systems, coupled through vertical flow in the aquitard. The mesh discretization was very coarse, with the minimum spacing being 1.6 km (1 mile).

The mines at the C-a and C-b tracts (room-and-pillar mine for the then-proposed surface retorting facilities) were idealized as a 10.4-km^2 (4-mi^2) excavation in the upper aquifer and the aquitard. Water was assumed to drain into the mine and to be pumped out so that the mine would remain dry at all times. Based on this, mine inflow and disturbance to groundwater potentials in the basin were computed.

The Weeks et al. study was a comprehensive preliminary investigation utilizing all available data at that time, and it forms a sound basis for further detailed studies. However, certain modifications are required to accommodate newly proposed development scenarios (room-and-pillar mining with surface retorting has been replaced by MIS retorting) and improved understanding of the physical problem. First, Weeks et al. (1974) treated the mine as an open-cast, 10.4-km^2 excavation. This, however, is not realistic for the MIS scheme which will not have any ex-

cavation at the surface. Indeed, water from the 10.4-km^2 area overlying the mine will actually drain into the mine, a feature which was not considered in the USGS model. Secondly, because theirs was an areal confined-flow model, they could not realistically treat the desaturation process. They attempted to account for unconfined flow by arbitrarily changing specific storage from 0.001 to 0.1 when the hydraulic head drawdown exceeded 30 m (98 ft) in the upper aquifer. Although this approach was acceptable, considering their scale of interest and the preliminary nature of their work, there is a need to investigate the drainage mechanism in a more detailed fashion, taking into account the desaturation process and the accompanying reduction in hydraulic conductivity.

Tipton and Kalmbach, Inc. (1977)

The Tipton and Kalmbach (T-K) study, an engineering analysis of the economics of dewatering by internal drainage at the C-b tract, used an analytic-solution approach. Because of the limitations of this approach, their model was highly idealized. The model consisted of a two-layered system, the upper and lower aquifers. Flow within each aquifer was purely confined and horizontal without any cross flow; leakage from the aquitard was neglected. The growing mine was represented as a large hole or well whose area equaled the area of mine development. Water was assumed to drain into the hole at a constant potential or drawdown. The assumed constant drawdown was 320 m (1050 ft) for the upper aquifer and 473 m (1550 ft) for the lower aquifer. Based on this model, the inflow rate at any given time was computed as the sum of inflows using the method of Jacob and Lohman (1952).

Just as the Weeks et al. (1974) model, the T-K study ignores the vertical drainage of water from the overburden above the mine through the mine roof. Secondly, drainage of water into the mine from the lower aquifer is assumed to be horizontal, while in fact water from the lower aquifer should be expected to enter the mine vertically through the floor. Finally, the T-K study ignores recharge at the surface as well as the role of the desaturation process and the consequent permeability reduction. Unlike the Weeks et al. (1974) study, however, the T-K investigation considered the time-dependent expansion of the mine.

Golder Associates (1977)

Golder Associates (1977) investigated various water management scenarios using a computational approach combining numerical and analytic methods. A three-layered model, consisting of an upper confined (or unconfined) aquifer, a middle aquitard, and a lower confined aquifer, was used. The mine, which expanded with time, was assumed to be a disc-shaped opening. Water was assumed to drain into the mine at atmospheric pressure. Golder Associates assumed horizontal flow in the two bottom zones and both vertical and horizontal flow in the upper aquifer in the presence of anisotropy. It was further assumed that there was no interformational flow between the three zones.

Because of these simplifying assumptions, the two bottom zones could be handled analytically using conventional well test equations such as the Theis equation. Vertical movement of water from the lower aquifer into the mine was approximated by modifying the horizontal flow assumption in that aquifer. The upper aquifer was analyzed using a numerical (finite element) model which accounted for the transient move-

ment of the water table. In the actual simulations, however, conservative estimates of inflow from the upper aquifer were first obtained by fixing the water table in time (allowing for recharge at the water table). Parametric studies were carried out with fixed geometry mines to investigate the influence of phreatic surface movement on the mine inflows.

Golder Associates used a reasonable geometry for the mine configuration, taking into account the growth of the mine, and they gave some consideration to the movement of the water table under special conditions. However, their model neglected cross-flow between the zones, and their analysis of water table movement did not take into account the effects of desaturation and the consequent permeability reduction.

Banks et al. (1978)

For hydrology simulation in the Piceance Creek Basin, Banks et al. (1978) modified Sun Company's 3-D Beta digital model traditionally used for hydrocarbon reservoirs. The model can simulate both homogeneous and heterogeneous reservoir rock characteristics using a gridded layer system as well as performance for single or multiple interrelated reservoirs. This model uses input data not directly derived from field pumping tests, i.e., it uses porosities and permeabilities instead of storage coefficients and transmissivities.

Banks et al. used a four-layer system (atmosphere plus three aquifer layers) in their basin-wide hydrology model. The model first simulated the steady-state conditions in the basin, and basin-wide potentiometric maps of upper and lower aquifers were computed.

The model was used to simulate three independent dewatering opera-

tions for variously sized pits. This model did not differentiate between discharge from storage and discharge from intercepted groundwater. Dewatering in this model means depressurizing, i.e., reducing the pressure within the grid cell to atmospheric pressure (15 psi). The effects of desaturation and mine growth were not considered.

Robson and Saulnier (1980)

Robson and Saulnier (1980) investigated hydrogeochemistry and solute transport in the Piceance Basin using a three-dimensional groundwater model developed by Intercomp, Inc. (1976). They conceptualized the basin as a five-layer system. The entire flow region was represented by 9x14 cell blocks. The aquifer system was assumed to be confined, and unsaturated flow was not considered in this analysis. Therefore, transient water-table conditions near an active mine at the time of dewatering are not simulated by the model. Solution of the groundwater flow equation was achieved by a finite difference scheme. It was assumed that the retorted region had a fixed geometry and that the flow regime is saturated. Anisotropy was included in the model. From the existing data, they concluded that the ratio of lateral permeability to vertical permeability could reach values of 500 in the bottom-most layers. Recharge was included in this study, and it was generally based on values given by Weeks et al. (1974). This study emphasized the groundwater quality changes that would occur as a result of mine dewatering or leaching of saline minerals.

SCOPE OF PRESENT WORK

The present work investigates the disturbance of the subsurface fluid flow regime around the proposed MIS facilities at the C-a and C-b

tracts. It represents the underground workings as an expanding disc-shaped region. A variable number of layers is used, and interaction between the layers is permitted. The study considers saturated and unsaturated flow under isothermal conditions. Temperature effects accompanying the retorting process, rock-water interactions, and chemical transport mechanisms are not considered.

Weeks et al. (1974) presented a comprehensive study of the hydrogeology of open-pit mining in the Piceance Creek Basin. However, in their analysis, the mine was idealized as a 10.4-km^2 (4-mi^2) excavation in the upper aquifer and the confining layer. Furthermore, unconfined conditions were approximated by changing the storage coefficient to the specific yield in an arbitrary fashion. The Tipton and Kalmbach, Inc. (1977) study, which considered the time dependent expansion of the mine, assumed a constant drawdown and ignored the effect of desaturation and cross-flow between the layers. Golder Associates (1977) analyzed a reasonable geometry for the mine configuration but assumed no coupling between the three zones and did not consider desaturation and subsequent permeability reduction. In Banks et al. (1977) and in Robson and Saulnier (1980), the flow was assumed to be confined and desaturation was ignored.

The present work is an attempt to overcome limitations in previous studies by treating mine dewatering as a saturated-unsaturated flow problem for an expanding retorted region with full interaction between various layers. The unsaturated regime is governed by utilizing the pressure head (pressure head = hydraulic head - elevation head) dependencies of hydraulic conductivity and saturation in the transient flow equation.

The geologic idealization of the hydrologic system is similar to that used by previous investigators. Parameters such as permeability and storativity used in this analysis are similar in magnitude to those used by previous workers.

This work is a semi-site specific, generic study because of the paucity of field data required to characterize the system. Although we now possess powerful computational tools to synthesize field data, we are handicapped in the present study by lack of sufficient data on unsaturated properties to adequately characterize the field problem. Therefore, we have chosen the approach of sensitivity analysis to identify the key parameters that govern system behavior. Hopefully, the results of the sensitivity study will lead to efforts to acquire the necessary field data.

The lack of data has also hampered our ability to model surface water/groundwater interactions at the Piceance Creek and Yellow Creek. Thus, we will only estimate probable groundwater level declines at the approximate location of these creeks.

DESCRIPTION OF THE C-a AND C-b TRACTS

In 1974, the federal government, through the Department of the Interior, offered for lease six experimental sites of approximately 5,100 acres each--two in each of the states of Colorado, Utah, and Wyoming. A major objective of this prototype leasing program was to develop environmentally acceptable methods to exploit the nation's oil shale reserves.

The two Colorado tracts, C-a and C-b, are located in the Piceance Basin in western Colorado. The C-a tract consists of 20.60 km^2 (5090

acres) of land which was awarded to Gulf Oil Corp. and Standard Oil Co. (Indiana) in January 1974. This tract is located on the west side of the Piceance Creek Basin about five miles east of the Cathedral Bluffs skyline in Rio Blanco County (Figure 1). The tract was originally slated for open pit mining. The current plans for the development of tract C-a are described in the revised Detailed Development Plan (DDP) of Rio Blanco Oil Shale Project (RBOSP) and call for MIS retorting. The C-a tract will be developed over a 40-year period. During the first 10 years, the Modular Development Phase (MDP), field MIS experience will be gained by burning a limited number of small retorts. During the next 30-years, the Commercial Phase, commercial-sized retorts will be designed and operated based on experience gained during the MDP phase. A commercial industry will be developed over this period, starting with 50,000 bbl/d and peaking at 76,000 bbl/d at the end of the 40-year development period.

The C-b tract is a 20.62-km^2 (5094-acre) tract located in Colorado's Piceance Creek Basin. At its closest, the C-b tract is about 1.76 km (1.1 miles) from the Piceance Creek. In 1973, this tract was estimated to contain 723 million barrels of shale oil at an average of 30 gallons of oil per ton of shale. The tract was originally leased to Atlantic Richfield, Ashland Oil, Shell Oil, and The Oil Shale Corporation (TOSCO) for development by room-and-pillar mining and surface retorting. By 1976, all of the participants but Ashland had withdrawn, and Ashland entered into an agreement with Occidental Oil Shale, Inc. to develop the tract using Occidental's MIS technology. In 1979, Ashland withdrew from the agreement and was replaced by Tenneco.

The revised Detailed Development Plan (Ashland Oil, Inc. and Shell

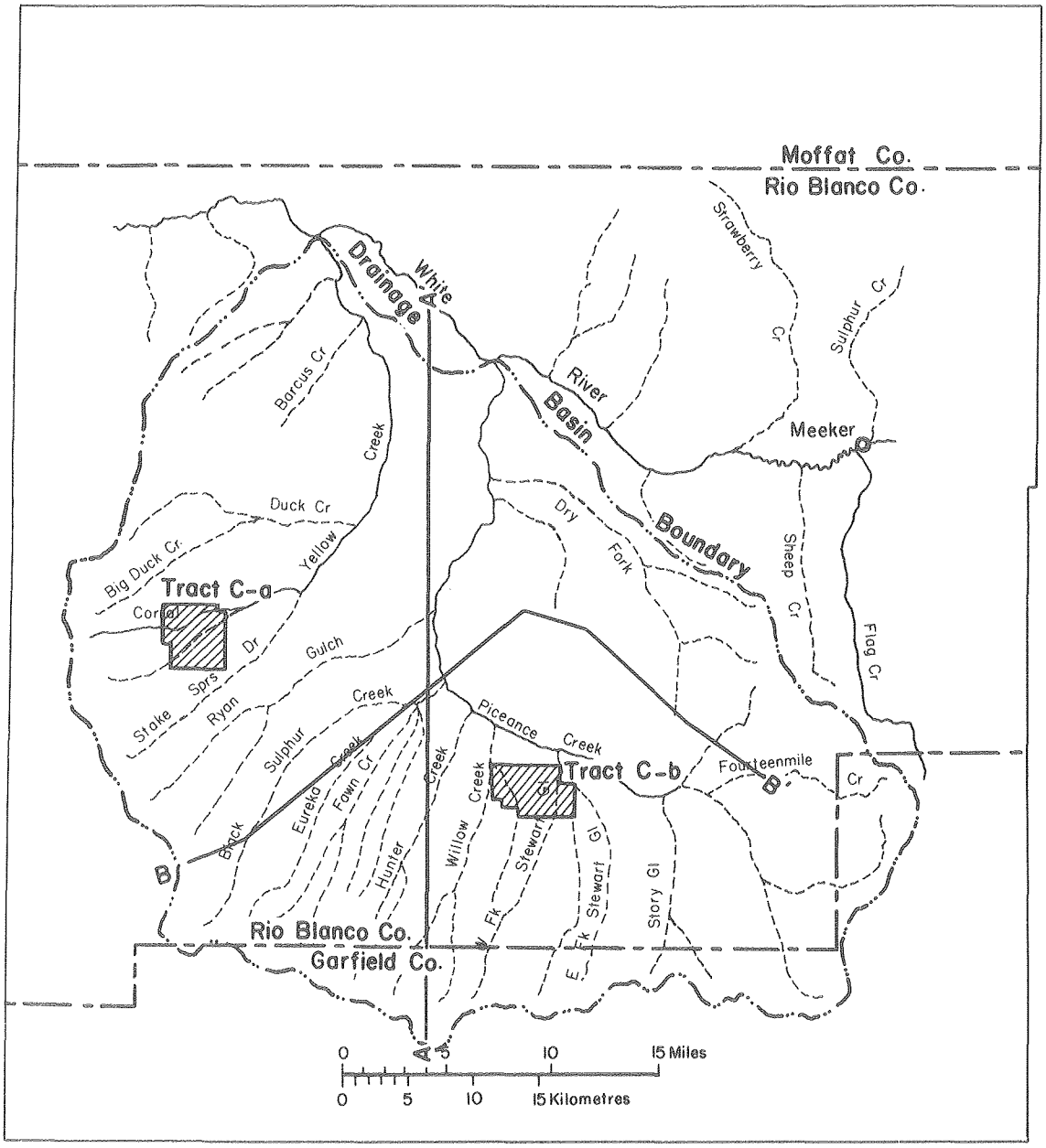

FXBL 8011-2286

Figure 1. Location of the Piceance Basin and prototype oil-shale lease tracts C-a and C-b (after Weeks et al., 1974).

Oil Co., 1976) proposes to produce 57,000 bbl/d of shale oil by 1985 using the MIS technology. Retorts will be developed in groups or clusters with several retorts being operated simultaneously. Three major shafts are presently being excavated and surface facilities are under construction.

THE PICEANCE CREEK BASIN

The federal tracts C-a and C-b are located within a small basin comprising the area drained by the Yellow and Piceance Creeks. This basin, referred to here as the Piceance Basin (Weeks et al., 1974), has an area of 2330 km^2 (900 mi^2), and it is part of the Piceance Creek structural basin with an areal extent of 4140 km^2 (1600 mi^2) Figure 1 shows the location of the tracts in the Piceance Basin.

The topography of the basin is one of ridges and valleys with local relief of 60 to 180 m (200 to 600 ft). The climate of the basin is semi arid with annual precipitation ranging from 254 mm to 640 mm (10 to 25 in) between altitudes of 1680 m (5500 ft) and 2745 m (9000 ft). Temperatures range from less than -40°C (-40°F) in the winter to more than +40°C (104°F) in the summer. The number of frost free days per year varies from 120 days at lower altitudes to 50 at higher altitudes (Weeks et al., 1974).

GEOLOGY

Rock outcrops in the basin range in age from Cretaceous to Quaternary. We are concerned primarily with the Green River and Uinta Formations of Eocene age and the Quaternary alluvium in the stream valleys, which contain the principal aquifers. Permeability in these two formations appears mainly to be due to fractures and faults. The Green River

Formation consists of the Douglas Creek Member, Garden Gulch Member, and Parachute Creek Member in ascending order (Cashion and Donnell, 1974) in most parts of the basin with the addition of the Anvil Points Member in the eastern margin of the basin. Figures 2 and 3 illustrate sections A-A' and B-B' shown in Figure 1. Stratigraphy of the Piceance Creek Basin is summarized in Table 2.

The Douglas Creek Member consists mainly of sandstone. It is exposed in the southern and western margins of the basin with a maximum thickness of 244 m (800 ft). The Garden Gulch Member overlies the Douglas Creek Member and consists of shaly, dolomitic marlstone. Its maximum thickness is 275 m (902 ft) in the southwest and northwest margins. Both the Douglas Creek Member and the Garden Gulch Member are relatively impermeable. The Anvil Points Member is the dominant member in the eastern and southeastern margins of the basin and consists primarily of sandstone and some marlstone. Maximum thickness of the Anvil Points Member is 509 m (1670 ft) in the southeast. The Parachute Creek Member overlies the Garden Gulch Member or the Anvil Points Member, and it is composed of dolomitic marlstone (oil shale) and soluble minerals.

The Parachute Creek Member consists of three zones. The lower zone is a high resistivity zone rich in kerogen and sodium minerals, relatively unfractured, and relatively impermeable with a thickness of 61 to 270 m (200 to 900 ft) (the main saline, R-4, and saline zones). Overlying the high resistivity zone, there is a leached fractured zone with relatively high permeability, ranging in thickness from 120 m to 200 m (400 to 700 ft) in the central part of the study area (leached zone). The Mahogany Zone overlies the leached zone and consists of kerogen-rich strata with a thickness of 30 to 60 m (100 to 200 ft) extending

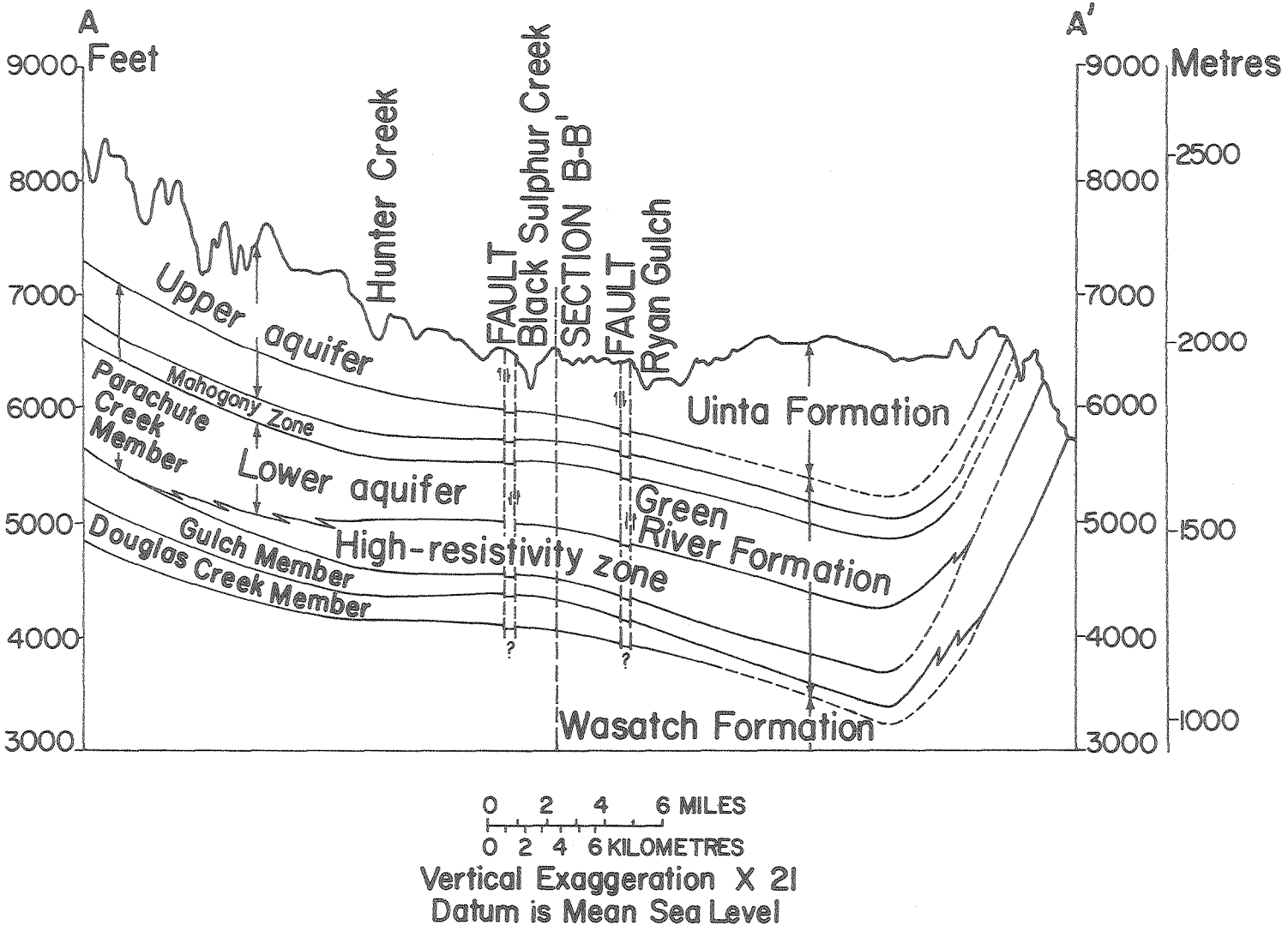

Figure 2. Geologic section through the Piceance basin. Section is located in Figure 1 (after Weeks et al., 1974).

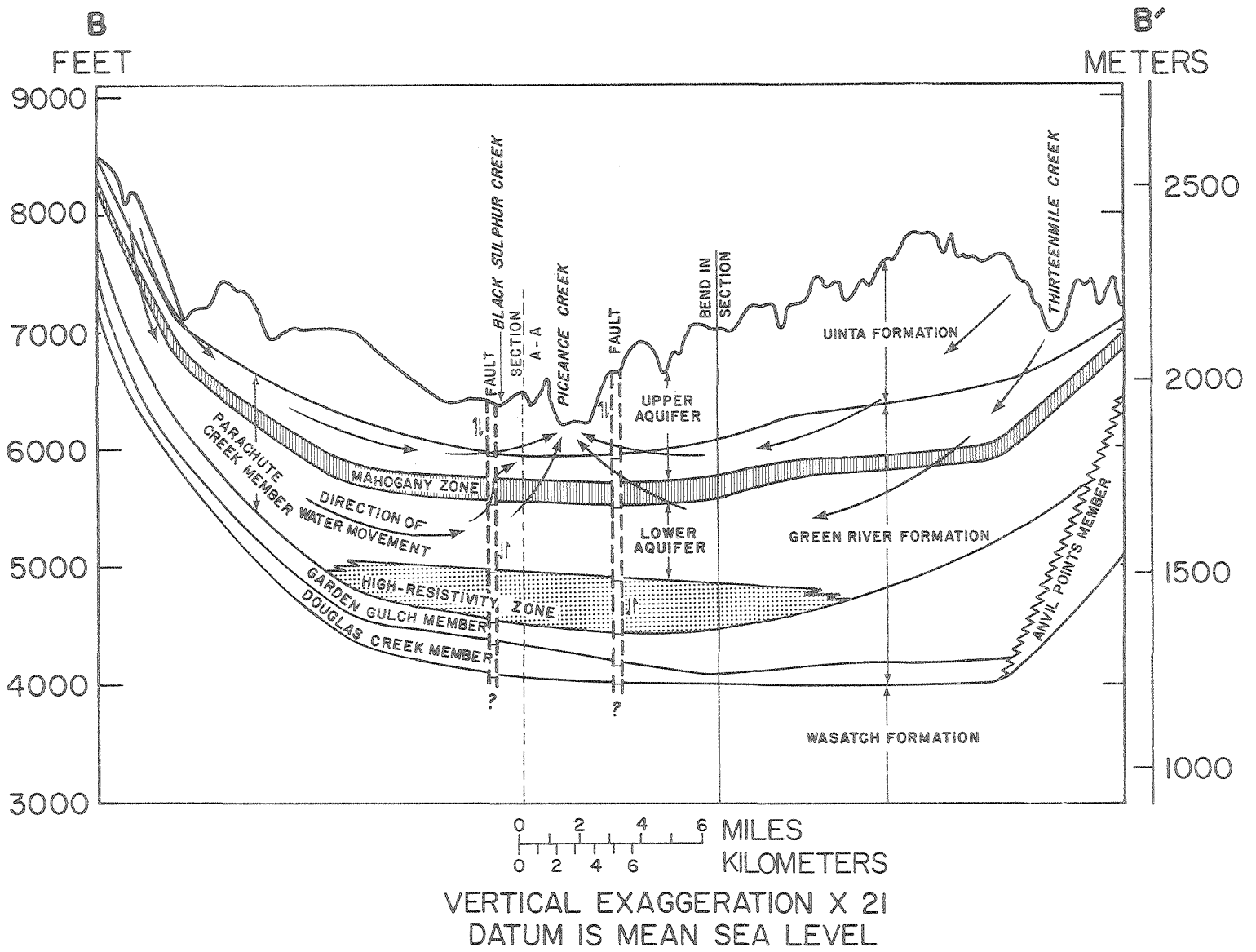

Figure 3. Geohydrologic section through the Piceance basin showing relation of the aquifers to the Green River and Uinta Formations. Section located in Figure 1 (after Weeks et al., 1974).

Table 2. Dominant stratigraphy and mineralogy of the Green River Formation, Piceance Creek Basin, Colorado (Fox, 1980).

Geologic Unit	Unit Subdivisions		Lithologic Description	Major Minerals
Valley Alluvium 0'-140'	--		Sand, gravel, clay	Quartz Dolomite
Uinta Formation 0' - 1250'	--		Mainly sandstone and siltstone with minor amounts of low-grade oil shale and barren marlstone	
Green River Formation	Parachute Creek Member 500' - 1600'	Upper Part of Parachute Creek Member		
		Mahogany Zone	Moderate- to high-grade oil shale	Dolomite Quartz
		Leached Zone	Low- to high-grade oil shale	Dolomite Albite Quartz Illite
		Main Saline Zone	Saline minerals and moderate- to high-grade oil shale	Nahcolite Dolomite Quartz
		R-4 Zone		
		Saline Zone		
	Garden Gulch Member 0' - 900'		Mainly clayey shale and low- to moderate-grade oil shale	Quartz Dolomite
	Douglas Creek Member 0' - 800'		Mainly sandstone with minor amounts of limestone	--
	Anvil Points Member 0' - 1670'		Shale, sandstone, marlstone	--

Source: Modified from National Academy of Science (1978).

throughout the basin as a more or less continuous layer (Smith, 1980). The Mahogany Zone is the richest persistent oil shale interval in the section and is the zone of principal interest for oil shale exploitation. There are, of course, local zones in the deeper part of the basin equally as rich as the Mahogany Zone.

The Uinta Formation overlying the Parachute Creek Member consists of sandstone, siltstone, and marlstone rocks. The thickness of the formation varies from 0 to 380 m (0 to 1250 ft) and generally thickens from west to east.

Quaternary alluvium consists of unconsolidated gravel, sand, and clay derived from the Uinta Formation. The alluvium is locally highly permeable and is an important aquifer in the major stream valleys, except where thick clay deposits exist as described by Coffin et al. (1968) where there are indications of low permeability. For a more detailed description of the geology of the Piceance Creek Basin, refer to Donnell (1961) and Cashion and Donnell (1974).

HYDROLOGY

The major geohydrologic investigations are those of Coffin et al. (1971) and Weeks et al. (1974) from which most of the information presented here is extracted. Any disturbance to the hydrologic environment will affect the quantity and quality of surface and ground waters in the basin. Oil shale development is no exception. A knowledge of the initial conditions of the hydrologic system is essential in order to understand and analyze the impact of MIS retorting.

Surface Water

The major rivers in the area are the Colorado River and the White

River. They flow westward on the western slopes of the Rocky Mountains in Colorado. A large part (2297 km^2 or 887 mi^2) of the basin in the northern part is drained by the White River and its tributaries, mostly by the Piceance and Yellow creeks. Piceance and Yellow creeks drain 1629 km^2 and 668 km^2 (629 mi^2 and 258 mi^2), respectively.

Over 75% of the flow in Piceance and Yellow Creeks is base flow, some derived as recharge from snow melt and some from rainfall. The primary source of stream flow in the Piceance Creek and Yellow Creek drainage basins is snow melt. Precipitation occurs at higher elevations between November and March and melts in the spring as temperatures rise. Mean daily stream flow increases during the snow melt period of March through June, recedes during the summer months, and is some from rainfall. is maintained by groundwater discharge which moves through the alluvium into the stream channels or appears as springs along the valley floors. Most of the total precipitation is lost through evapotranspiration (Wymore, 1974).

Using estimates of precipitation, temperature, and other climatic factors, Wymore (1974) developed estimates of evapotranspiration losses for the basin, and he arrived at the annual water balance of the basin. Wymore's (1974) estimate of average annual outflow for the Piceance Creek drainage basin (16.16 x 10^6 m^3 or 13,100 ac-ft) is very close to the eight-year average annual flow derived from gaging stations records (16.50 x 10^6 m^3 or 13,377 ac-ft).

It should be pointed out that most of the basin water yield, about 29.61 x 10^6 m^3/year (24,000 ac-ft/year), originates from above 2134 m (7,000 ft), or elevations above both the C-a and C-b tracts. Approximately 2060 hectares (5100 acres) in the Piceance Basin and 81 hectars

(200 acres) in the Yellow Creek Basin are irrigated annually. Irrigation diversions begin in mid-March and continue through November. Streamflow losses from consumptive use by crops and evapotranspiration losses associated with irrigation practices have a marked influence on the stream flow hydrograph from March to November.

Groundwater

The major water-bearing strata are located in the Uinta and Green River Formations. The Garden Gulch Member, which consists of marlstone, is relatively impermeable and forms the lower boundary of the aquifer system in much of the Piceance Basin. The Parachute Creek Member which overlies the Garden Gulch Member contains the most permeable materials in the Green River Formation with greater thickness and porosity. Water wells which are open to the Parachute Creek Member yield as much as 0.06m^3/sec (1000 gpm) for short periods although 0.012 to 0.024 m^3/sec (200 to 400 gpm) is typical. The Uinta Formation overlies the Parachute Creek Member, and wells completed in this formation yield as much as 0.018 m^3/sec (300 gpm) although yields of less than 0.006 m^3/sec (100 gpm) are more common. The depth to the saturated zone varies from one place to another, and it reaches 164 m (500 ft) at higher ridges. Since little groundwater development has been done there, the basin is in equilibrium which means that change in storage is negligible or inflow to the basin is nearly equal to outflow. Estimates of groundwater storage in the Uinta and Green River Formations in the basin reach up to 31 billion m^3 (25 million ac-ft). The direction of groundwater flow is toward the north central parts of the basin along the axis of the main synclinal structure.

The recharge pattern in the basin by precipitation given by Weeks

et al. (1974) indicates that most recharge occurs in western, southern, and eastern elevations of the basin. Although according to this pattern there is no recharge on the C-b tract, the recharge over the area enclosed by the modeled zone will be considered in our modeling efforts. Groundwater discharge from the basin occurs mostly to creeks with some discharge directly to the White River in the northern parts of the basin.

For practical, computational purposes, some investigators have idealized the basin as consisting of two major aquifers, an upper aquifer and a lower aquifer. However, in most parts of the basin, the two aquifers are effectively separated by a confining layer called the Mahogany Zone (Smith et al., 1979). Furthermore, in some parts of the basin, an alluvial aquifer with distinct properties overlies the upper aquifer. Therefore, the aquifer system generally consists of three aquifers and one confining layer (aquitard). Although in most modeling efforts, including the present work, the alluvial aquifer has been incorporated into the upper aquifer, in the following section, the characteristics of four layers will be briefly discussed.

The Alluvial Aquifer. The areal extent of this aquifer is limited. It consists of gravel, sand, and clay of variable thickness throughout the basin, attaining a maximum of about 43 m (140 ft). Maximum saturated thickness is approximately 31 m (100 ft). Permeability is generally high, and the transmissivities have been estimated to range from 250 m^2/day to 1900 m^2/day (2700 to 20,000 ft^2/day). The alluvial aquifer is unconfined and, because of its limited areal extent, it can be treated as part of the upper aquifer.

The Upper Aquifer. The saturated thickness extending from the

Mahogany Zone to the phreatic surface is generally referred to as the upper aquifer. It consists of fractured, lean oil shale (marlstone) of the Parachute Creek Member above the Mahogany Zone and fractured marlstone, siltstone, and sandstone of the Uinta Formation. The thickness of the upper aquifer increases eastward. At the C-b and C-a tracts, the average thickness of the upper aquifer is 325 m (1066 ft) and 79 m (260 ft), respectively. Figures 4 and 5 illustrate the location of the upper and lower aquifers with respect to the geological formations on tracts C-a and C-b and also the interval of interest for oil exploitation. The letters R and L refer to rich and lean oil-shale layers in these figures.

It is generally believed by earlier workers, that within the zones of interest, permeability is mainly due to fracture porosity. The marlstone beds in the lower part of the aquifer are locally leached, more brittle and therefore more susceptible to fracturing, causing higher permeability in that part of the aquifer (Tipton and Kalmbach, 1977). The transmissivity values vary from 0.7 to 88 m^2/day (8 to 1000 ft^2/day). Although short-term pumping tests indicate confined conditions, most of the upper aquifer is generally believed to act as an unconfined aquifer. The limited aquifer tests indicate that the storage coefficient of the upper aquifer is on the order of 10^{-3}. This value is often used for modeling purposes where the upper aquifer is assumed to be confined. In areas where the upper aquifer outcrop occur, Weeks et al. (1974) used a specific yield of between 10^{-2} and 10^{-1}.

At the C-a tract, the upper aquifer consists mainly of the Mahogany Zone overlain by A-Groove (Figure 4). Below the Mahogany Zone, alternating layers of lean and rich oil shale extend down for approximately

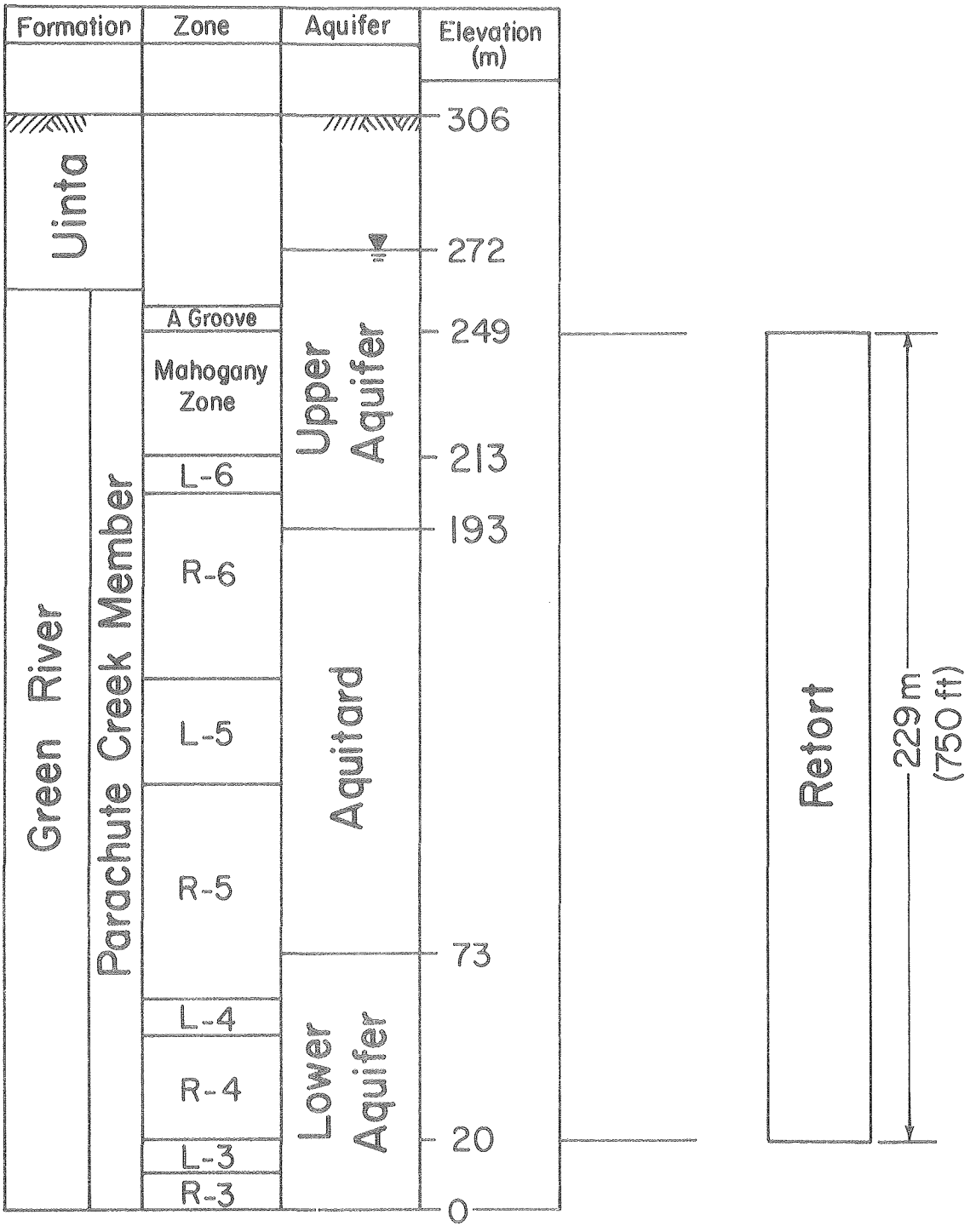

Figure 4. Stratigraphy of the C-a tract and location of the mining zone. R stands for the rich oil shale zone and L for a lean oil shale zone (After RBOSP, 1977). Datum is bottom of R-3 zone.

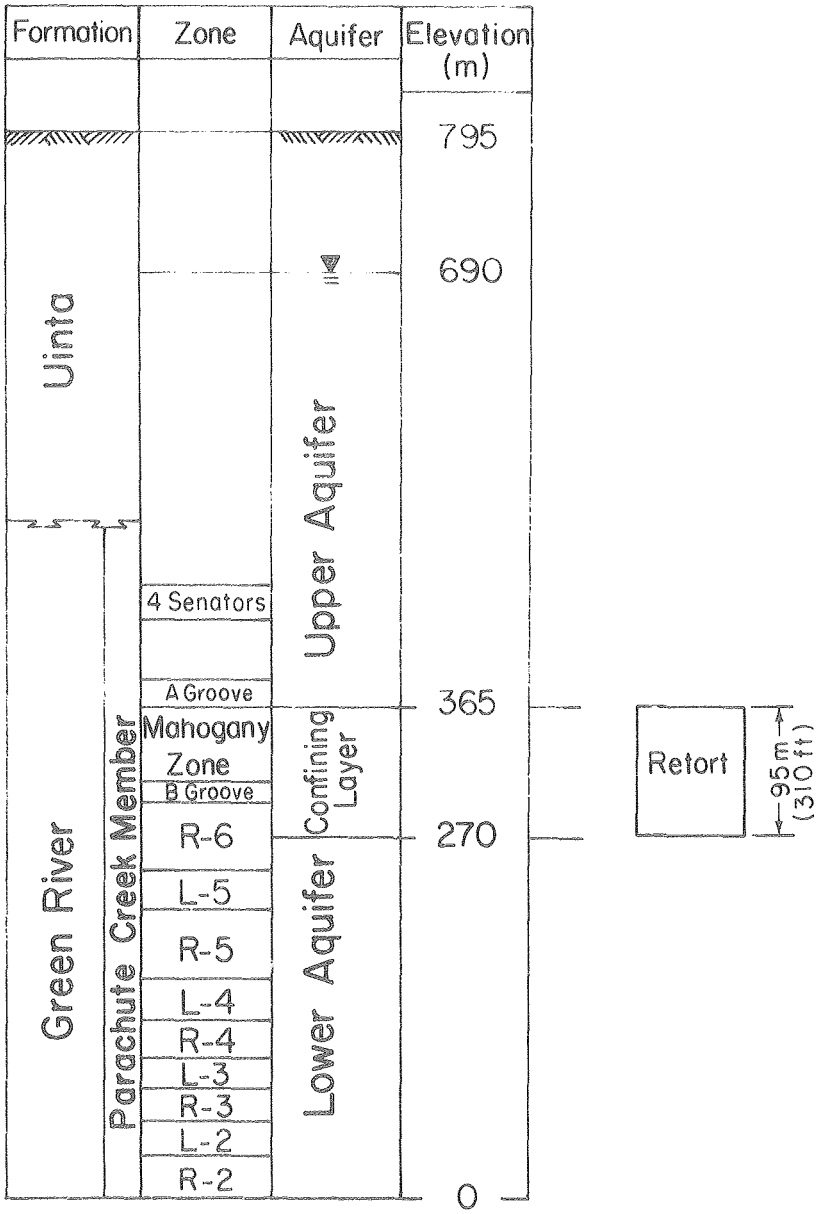

FXBL 8011-2306

Figure 5. Stratigraphy of the C-b tract and location of the mining zone. R stands for a rich oil shale and L for a lean oil shale zone. Datum is bottom of R-2 zone.

200 m (650 ft) (RBOSP, 1977).

At the C-b tract, the upper aquifer consists of various zones with different material and hydraulic properties. A lean oil shale zone, which is more fractured than other parts of the aquifer, exists between the Four Senators Zone and A Groove (Figure 5). The A Groove, which is located on top of the Mahogany Zone, is highly conductive to water. The A Groove is about 5 to 8 m (16 to 26 ft) thick. Permeability of materials above and below the A Groove in both vertical and horizontal directions is much lower than that of the A Groove.

The Confining Layer. Below the A Groove, a confining layer called the Mahogany Zone extends throughout the basin. It hydraulically separates the upper and lower aquifers except in recharge and discharge areas. Vertical exchange of water and solutes between the aquifers through the confining layer is possible through fractures present in the Mahogany Zone. Although the Mahogany Zone is considered as part of the lower aquifer in Figure 5, its material and hydraulic properties are quite different. The thickness of the Mahogany Zone at the C-a and C-b tracts are 36 m and 55 m (118 ft and 180 ft), respectively. Contradictory values of hydraulic conductivity (both vertical and horizontal) have been reported for the Mahogany Zone ranging from nonmeasureable (Weeks and Welder, 1974) to 0.11 m/day (0.36 ft/day) obtained from isolated intervals in the Mahogany Zone (Golder Associates, 1977). In the Weeks et al. (1974) model, a vertical hydraulic conductivity of 4×10^{-4} m/day is assumed. If the Mahogany Zone were impermeable, much larger hydraulic differences between the lower and upper aquifers would be developed than have been observed (Weeks et al., 1974). Recently, it has been emphasized by Smith (1980) that the confining layer is continu-

ous throughout the system, and the water yield in vertical MIS retorts is extremely small, indicating much lower transmissivities. Smith also points out that the Mahogany Zone is broken up in the C-b tract, and it would perhaps be better to shift the site to another location. An aquitard is present on the C-a tract which extends from a depth of approximately 100 m (330 ft) to the bottom of the R-5 layer (Figure 4). The data on hydraulic properties of this layer are scarce.

The Lower Aquifer. The lower aquifer consists of fractured oil shale and marlstone of the Parachute Creek Member underlying or including the Mahogany Zone. The secondary porosity and permeability have been enhanced by solution of primary minerals, mostly nahcolite (Weeks et al., 1974). The thickness of this aquifer varies from place to place and in the C-a and C-b tracts, it is approximately 73 m and 270 m (239 ft and 886 ft), respectively. The bottom of the lower aquifer lies on the relatively impervious materials of the Garden Gulch Member. It is at this depth in the central part of the basin that the Saline Zone begins.

The data on transmissivities are highly variable and range up to 180-m^2/day (2000 ft^2/ day). The existing data are derived from a number of aquifer tests, but because they represent a small area of influence, the values may not be typical. The transmissivity data for the lower aquifer on the C-a tract appear to be more representative than that of the upper aquifer. Pumping test data indicate that the transmissivity of the lower aquifer is about 90 m^2/day (1000 ft^2/day) (Rio Blanco Oil Shale Project, 1977). The storage coefficient data are based on aquifer tests on three sites in the basin, and it is on the order of 10^{-4} (Weeks et al., 1974). In areas where the lower aquifer is exposed, a specific

yield of 10^{-1} has been assumed.

PROBLEM DESCRIPTION

The problem is idealized by assuming that the retorted region is a disc-shaped area that starts at the axis of symmetry of the flow region and extends radially outward with time. The flow region is assumed to be bounded by impermeable boundaries except on the upper boundary where recharge occurs. Seepage into the retorted region takes place through the upper surface, the lower surface, and the periphery of the disc-shaped volume. As desaturation proceeds, water table profiles evolve in time. A schematic diagram of the flow region, expanding retort, hypothetical water table profiles, and desaturated zones are shown in Figure 6.

PROPOSED MINE DEVELOPMENT

Internal drainage is used for dewatering at both tracts C-a and C-b in this analysis. Thus, underground mine development is the forcing function in our problem.

The C-a Tract

The proposed mine dewatering system at tract C-a will consist of pumping wells and mine drainage through drifts and underground workings (Rio Blanco Oil Shale Project, 1977). This system will be continually modified with the addition of new wells and abandonment of old wells as the mine expands in time. The present study is based only on dewatering by internal drainage.

The geometry of retorts varies according to the phase of the project. In the first phase (MDP) of the project, the retorts have dimensions of 30 m x 30 m (100 ft x 100 ft) in plan and 122 m (400 ft) in

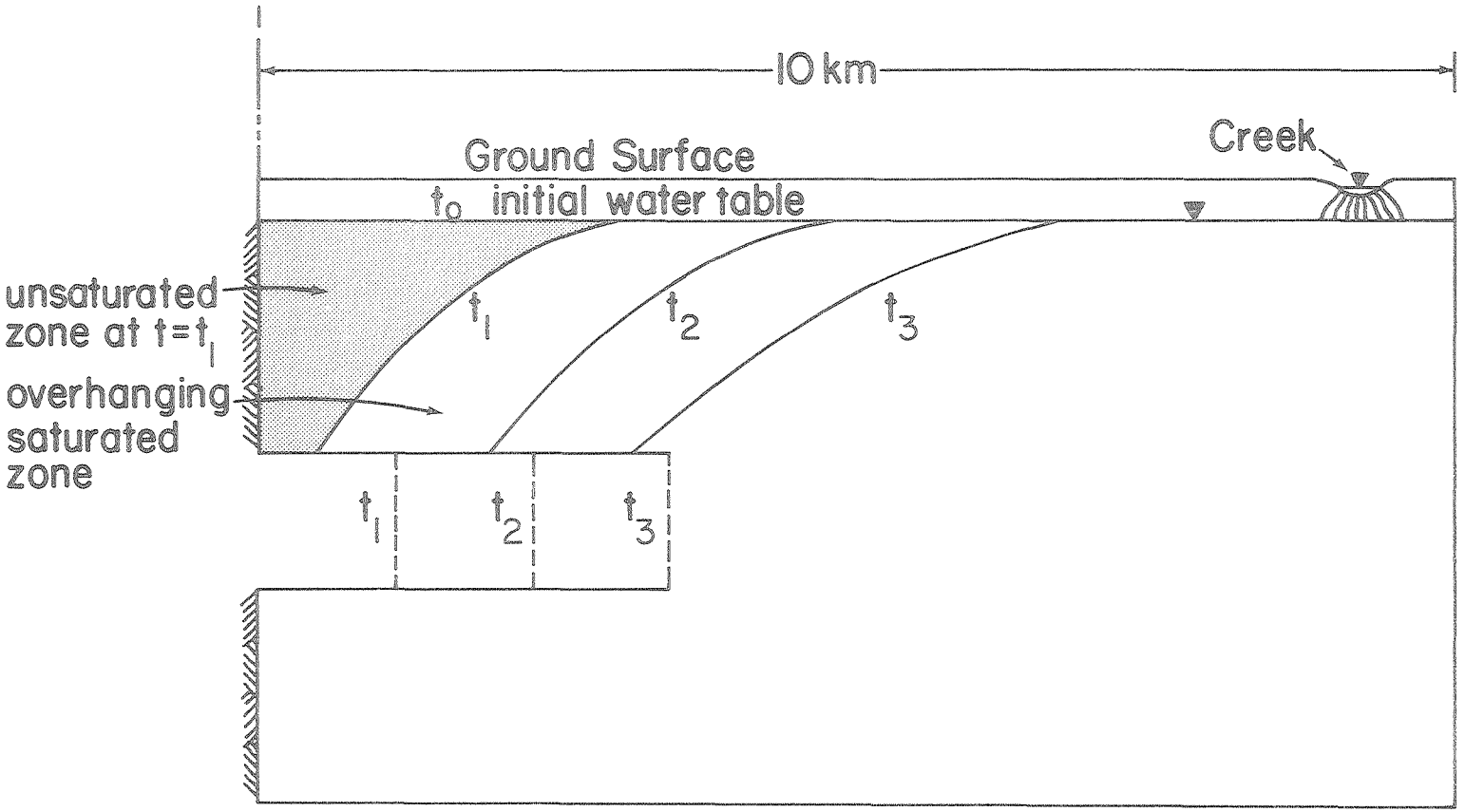

FXBL 8011-2305

Figure 6. Schematic diagram of the flow region, expanding retort, and hypothetical water table profiles.

height. However, in the commercial phase, the retorts will have the dimensions of 46 m x 92 m (150 ft x 300 ft) in plan and 229 m (750 ft) in height. Only commercial-sized retorts are used in this study.

The retorting interval in the commercial phase begins from the top of the Mahogany Zone and extends to the bottom of the R-4 Zone as shown in Figure 4. According to the Revised Detailed Development Plan (Rio Blanco, 1977), for 30 years of production on one-half of the tract, 932 retorts will be developed covering a plan area of approximately 390 hectares (960 acres). Assuming an areal extraction ratio of 50%, the retorted area will advance at approximately 26 hectares (64 acres) per year. Figure 7 shows the expansion of the retorted area with time.

The C-b Tract

According to the Tipton and Kalmbach analysis, internal mine drainage is preferable to deep wells for dewatering the C-b tract because dewatering wells must necessarily penetrate far below the retort level, unfavorably affecting economics. Additionally, they may result in pumping poorer quality water to the surface. Another reason for not using deep wells is that near ultimate dewatering levels, the yield of the wells may be very small and additional wells may be required (Tipton and Kalmbach, 1977). Since the present study considers dewatering through internal drainage as the retorted area expands with time, information on mine development is an essential input to the groundwater model.

The smallest physical unit in the proposed MIS system for the C-b tract is a retort with dimensions of 61 m x 61 m (200 ft x 200 ft) in plan and 95 m (310 ft) in height. The volume of each retort is 0.35 million m^3 (12.4 million ft^3). The retorts are created subsequent to

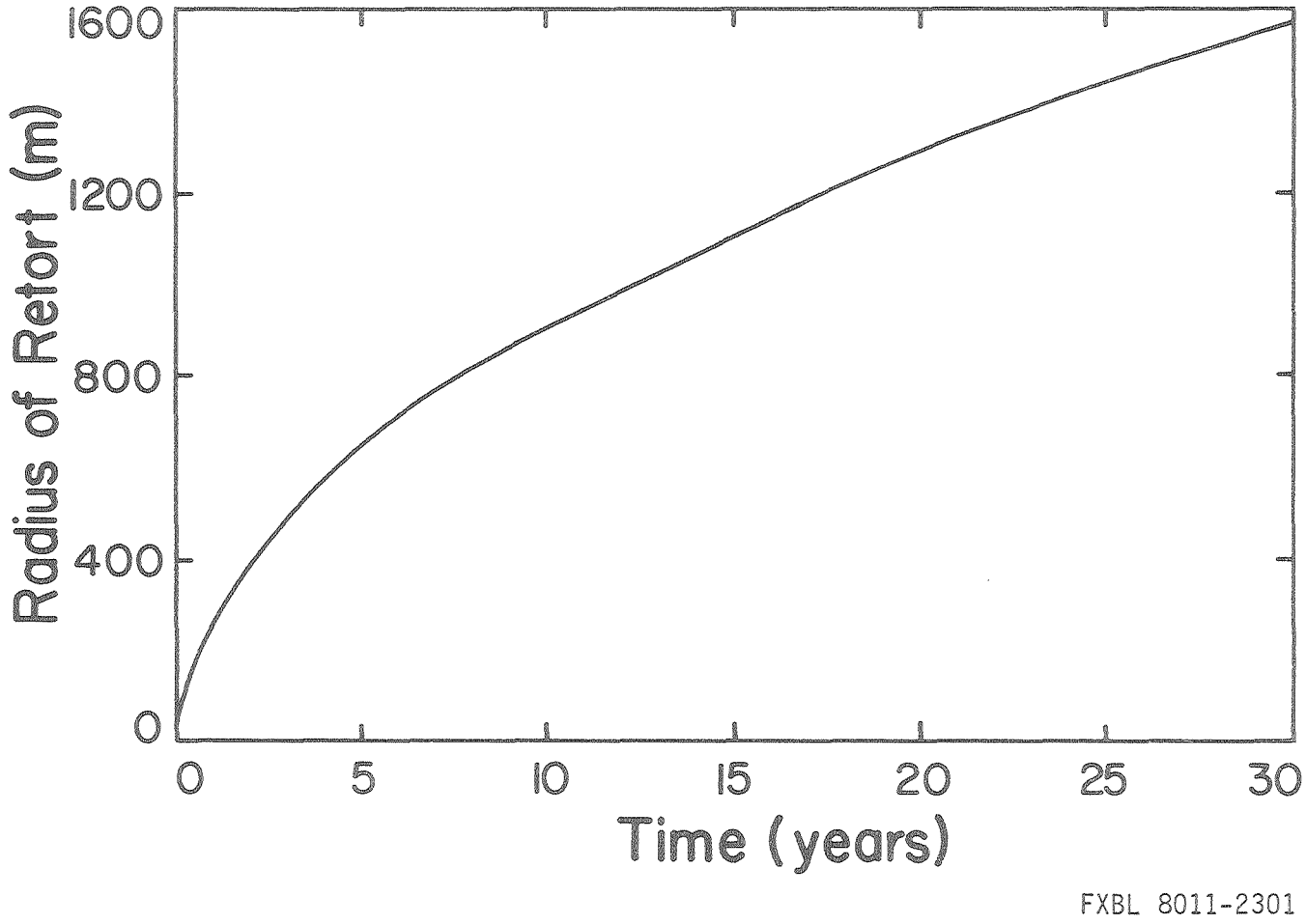

Figure 7. Rate of expansion of the retorted area with time at the C-a tract.

mining and hoisting 20 to 25% of the in-place material to the surface in order to provide sufficient void space prior to rubblization.

The retorting interval of interest starts just below the top of the Mahogany Zone and ends just above the bottom of the R-6 Zone as shown in Figure 5. Individual retorts are separated by pillars. The plan area of pillars associated with each retort will be about 60% of the retort area. A collection of eight retorts forms a cluster and 32 clusters form a panel. At a production level of 9120 m^3/day (57,000 bbl/d), 15 panels will be developed during the 60-year life of the project. Therefore, each panel lasts four years (Energy Development Consultants, Inc., 1980).

Since each panel consists of 256 retorts, the rate of retort development will be 64 per year. Taking the total area of retorts and panels into account, the rate of development of the retorted region will be approximately 38 hectares (94 acres) per year in plan. Using this rate of retort expansion represented in cylindrical geometry, the increase in the radius of the retorted area with time is as shown in Figure 8. Although the areal development may not be precisely circular, the radial concept employed here is a reasonable first approximation.

Access to retorts, clusters, and panels will be through five vertical shafts as follows: a 1.83 m (6 ft) diameter temporary gas shaft; a 3.6 m (12 ft) diameter ventilation/escape shaft; and three 10.3 m (34 ft) diameter production, service, and product gas shafts. Since the volume of the shafts is negligible compared with the total volume of the disturbed material, their presence is ignored in the simulations.

MATERIAL DISTRIBUTION AND PROPERTIES

The stratigraphy of the C-a and C-b tracts indicates that the medi-

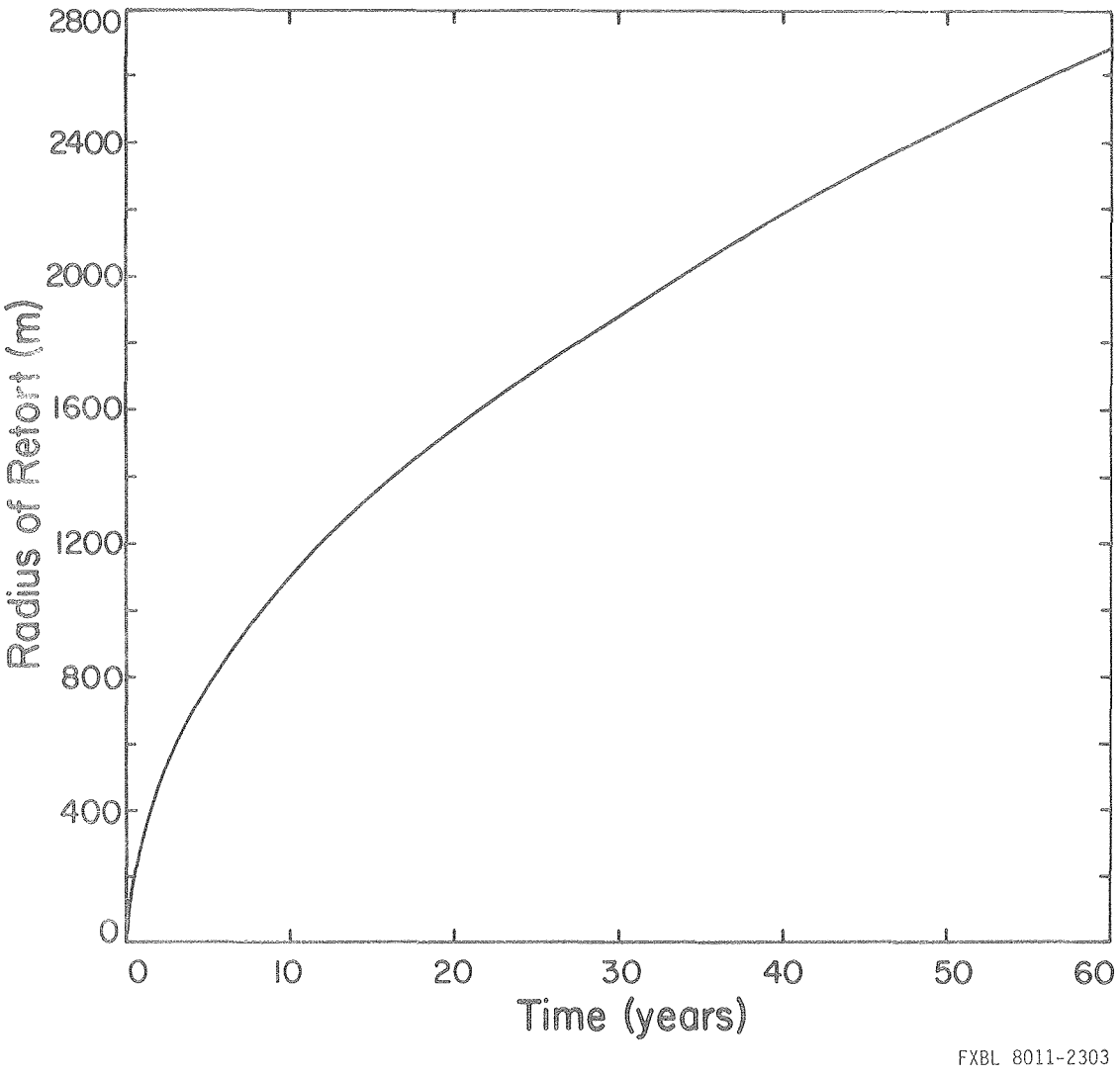

Figure 8. Rate of expansion of the retorted area with time at the C-b tract.

um is inhomogeneous and anisotropic. The general stratigraphic succession consists of the upper aquifer (including the alluvial zone), the confining layer, and the lower aquifer. The thickness of the flow region for the C-a and C-b tracts is taken to be 272 m (892 ft) and 690 m (2260 ft) from the bottom of the lower aquifer to the average position of the water table, which is about 34 m and 100 m (111 and 330 ft) below the land surface, respectively. The locations of the upper aquifer, the Mahogany Zone, and the lower aquifer and their thicknesses for the two tracts are given in Figures 4 and 5. The range of properties of the materials encountered in the field and used or considered by previous investigators are summarized in Table 3 (Weeks et al., 1974; Tipton and Kalmbach, 1977; Golder Associates, 1977; Robson and Saulnier, 1980).

Fractured Versus Porous Media

There is a general belief among those who have studied the Piceance Creek Basin geology that much of the flow at depths may be controlled largely by fractures. At the outset, therefore, one would like to simulate the system as a fractured medium. However, the modeling of fractured systems for fluid flow is beset with considerable difficulty. Modeling discrete fractures is a very tedious procedure requiring large amounts of detailed data on orientation, spacing, and aperture of fractures. Modeling large flow systems (of the order of several square kilometers) using discrete fractures is neither economical nor justifiable from data available in the present work. Under the circumstances, it is general practice to treat large fractured rock systems as equivalent porous media. The earlier workers who modeled Piceance Creek Basin hydrogeology followed this approach, and we also shall follow the same ap-

Table 3. Hydraulic parameters considered by various investigators

Parameter	Study[a]	Upper Aquifer	Confining Layer	Lower Aquifer
Thickness, m	W	V[e]	V	V
	T-K	330	55	315
	GA[c]	310	95	275
	RS	V	V	V
Transmissivity, m^2/day	W	6.5-25.0	0.022[b]	12.1-62.0
	T-K	21.7	--	5.5
	GA	2.41[c]	1.92[c]	1.98[c]
	RS	V	V	V
Storage coefficient	W	10^{-3}	--	10^{-4}
	T-K	$1x10^{-3}$-$5x10^{-2}$	--	$1x10^{-3}$-$5x10^{-2}$
	GA	$3x10^{-4}$	$0.93x10^{-4}$	$2.7x10^{-4}$
	RS[d]	$1.4x10^{-4}$	$1.3x10^{-5}$	$1.6x10^{-4}$
Specific yield (drainable porosity)	W	0.1	--	0.01-0.1
	T-K	0.01-0.15	--	--
	GA	0.01-0.1	0.01	0.01-0.02
	RS	0.01	0.01	0.01

[a] W = Weeks et al.; T-K = Tipton and Kalmbach; GA = Golder Associates; RS = Robson and Saulnier.

[b] Obtained from leakance value of $4x10^{-4}$ m/day.

[c] Based on equivalent hydraulic conductivity obtained from vertical and horizontal conductivites of different zones.

[d] Based on thickness of the aquifers used in the present study.

[e] V = Variable.

proach in the present work. An added justification for this is that most of the well tests have been interpreted in terms of homogeneous porous media to obtain hydraulic conductivity and storage. As far as our current ability to hydrogeologically characterize the C-a and the C-b tracts is concerned, the equivalent porous medium approach will provide a reasonable estimate of probable system behavior for purposes of making engineering decisions.

Degree of Saturation

In the groundwater models cited earlier, flow is assumed to take place in a fully water saturated medium. In situations where water physically drains out of the pore space and the medium becomes unsaturated, the above treatment may lead to erroneous conclusions. In the unsaturated state, the main contribution to drainage is from the desaturation of pores which far exceeds the compressibility of either water or the solid skeleton. Analysis of flow in borehole infiltration tests by Stephens and Neuman (1980) demonstrates that the classical free-surface approach gives a distorted view of the flow pattern. They also show that a significant percentage of the flow takes place under unsaturated conditions and indicate that disregarding the unsaturated flow may result in an underestimation of unsaturated hydraulic conductivity of fine-grained soils by a factor of two, three, or more. It is therefore important that unsaturated flow be given due consideration in the present analysis.

The treatment of unsaturated flow requires, a priori, a knowledge of the variation in degree of saturation, S, with pressure head, ψ, (pressure head = hydraulic head - elevation head) and the variation in

hydraulic conductivity, K, with pressure head. Both of these properties are strong functions of particle size and particle size distribution of the materials comprising the aquifer system.

A typical saturation-pressure head (S-ψ) relation for a coarse-grained material is shown in Figure 9. Change in saturation results in absorption (increase) or release (decrease) of water from storage. As saturation reduces to less than 100%, a negative gage pressure develops which is usually referred to as soil moisture suction.

Upon applying suction to a saturated soil with $\psi = 0$, the soil does not physically desaturate until the applied suction exceeds a critical "air entry" value, ψ_A, which is a function of the texture of the medium. In general, one would require lower suctions for initiation of desaturation in coarse-grained soils as compared with fine-grained soils. The air entry value for the well-graded sand shown in Figure 9 is 0.20 m (0.66 ft) of water. In any case, in the range of $\psi_A < \psi < 0$, although the soil has negative pore pressure, it remains saturated. It is evident from Figure 9 that below a certain pressure head in the unsaturated region, further reduction in pressure head is associated with only minute changes in saturation. This degree of saturation is referred to as "residual saturation". Figure 9 also illustrates that the dependence of S on ψ is not unique, and it depends on whether the system is in the drying cycle or the wetting cycle. This phenomenon is called hysteresis. Although the numerical model used in the present study can handle the hysteresis effect, it is ignored in the simulations because of lack of experimental data.

The S-ψ relationship is usually obtained from laboratory experiments by subjecting the soil column to various suctions. In the case of

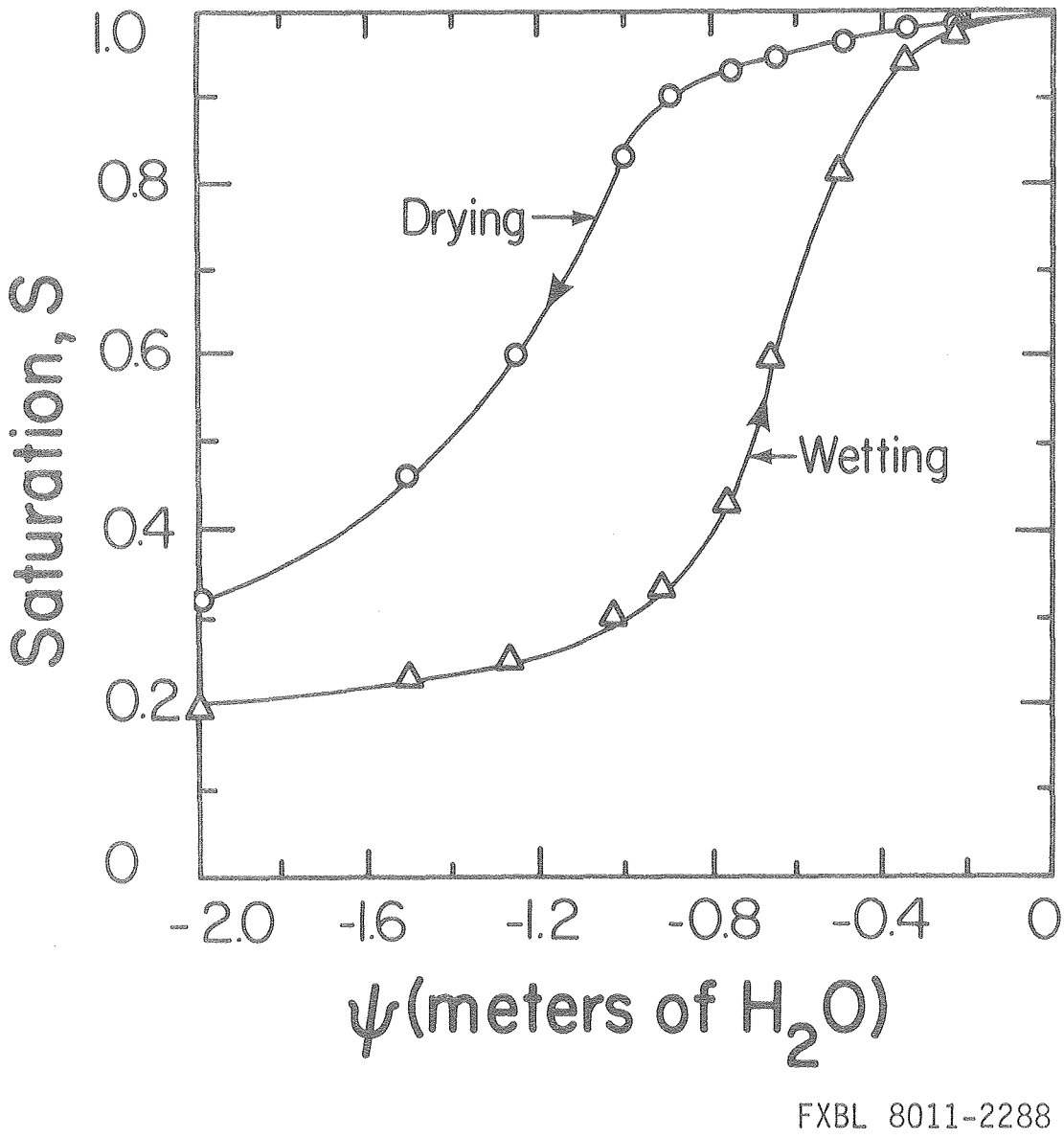

Figure 9. Variation of saturation with pressure head for Del Monte sand (after Liakopoulos, 1965).

fine-grained materials, this relation is obtained by the pressure membrane apparatus providing saturation values at very low suctions.

At this point, a digression is necessary to discuss the S-ψ relationship with respect to fractured rock masses. We recall here that we chose to treat the C-a and the C-b tract systems as equivalent porous media although their fractured nature is recognized. The subject of partially saturated fluid flow has been developed over the decades mainly by soil physicists who have been almost exclusively concerned with real porous media. As far as we know, little is available in the literature concerning the unsaturated characteristics of large-scale fractured masses. As such, we have no quantitative guidance to model this phenomenon accurately in the present work. Yet, we know that physically, the region above the expanding retort will continue to drain with time and eventually has to desaturate. Qualitatively, we know that this phenomenon has to be given consideration in the modeling. Under the circumstances, we have chosen more than one S-ψ relationship with a view to estimating their role in the overall desaturation process. Certainly, there is a need to systematically study this topic as a research and development problem. With the proposed step-up in the development of coal, lignite, and other natural resources, the time and effort spent to investigate the desaturation behavior of fractured rock masses will prove to be of practical benefit in more than one energy-related industry.

Hydraulic Conductivity

The dependence of hydraulic conductivity on pressure head for a coarse-grained material is shown in Figure 10. Tremendous reductions in

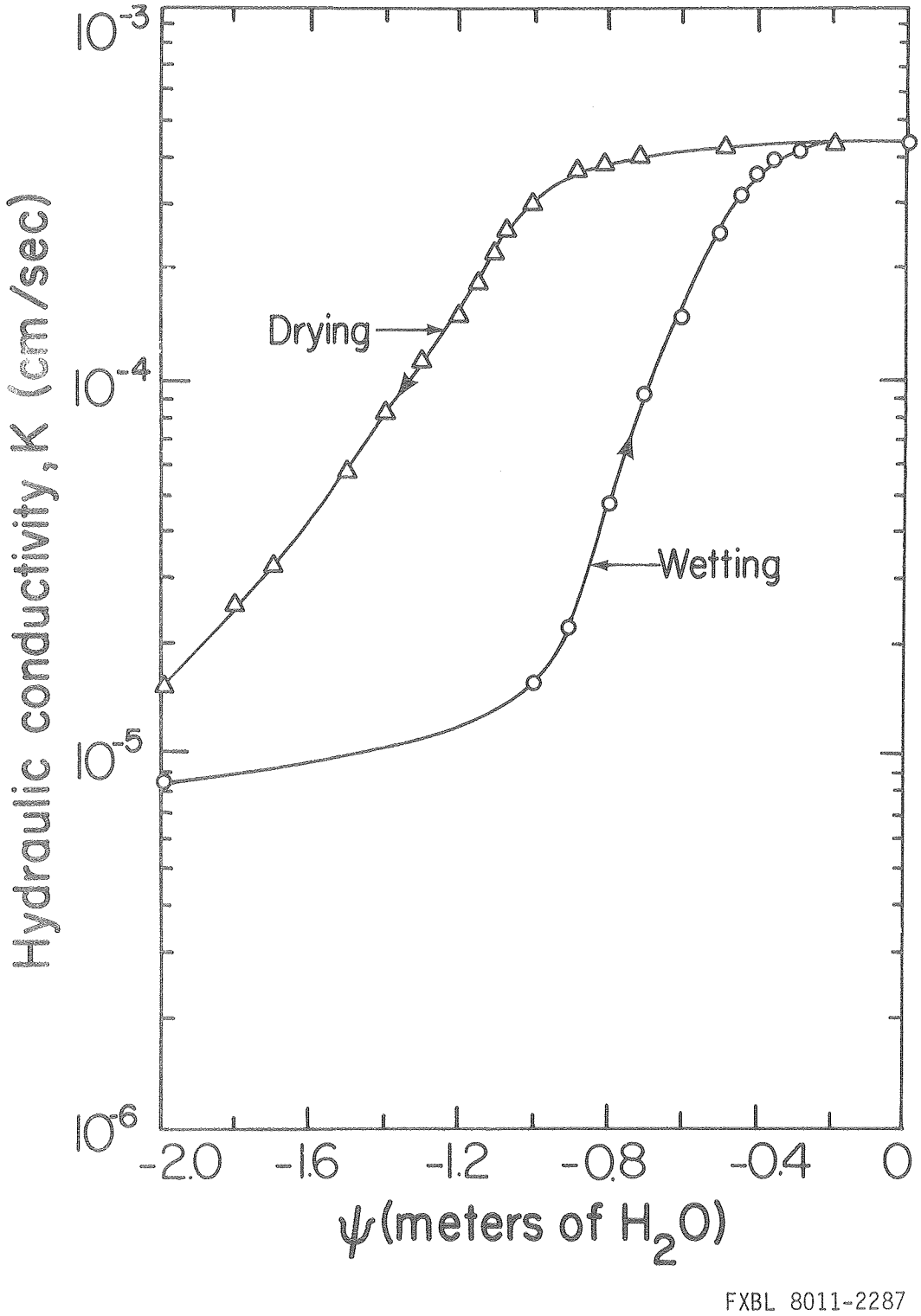

Figure 10. Variation of hydraulic conductivity with pressure head for Del Monte sand (after Liakopoulos, 1965).

hydraulic conductivity are observed as desaturation proceeds, indicating a strong dependence of K on ψ. In analyzing unsaturated flow using numerical methods, it is customary to compute the K-ψ relationship based on fundamental properties of the medium. This can be achieved by various approaches, all of which depend primarily on pore-size distribution. The Millington-Quirk equation can be cited as one of the most commonly used methods of evaluating hydraulic conductivity in the unsaturated state. It requires a knowledge of saturated hydraulic conductivity and pore-size distribution which in turn can be obtained from the soil-moisture characteristic curve (Millington and Quirk, 1961).

Initial Conditions

The system consists of a layered, anisotropic saturated system which evolves in time into a saturated-unsaturated system. Thus, the physics is governed by the transient equation of saturated-unsaturated groundwater flow. The flow region is initially assumed to be hydrostatic with hydraulic heads of 270 and 690 m (886 and 2260 ft) for the C-a and C-b tracts, respectively. In the present model, we shall ignore the region from the land surface to the average position of the water table. In other words, we start with a fully saturated system which undergoes desaturation with time.

Boundary Conditions

The flow region, as shown in Figure 6, is assumed to be surrounded by impermeable boundaries located far away from the axis of symmetry. The flow is axisymmetric with no flow across the axis of symmetry. The bottom of the flow region is impermeable. The flow region extends radi-

ally to a distance where no boundary effects can be observed during the dewatering phase. Recharge at the upper surface of the flow region (initial water table) is assumed to be zero for all cases considered in the sensitivity analysis. However, for long-term simulations of dewatering on tracts C-a and C-b, recharge is taken into account. Flow into the retorted region takes place from the exposed bottom of the upper aquifer, from the exposed top of the lower aquifer, and from the periphery of the disc-shaped retorted region.

THE NUMERICAL MODEL

The numerical model divides the flow region into appropriately small subregions and satisfies the conservation equation for transient saturated-unsaturated flow for each such subdomain. The resulting set of implicit equations is solved simultaneously for the average time derivative in each subdomain (Narasimhan and Witherspoon, 1977 and Narasimhan et al., 1978).

THE GOVERNING EQUATION

For a small volume element undergoing deformation with time, the equation of conservation of mass combined with Darcy's law yields (Narasimhan and Witherspoon, 1977):

$$G + \int_{\Gamma} \rho_w \frac{k\rho_w g}{\mu} \nabla (z+\psi) \cdot \vec{n} d\Gamma = \frac{d}{d\psi} (\rho_w V_s e S) \frac{D\psi}{Dt} \qquad (1)$$

where

ρ_w = mass density of water,
k = absolute or intrinsic permeability,
g = acceleration due to gravity,
μ = coefficient of viscosity,
z = elevation head,
ψ = pressure head,
$\vec{n}$ = outward unit normal to $d\Gamma$,
Γ = bounding surface of volume element of flow region,
G = source,
V_s = volume of incompressible solids of the finite subregion,
e = void ratio,
S = degree of saturation,
t = time,
$\frac{D}{Dt}$ = material derivative.

In Eq. (1), $\frac{d}{d\psi}(\rho_w V_s eS) = M_c$ is defined as the fluid mass capacity of the volume element. Upon differentiation and simplification, the following expression for M_c is obtained (Narasimhan and Witherspoon, 1977):

$$M_c = V_s \rho_w \left(Se\rho_{wo}\beta g + \frac{S\gamma_w \chi' C_c}{2.303\sigma'} + e\frac{dS}{d\psi}\right) \qquad (2)$$

where

β = compressibility of water,
ρ_{wo} = mass density of water at atmospheric pressure,
γ_w = specific weight of water,
C_c = coefficient of consolidation,
σ' = effective stress,
$\chi' = \chi + S\frac{d\chi}{d\psi}$

and χ' is Bishop's parameter relating pore pressure to effective stress in a partially saturated soil. The three terms on the right hand side of Eq. (2) represent three distinct quantities. The first term expresses the expansion of water as hydrostatic pressure changes. The second term represents the deformability of the soil skeleton, and the last term denotes desaturation of the pores. Under many circumstances where flow takes place in an unsaturated state, the last term of Eq. (2) is dominant. However, many workers (e.g., Golder Associates) choose to treat the desaturation term through an equivalent specific yield coefficient.

Equation (1) is highly nonlinear because M_c and K are both strongly dependent on ψ.

METHOD OF SOLUTION

The solution described here will assume a small subregion of the flow region (Figure 11) in which the lines joining the nodal point ℓ to its neighbors are normal to the interfaces between the respective elements. Applying Eq. (1) to this volume element, we can write:

$$G_\ell + \sum_m \rho_w \frac{k\rho_w g}{\mu} \left[\frac{(z_m + \psi_m) - (z_\ell + \psi_\ell)}{d_{\ell,m} + d_{m,\ell}} \Gamma_{\ell,m}\right] = M_{c,} \frac{\Delta\psi_\ell}{\Delta t} \tag{3}$$

Defining $\rho_w \frac{k\rho_w g}{\mu} \frac{\Gamma_{\ell,m}}{d_{\ell,m}+d_{m,\ell}} = U_{\ell,m}$ as the conductance of the interface between elements ℓ and m, Eq. (3) including the boundary effects, can be written as:

$$G_\ell + \sum_m U_{\ell,m} (\bar{\phi}_m - \bar{\phi}_\ell) + \sum_b U_{\ell,b} (\bar{\phi}_b - \bar{\phi}_\ell) = M_{c,\ell} \frac{\Delta\psi_\ell}{\Delta t} \tag{4}$$

where ϕ is the total head and

$$\begin{aligned} \bar{\phi}_m &= \phi_m^o + \lambda \Delta\phi_m \\ \bar{\phi}_\ell &= \phi_\ell^o + \lambda \Delta\phi_\ell \end{aligned} \tag{5}$$

In the above equations, λ can assume values of 0, 0.5, or 1 for explicit forward difference, central difference, or fully implicit schemes, respectively. By quasi-linearization, Eq. (4) may be reduced to a system of algebraic equations. These algebraic equations are solved using a Point Jacoby type accelerated iterative scheme with a mixed explicit-implicit strategy (Edwards, 1972; Narasimhan et al., 1978).

The numerical model, called TRUST, is capable of solving transient saturated-unsaturated isothermal flow in one, two, or three dimensions for simple or complex geometrical configurations under various initial and boundary conditions. Anisotropy of the media can be handled by the

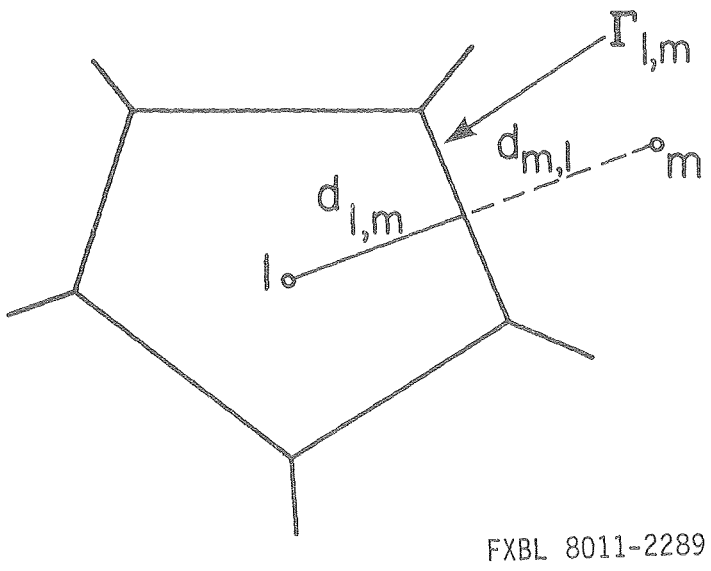

Figure 11. Volume element for node ℓ.

model by orienting volume elements in such a maner that their boundary surfaces are perpendicular to the principal direction of anisotropy.

RESULTS

This section discusses the results of the various simulations that were carried out. As will be seen subsequently, the C-b tract was subjected to a far more detailed analysis than the C-a tract. The reason for this is that we started our work with the C-b tract and performed parametric studies for this site before taking up the C-a tract. We believe that although the C-a tract is more fractured than the C-b tract, the sensitivity analysis of the C-b tract provides enough information about the relative importance of the different parameters and that further sensitivity studies with the C-a tract are not essential.

Two broad scenarios were considered for the C-b tract. In the first, the retorted region was assumed to have a fixed geometry, while in the second, the geometry of the retorted region was allowed to vary with time. Analysis of the fixed geometry scenario is carried out in order to show that such treatment is a gross simplification of the more complex and realistic case of the expanding retort. All the parametric studies and the long-term simulations were done with a variable geometry.

The flow region for the C-b tract is shown in Figure 12. The entire flow region is assumed to consist of an upper aquifer and a lower aquifer with a confining layer between the two aquifers representing the interval of interest for retorting. Flow into the disc-shaped retorted volume takes place through the upper and lower surfaces as well as the periphery of the retorted region. At these surfaces, the pressure is assumed to be atmospheric, implying that hydraulic head is equal to eleva-

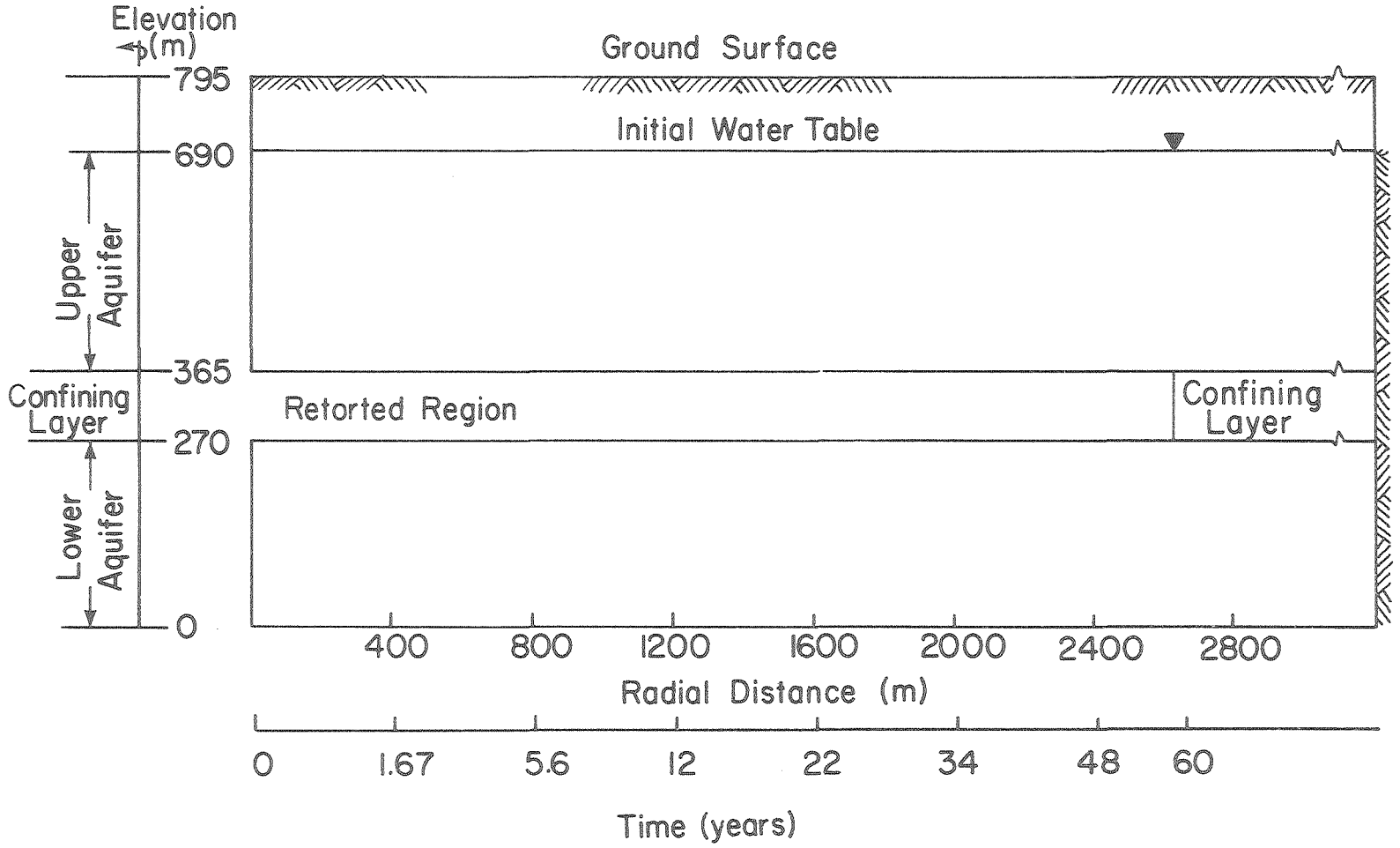

Figure 12. Schematic diagram of the axisymmetric flow region and location of the front of the retorted region as a function of time for the C-b tract.

-tion above datum. Also, it is assumed that water is instantaneously pumped out of the mine.

Analysis of flow requires a knowledge of the relationships between saturation and pressure head and between permeability and pressure head. Figure 13 shows two hypothetical saturation-pressure head relationships, $S(\psi)_1$ and $S(\psi)_2$, used in this study. They correspond to two distinct types of material behavior under desaturation. $S(\psi)_1$ represents a material with a low degree of residual saturation (20%) and high drainable porosity. $S(\psi)_2$ represents a material which has a higher residual saturation and, hence, a smaller drainable porosity. $S(\psi)_1$ and $S(\psi)_2$ could represent the behavior of coarse-grained and fine-grained materials, respectively. Figure 14 shows the relationship between permeability and pressure head used in the sensitivity analysis. Conductivity in this figure is expressed in terms of intrinsic permeability defined as:

$$k = K \frac{\mu}{\rho_w g} \tag{6}$$

where K = hydraulic conductivity. Since the lower aquifer remains saturated at all times, a constant saturated permeability is assumed.

DEWATERING A FIXED RETORTED REGION

Since the fixed-geometry scenario is only an approximation to the more complex scenario of an expanding retort area, the comparison of the results of the two scenarios is worth investigating. For the fixed-geometry scenario, it is assumed that a cavity the size of the area to be ultimately retorted is created without disturbing the flow pattern prior to simulation. The thickness of the cavity is equal to the mining interval. It is further assumed that at time zero, the radius of the retorted region is 500 m (1640 ft) with a hydraulic head of 690 m (2260

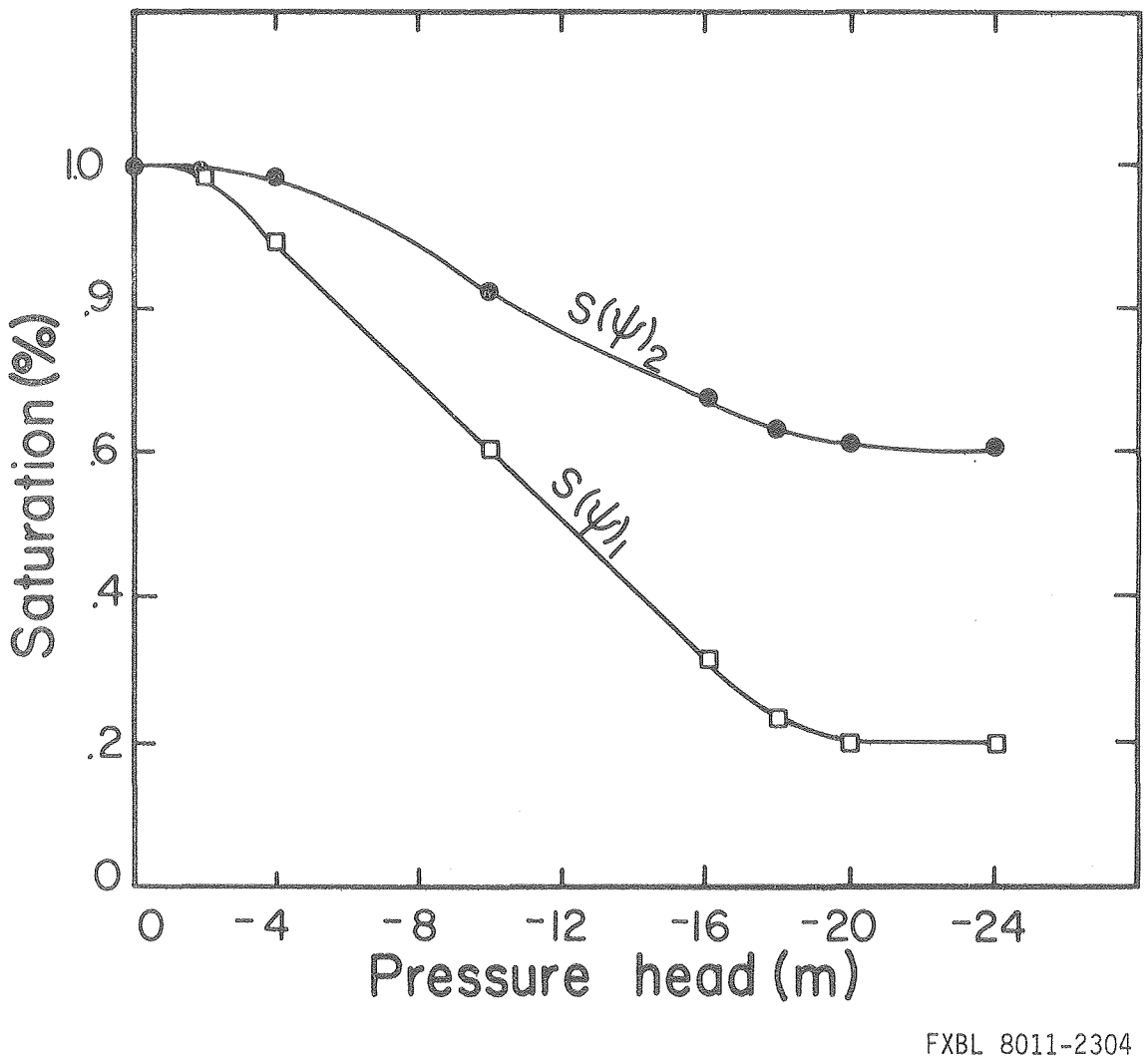

Figure 13. Percent saturation as a function of pressure head for two different materials assumed in this study.

ft) throughout the region. For this analysis, to avoid boundary effects, it is assumed that the aquifers and the confining layer extend radially to a distance of 10 km (6.35 miles).

Based on these assumptions, the dewatering of the region was simulated by TRUST for only two years as an approximation to the more realistic scenario of an expanding retort. In this analysis, the relationship between saturation and pressure head for the upper aquifer was assumed to be $S(\psi)_1$ (Figure 13). The permeability-pressure head relation was that given in Figure 14. The storage coefficient of the lower aquifer was taken as 1×10^{-4}. The porosity of all three layers was assumed to be 1%.

The inflow rate for a two-year simulation of dewatering in a retort of 500-m (1640 ft) radius is shown in Figure 15. The initial inflow rates are extremely high because at time zero, the retorted region is subject to very high potential gradients at all boundaries. Subsequent reduction in inflow rate is due to the lowering of the gradients and desaturation of the upper aquifer located above the retorted region. The gradual decrease in flow rate is reflected in the cumulative flow curve shown also in Figure 15. As desaturation proceeds, the phreatic surface (the surface of zero pressure head) becomes dynamic and continuously moves down within the flow region. It should be pointed out that flow in the unsaturated medium above the phreatic surface continues until the unsaturated hydraulic conductivity becomes extremely small. The properties of the medium, particularly the hydraulic conductivity of the upper aquifer, play an important role in both the magnitude of the inflow rate and the position of the water table profiles. These effects will be demonstrated for the case of the expanding retort. The results

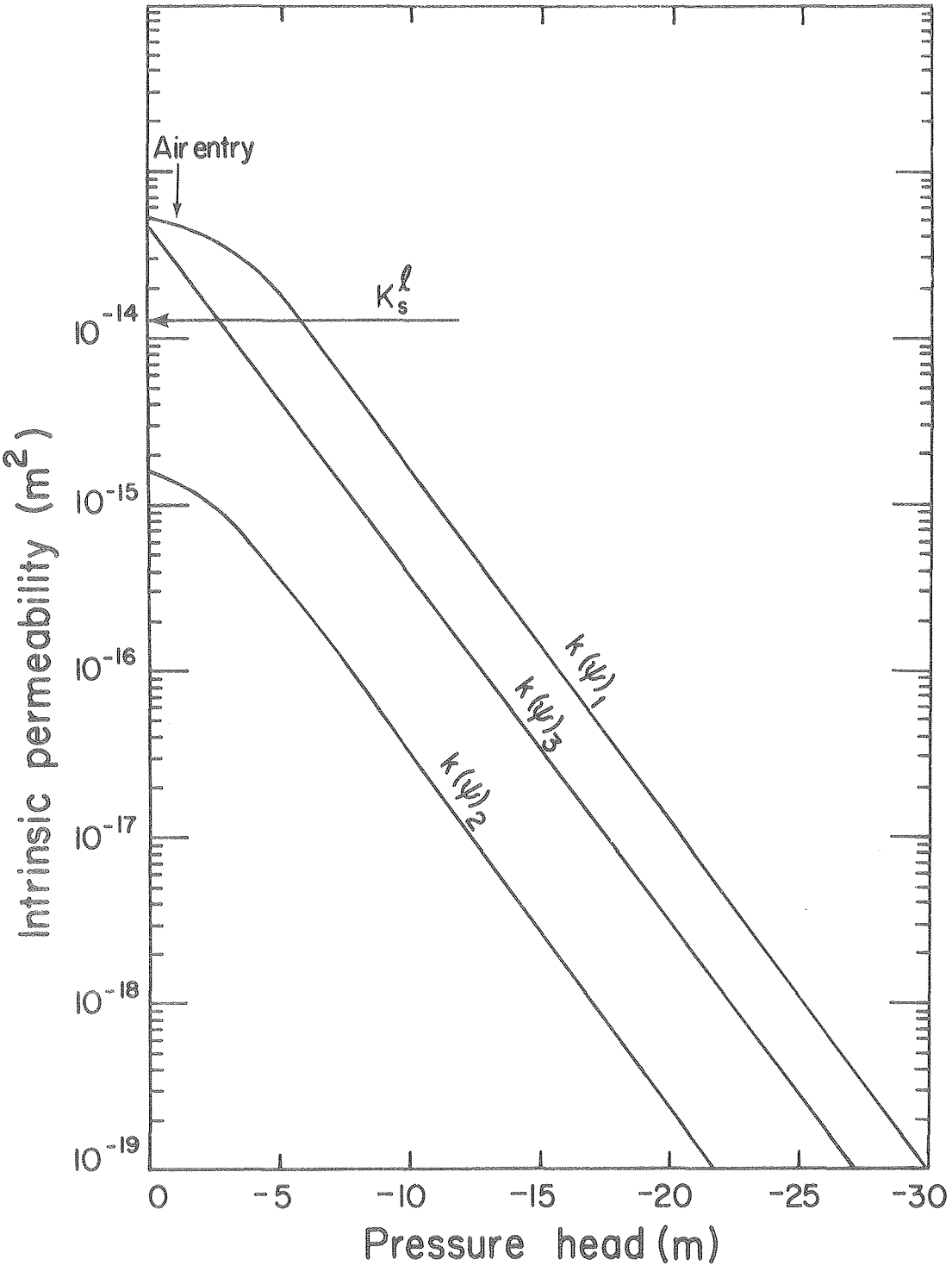

FXBL 8011-2300

Figure 14. The relationship between permeability and pressure head for three different materials undergoing desaturation. Saturated permeability of the lower aquifer, $k_s^\ell = 1.28 \times 10^{-14}$ m^2. Values shown were used in parametric studies only.

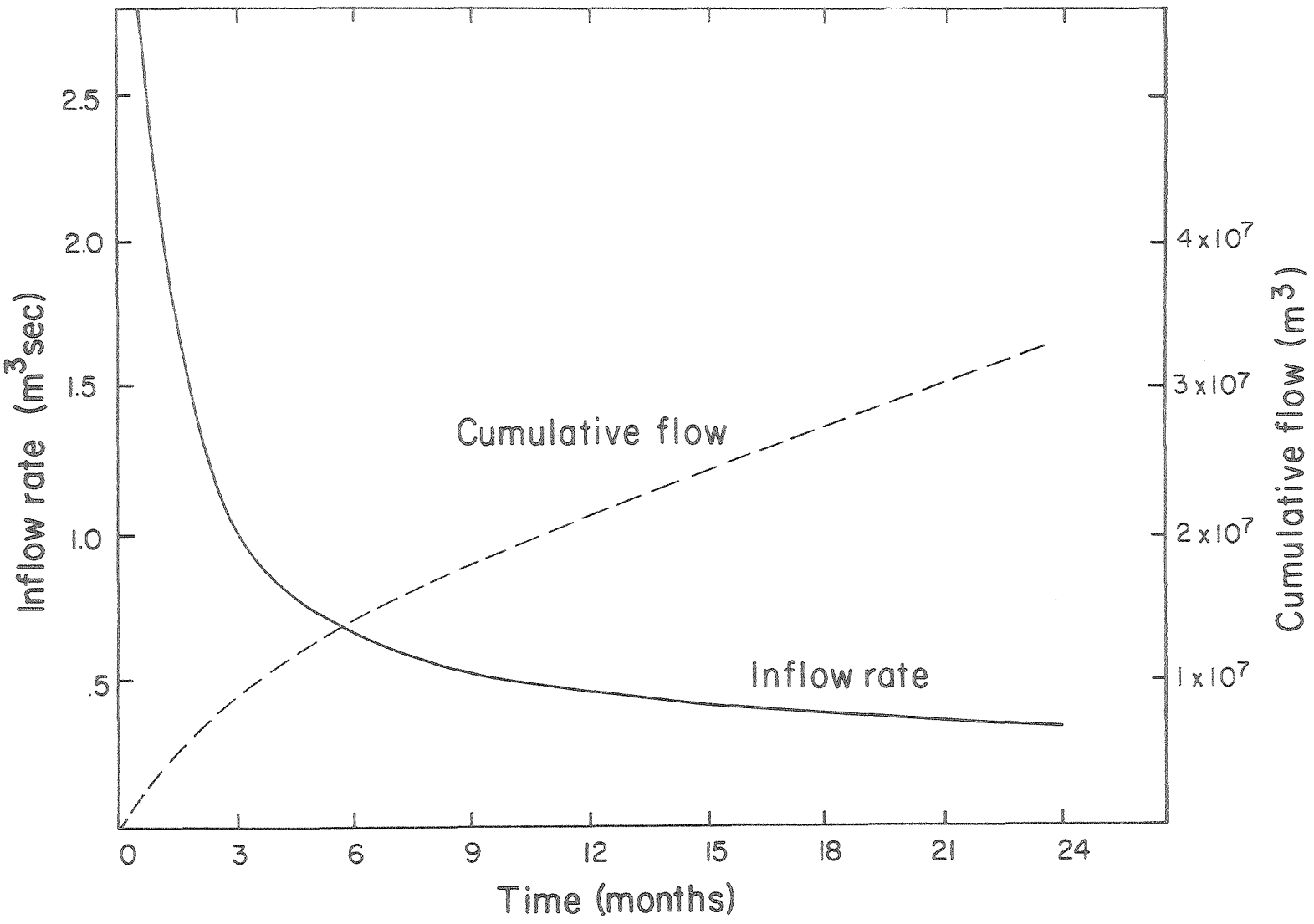

FXBL 8011-2299

Figure 15. Variation of inflow rate and cumulative flow with time for dewatering a retort with fixed geometry.

of the fixed geometry scenario will be compared with the expanding case after the expanding retort case is presented.

DEWATERING AN EXPANDING RETORTED REGION

This scenario, which is more realistic for dewatering an MIS site, requires a knowledge of the rate at which the effective (equivalent) radius of the retorted area (in plan) expands with time. This information is used as an input to the groundwater model. Based on information provided by the Energy Development Consultants, Inc. (1980), the rate of expansion of retorts will be 38 hectares (94 acres) per year. This rate of expansion is illustrated in Figure 8 for the 60-year life of the project at the C-b tract. The flow region for this scenario is shown in Figure 12 as a vertical section from the ground surface to a depth of 795 m (2608 ft). The average position of the initial water table is assumed to be at a depth of 105 m (344 ft) below land surface. The retorting interval of interest with a thickness of 95 m (310 ft) lies between the upper and lower aquifers, which have thicknesses of 325 m (1066 ft) and 270 m (886 ft), respectively. The time scale in Figure 12 indicates the position of the periphery of the retorted region with progressive exploitation.

Parametric Studies

The range of parameters given in Table 3 demonstrate the wide variability of hydraulic properties of the aquifer system under study. It is therefore important to explore the influence of each parameter on the overall response of the mine dewatering system and to evaluate its relative importance. The above considerations are not only essential for design purposes, but they will also dictate management alternatives for

ground and surface water resources. Sensitivity analyses of important parameters will provide guidelines for field and laboratory experimental programs that will be carried out in the future to better characterize the system.

The sensitivity analysis of mine dewatering is carried out for two years for an expanding retort at tract C-b. The following properties and parameters of the flow region are examined: 1) degree of saturation and its pressure head dependency, 2) hydraulic conductivity and its pressure head dependency, 3) material distribution, 4) porosity, and 5) anisotropy. Table 4 shows the various scenarios and cases that have been considered in this analysis. The unsaturated properties used in the sensitivity analysis are given in Figures 13 and 14. Table 5 summarizes the various cases that are considered in the sensitivity analysis and gives the magnitude of the saturated and unsaturated properties. For cases A through F, the porosity of the upper aquifer is assumed to be 0.28.

Material Distribution. The effect of material distribution, or the number of layers and their physical properties, on mine inflow rates is investigated by comparing cases A, C, and D (Table 5). Three different cases, namely a two-layer case, a three-layer case, and a five-layer case, were considered in the present study. In the two-layer case (A), only the upper aquifer is subject to desaturation and $S(\psi)_1$, and $k(\psi)_1$ are used to describe unsaturated properties. In the three-layer case, a confining layer is introduced between the upper and the lower aquifers. In the five-layer case, it is assumed that part of the confining layer, which has a smaller permeability, remains intact as a blanket around the retorted region. This simulates leaving a cap rock or zone of undis-

Table 4. Dewatering scenarios and cases considered for the C-b tract.

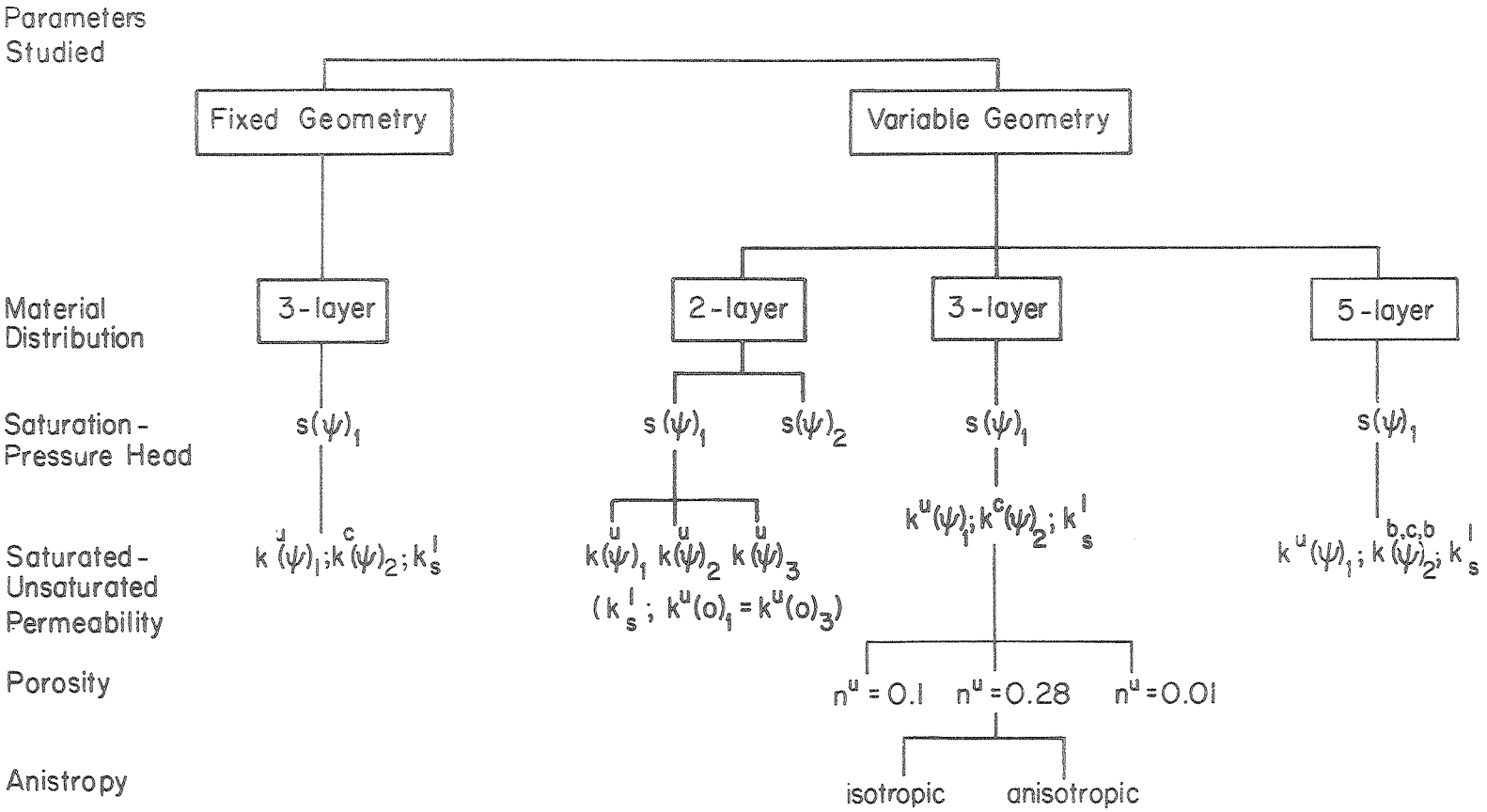

u = upper aquifer; l = lower aquifer; c = confining layer; b = blanket; n = porosity

FXBL 8011-2295

Table 5. Saturated-unsaturated properties considered in the sensitivity analysis.

Case	Layering	Unsaturated Properties		Saturated Properties		Porosity	Coefficient of Compressibility Pascal^{-1}
		Saturation (Fig. 13)	Permeability (Fig. 14)	Specific Storage	Permeability (m^2)		
A	Upper Aquifer	$S(\psi)_1$	$k(\psi)_1$	--	4.80×10^{-14}	0.28	10^{-9}
	Lower Aquifer	1.0*	--	1.14×10^{-5}	1.28×10^{-14}	0.01	--
B	Upper Aquifer	$S(\psi)_2$	$k(\psi)_1$	--	4.80×10^{-14}	0.28	10^{-9}
	Lower Aquifer	1.0	--	1.14×10^{-5}	1.28×10^{-14}	0.01	--
E	Upper Aquifer	$S(\psi)_1$	$k(\psi)_2$	--	1.30×10^{-15}	0.28	10^{-9}
	Lower Aquifer	1.0	--	1.14×10^{-5}	1.28×10^{-14}	0.01	--
F	Upper Aquifer	$S(\psi)_1$	$k(\psi)_3$	--	4.80×10^{-14}	0.28	10^{-9}
	Lower Aquifer	1.0	--	1.14×10^{-5}	1.28×10^{-14}	0.01	--
C	Upper Aquifer	$S(\psi)_1$	$k(\psi)_1$	--	4.80×10^{-14}	0.28	10^{-9}
	Confining Layer	$S(\psi)_1$	$k(\psi)_2$	--	1.30×10^{-15}	0.01	10^{-9}
	Lower Aquifer	1.0	--	1.14×10^{-5}	1.28×10^{-14}	0.01	--
G	Upper Aquifer	$S(\psi)_1$	$k(\psi)_1$	--	4.80×10^{-14}	0.10	10^{-9}
	Confining Layer	$S(\psi)_1$	$k(\psi)_2$	--	1.30×10^{-14}	0.01	10^{-9}
	Lower Aquifer	1.0	--	1.14×10^{-5}	1.28×10^{-14}	0.01	--
H	Upper Aquifer	$S(\psi)_1$	$k(\psi)_1$	--	4.80×10^{-14}	0.28	10^{-9}
	Confining Layer	$S(\psi)_1$	$k(\psi)_2$	--	1.30×10^{-14}	0.01	10^{-9}
	Lower Aquifer	1.0	--	1.14×10^{-5}	1.28×10^{-14}	0.01	--
I	Upper Aquifer	$S(\psi)_1$	$k(\psi)_1$	--	4.80×10^{-14}	0.28	10^{-9}
	Confining Layer	$S(\psi)_1$	$k(\psi)_2$	--	1.30×10^{-15}	0.01	10^{-9}
	Lower Aquifer	1.0	--	1.00×10^{-4}	1.28×10^{-14}	0.01	--
D	Upper Aquifer	$S(\psi)_1$	$k(\psi)_1$	--	4.80×10^{-14}	0.28	10^{-9}
	Blanket	$S(\psi)_1$	$k(\psi)_1$	--	1.30×10^{-15}	0.01	10^{-9}
	Mahogany Zone	$S(\psi)_1$	$k(\psi)_2$	--	1.30×10^{-15}	0.01	10^{-9}
	Blanket	$S(\psi)_1$	$k(\psi)_2$	--	1.30×10^{-15}	0.01	10^{-9}
	Lower Aquifer	1.0	--	1.14×10^{-5}	1.28×10^{-14}	0.01	--

*The lower aquifer is assumed to remain saturated at all times.

turbed rock in place to minimize flow through the retorted region. In all three cases, it is assumed that the lower aquifer remains saturated with a permeability of $k_s^{\ell} = 1.28 \times 10^{-14}$ m^2. Using the same values of permeability for the upper and lower aquifer in all three cases, the inflow rates are as shown in Figure 16. The result, as expected, implies that introducing a confining layer with a low permeability largely reduces the flow over a long period of time. A drastic reduction in flow is observed in the five-layer case where the retorted region is protected by a blanket of low permeability material. In the five-layer case, the inflow rate after two years of dewatering is about 40% of that of the three-layer case. This result may be important in situations where significant reduction of mine inflow rate is desired.

Saturation-Pressure Head Relation. One of the most important hydraulic properties of the aquifer system in the unsaturated regime is the path along which the fluid saturation changes as a result of a change in pressure head. The effect of the saturation-pressure head relationship is investigated by comparing cases A and B (Table 5). The cases use two hypothetical moisture characteristic curves (Figure 13). Hysteresis effects are neglected.

The results in Figure 17 indicate that mine inflow can be significantly affected by the saturation-pressure head relationship. In the case of higher residual saturation, both the inflow and the rate of increase in inflow rate are smaller and tend to stabilze with time. This suggests that a realistic description of saturated-unsaturated flow for a thick formation undergoing desaturation requires a knowledge of the saturation-pressure head relationship. The methodology for obtaining such relationships for large-scale modeling of thick unconfined aquifers

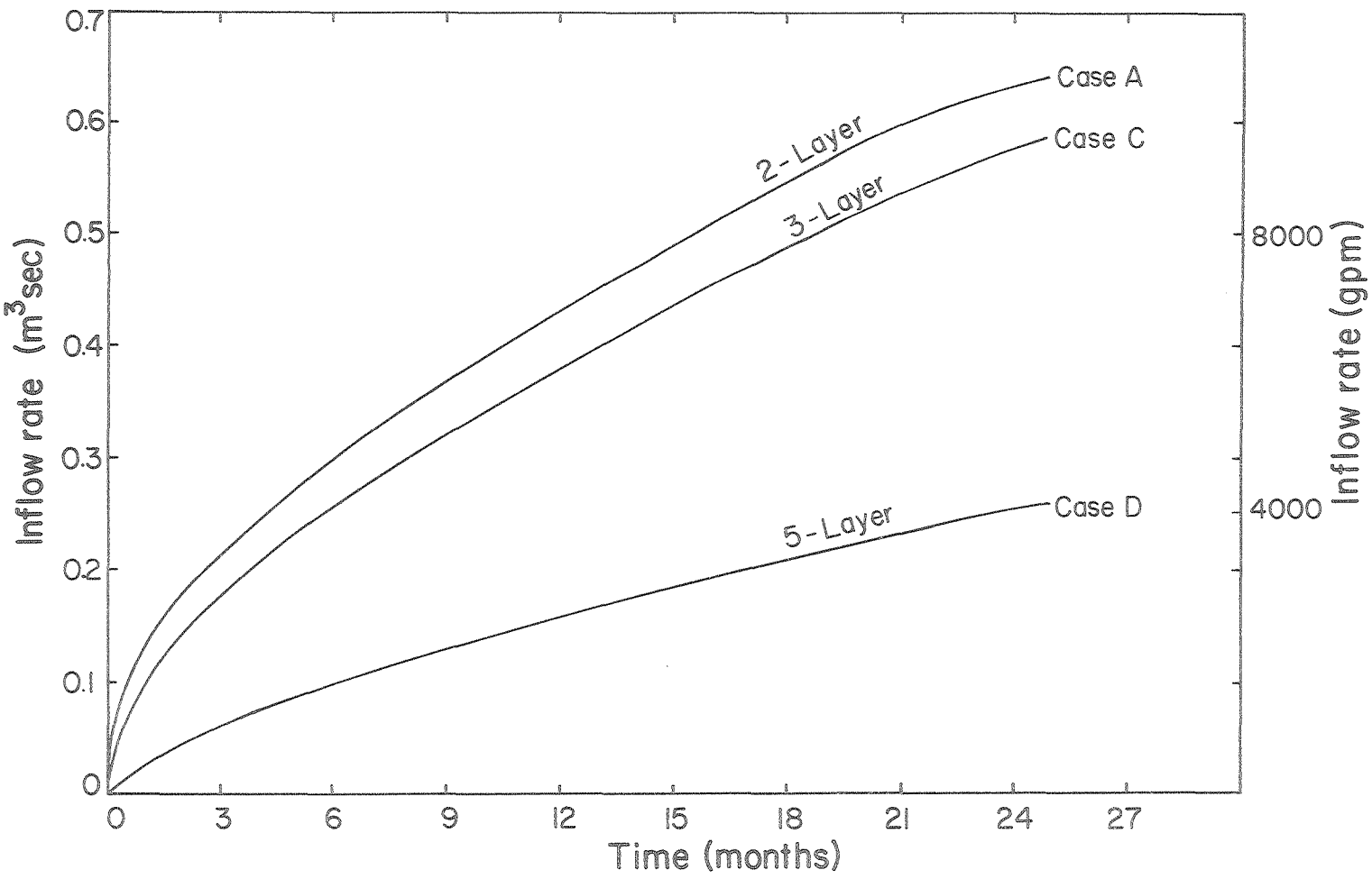

Figure 16. The influence of material distribution on inflow rate. In Case D, the retorted region is protected by a blanket of low permeability material on the top and bottom.

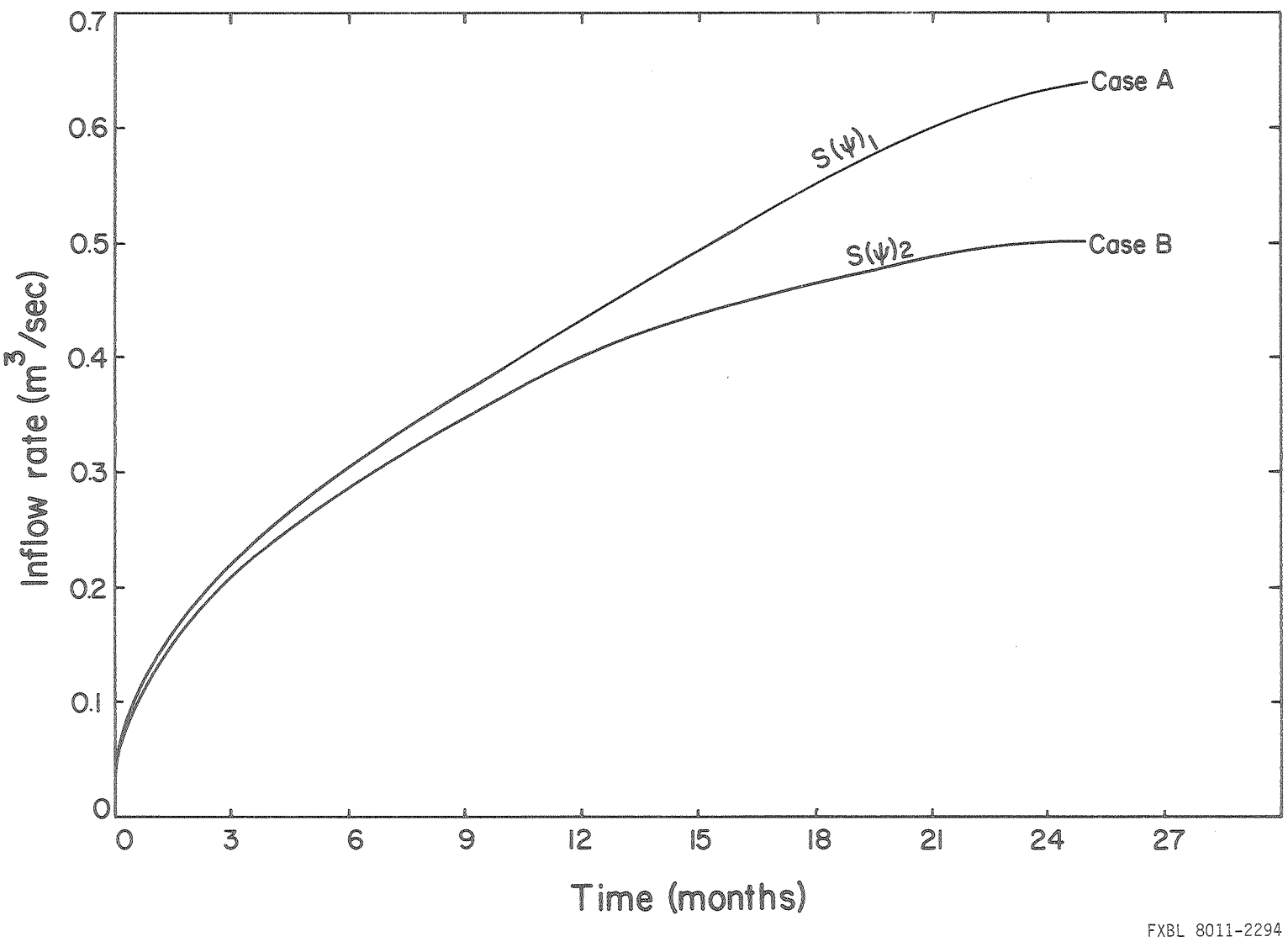

Figure 17. The influence of the saturation-pressure head relationship on inflow rate for a two-layered system.

remains to be explored.

Saturated-Unsaturated Hydraulic Conductivity. The effect of three different permeability-pressure head relationships on saturated and unsaturated hydraulic conductivity is investigated by comparing cases A, E, and F. As shown in Figure 14, $k(\psi)_1$ is 30 to 50 times greater than $k(\psi)_2$ over the entire range of pressure heads under consideration. $k(\psi)_3$ has the same saturated permeability as $k(\psi)_1$ but with lower values in the negative pressure head range.

The inflow rates for these three cases are shown in Figure 18. The difference in flow rate for $k(\psi)_1$ and $k(\psi)_3$ are due to differences in the permeability-pressure head relationship since they both have the same saturated permeability. The comparison between these two also indicates that for a period of about 10 days before the phreatic surface intersects the upper boundary of the retort, they both give the same inflow rate governed by saturated permeability. The large difference between the inflow rates for $k(\psi)_1$ and $k(\psi)_2$ is attributed to the difference in saturated-unsaturated permeability. This indicates the importance of realistic values for the unsaturated hydraulic conductivity.

Porosity. The effect of porosity of the upper aquifer is investigated by comparing cases C, G, and H all of which are three-layered and have the same saturated-unsaturated properties. Since most literature data indicates that the porosity of the confining layer in the lower aquifer is 1%, this parameter was not varied in the sensitivity analysis.

The available data on porosity of the upper aquifer show variations of 1% to 15%. To investigate the effect of porosity of the upper

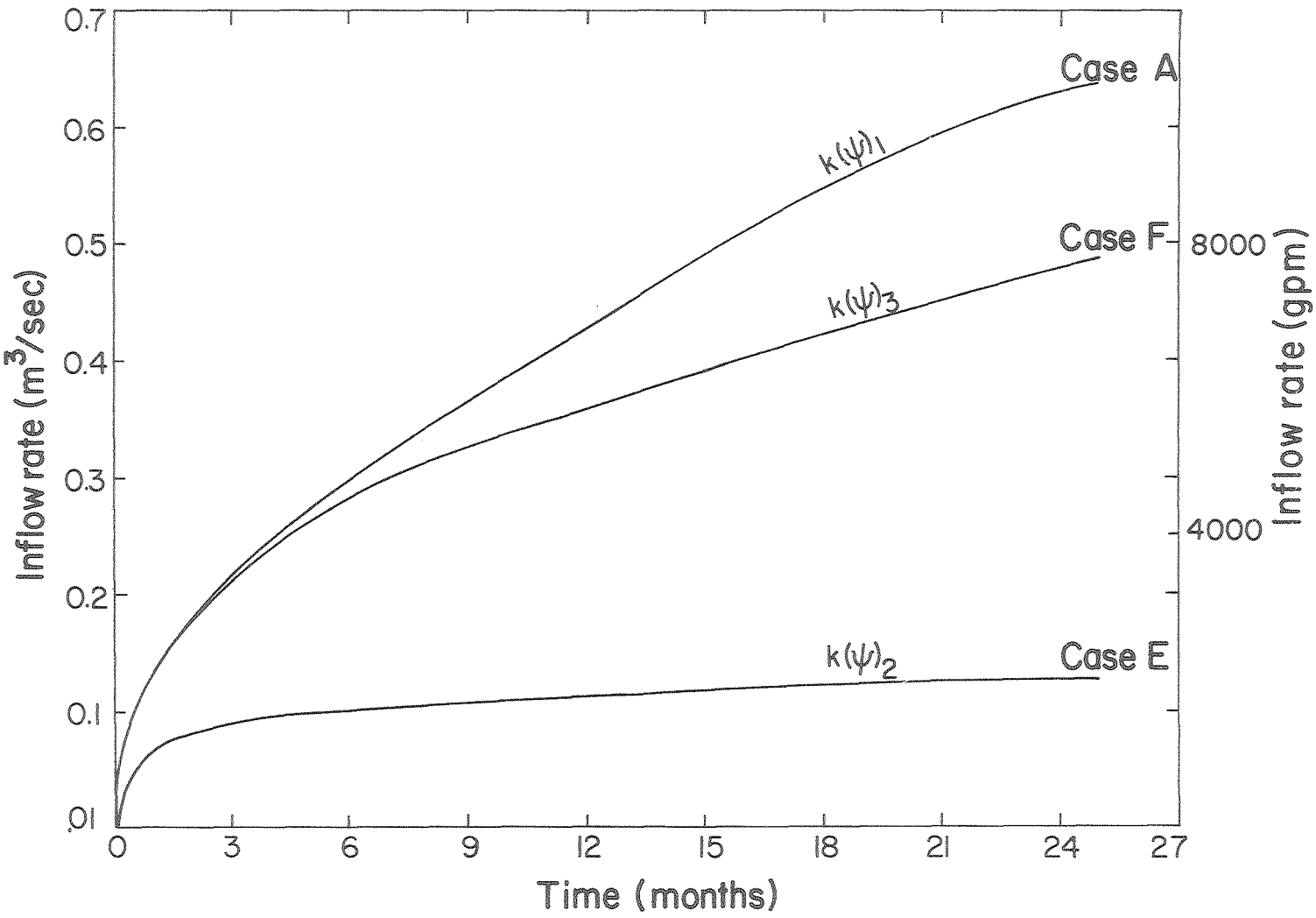

FXBL 8011-2309

Figure 18. The influence of the permeability pressure head relationship of the acquifer on the inflow rate for a two-layered system.

aquifer, porosities of 1% and 10% are assumed here for cases G and H, respectively and they are compared with the previous case C with the porosity of 28%. Other parameters for this analysis are given in Table 5.

The inflow rates for these three cases are shown in Figure 19. It is evident that porosity could have a significant effect on the inflow rate. The rate of increase in inflow rate with time for the low porosity case is much smaller than that of the high porosity case. This is expected because of the pronounced effect of porosity, appearing in the desaturation term ($e\frac{dS}{d\psi}$) of the fluid mass capacity of each volume element. The equal inflow rates for the three cases in the initial stages of dewatering is additional evidence for the effect of desaturation as compared to the fluid compressibility effect (first term of Eq. (2)).

Anisotropy. It is generally well known that sedimentary rocks often exhibit a greater ability to conduct water in the horizontal direction than in the vertical direction. The ratio between the two hydraulic conductivities may be as much as a factor of 100 or more. It stands to reason, therefore, that anisotropy in the vertical plane will have to be given due consideration in the study of dewatering problems. In order to evaluate the importance of anisotropy relative to isotropy, we used the ratios suggested by Robson and Saulnier (1980). The anisotropy ratios used are: upper aquifer, $K_V/K_H = 0.5$; aquitard, $K_V/K_H = 0.002$; lower aquifer, $K_V/K_H = 0.137$. The results of the simulation, presented in Figure 20, indicate that the inflow rate for the isotropic case may be twice as high as that for the anisotropic case.

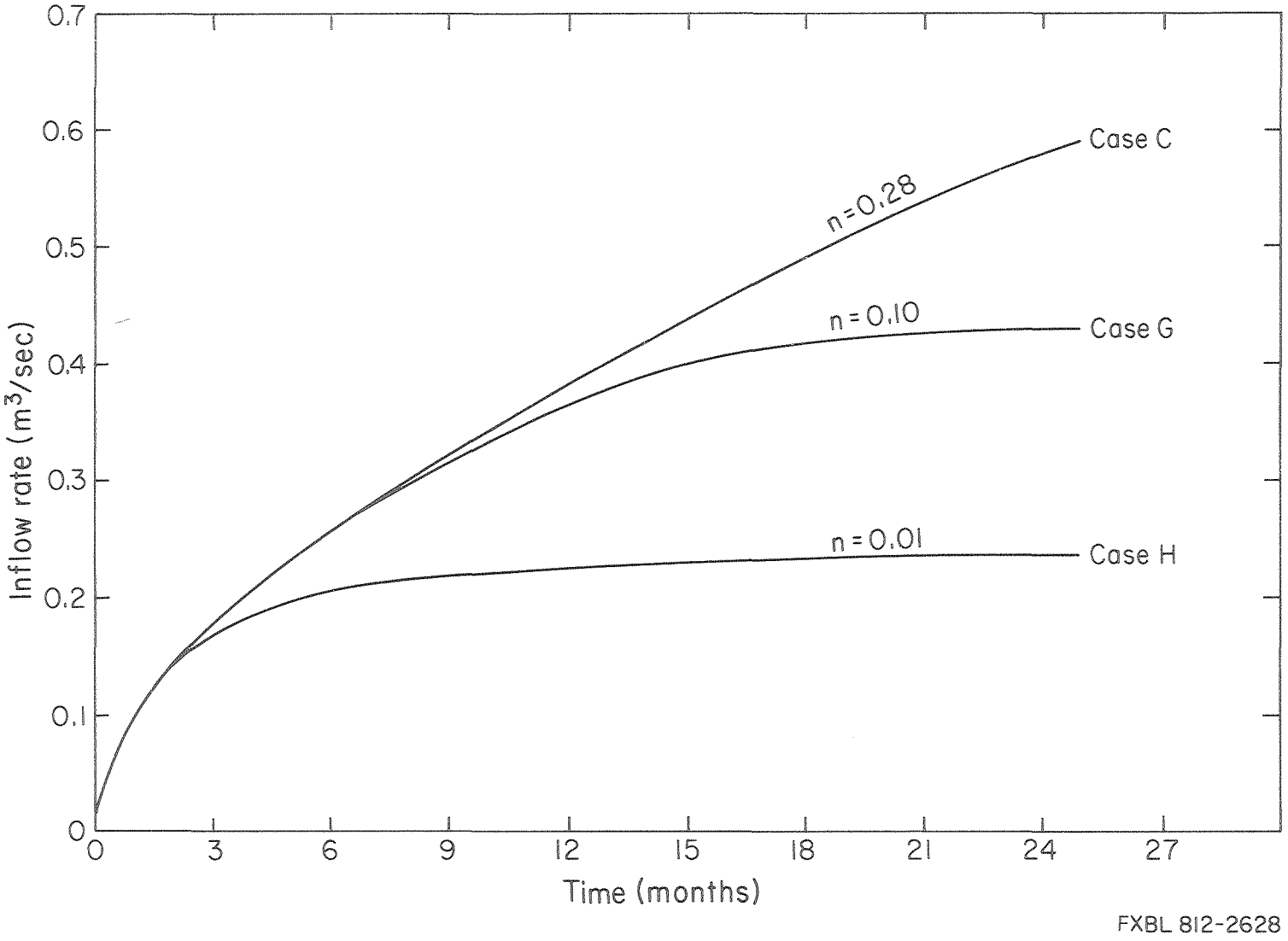

Figure 19. The influence of porosity (n) of the upper aquifer on inflow rate in a three-layered system.

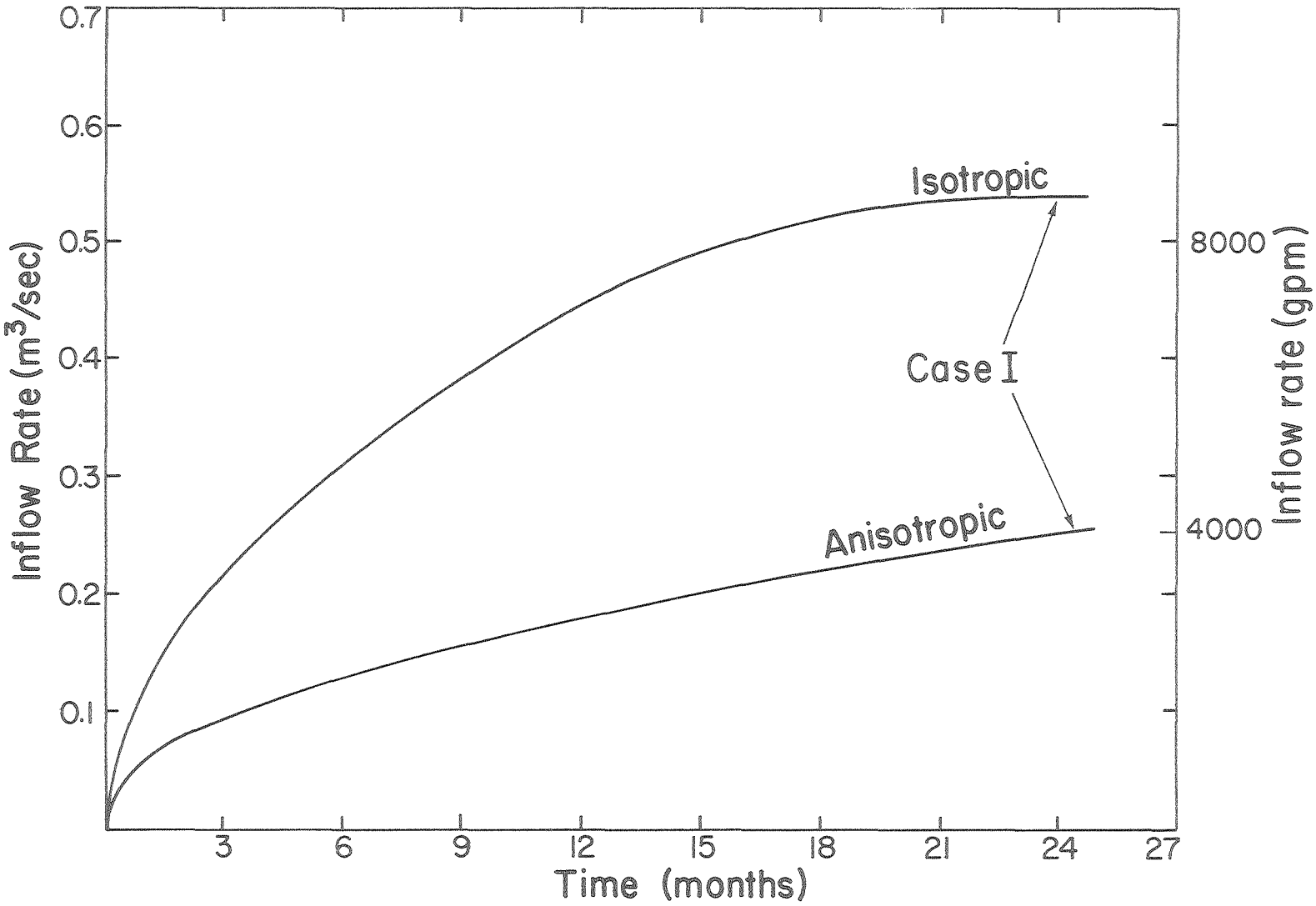

Figure 20. The influence of anisotropy on inflow rate in a three-layered system. $K_v^u/K_h^u = 0.5$; $K_v^c/K_h^c = 0.002$; $K_v^\ell/K_h^\ell = 0.137$.

SUMMARY

A Comparison Between Fixed Geometry And Variable Geometry

In the fixed geometry scenario (used by Weeks et al., 1974; Banks et al., 1978; and Robson and Saulnier, 1980), we assumed that a cavity of a given size is subject to flow across its boundaries at time zero under an initial head of 690 m (2260 ft). This creates extremely high gradients at the interface of the cavity and the flow region resulting in high initial inflow rates. This result is reflected in Figure 15 which shows very high inflow rates which rapidly decrease with time. This behavior is in contrast with that observed in the expanding retort scenarios where the inflow rates increase gradually as the size of the cavity grows in time. Therefore, analysis of flow in an expanding cavity by approximating fixed geometry is unrealistic, and the results can be misleading, particularly in the initial stages of dewatering.

Parametric Studies

The results of the parametric studies in terms of inflow rates after two years of dewatering are summarized in Table 6. Material distribution plays a significant role in controlling flow into the mine. In view of comments by Smith (1980), the results show that the existence of a blanket around the retorted region could drastically reduce inflow, providing more favorable conditions for retorting. For a better comparison between various cases, the results are shown in Figure 21. In general, lower residual saturations, higher permeabilities, and higher porosities tend to increase the inflow. In comparing cases A and E, it is evident that the increase in total flow rate into the mine at tract C-b is proportional to the increase in saturated-unsaturated permeability of the upper aquifer, indicating the impact of the unsaturated properties of the upper aquifer on the total mine inflow. The difference

Table 6. Summary of inflow rates from the parametric studies after after two years of dewatering for C-b tract.

Property	Case	Inflow Rate m^3/sec	Comments	
Material Distribution	A	0.63	2-layer case	
	C	0.57	3-layer case	
	D	0.26	5-layer case	
Saturation-Pressure Head	A	0.63	$S(\psi)_1$	Figs. 13, 17
	B	0.50	$S(\psi)_2$	
Permeability-Pressure Head	A	0.63	$k(\psi)_1$	
	F	0.47	$k(\psi)_3$	Figs. 14, 18
	E	0.12	$k(\psi)_2$	
Porosity	C	0.57	28% Porosity	
	G	0.43	10% Porosity	
	H	0.24	1% Porosity	
Anisotropy	I_1	0.54	Isotropic	Fig. 20
	I_2	0.25	Anisotropic	

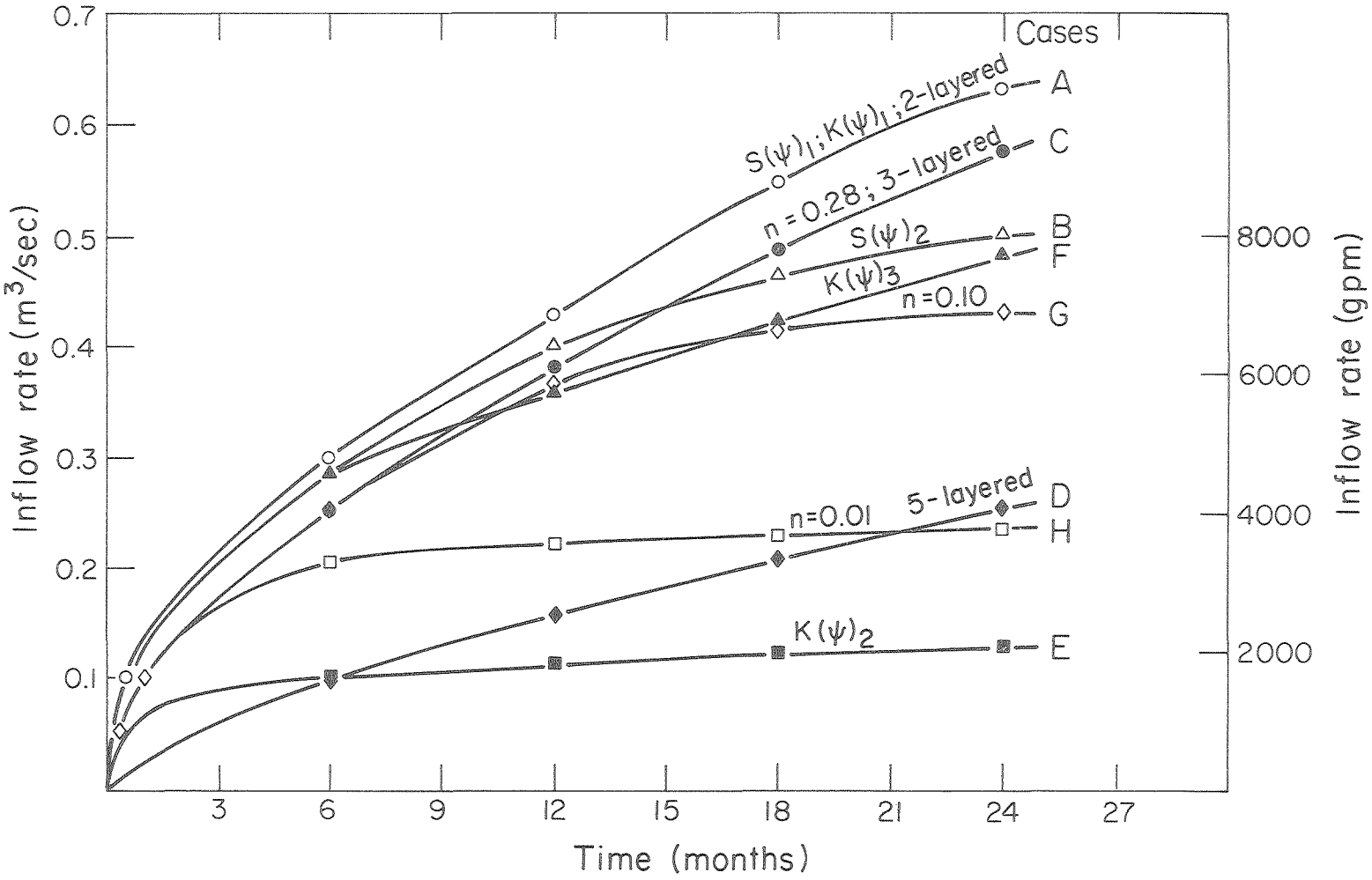

Figure 21. Inflow rate as a function of time for various cases considered in the parametric studies.

in inflow rates between cases A and F is due only to the difference in $k-\psi$ relationship in the unsaturated state ($\psi<0$) because they both have the same saturated permeability (Figure 14). In cases G and H, it is shown that an increase in porosity of the upper aquifer from 0.01 to 0.10 causes an 80% increase in inflow rate. The overall results indicate that, assuming proper conceptualization of the system with regard to material distribution, directional permeability and porosity are the key parameters that control mine inflows.

LONG-TERM SIMULATIONS OF DEWATERING

For purposes of understanding possible long-term consequences of MIS retorting, 30- and 60-year simulations were carried out for the C-a and C-b tracts respectively for the expanding retort scenario. The properties of the aquifer system used for these simulations are given in Table 7. The saturated hydraulic conductivities of the upper and lower aquifers are the same as those used by Tipton and Kalmbach, Inc. (1977), and they are within the range of values used by Robson and Saulnier (1980) and Golder Associates (1977). The porosities given in Table 7 are the total porosities.

The results of the sensitivity analysis presented earlier were based on assumed relationships for $S-\psi$ and $k-\psi$. In long-term simulations, we have reduced the number of assumptions by one, namely, the $S-\psi$ relationship shown in Figure 22. The unsaturated hydraulic conductivity is computed from the Millington-Quirk (1959, 1961) formula as follows:

$$K(\theta)_i = \frac{\rho_w g}{8\mu} \frac{\theta^p}{n^2} \sum_{j=1}^{n} (2j + 1 - 2i) r_j^2 \qquad (7)$$

where $r_1, \ldots, r_n$ are the radii of pores corresponding to n pore classes, θ is volumetric water content, and $K(\theta)_i$ denotes the hydraulic conduc-

Table 7. Properties used for long-term dewatering simulations.

Property	Upper Aquifer	Confining Layer	Lower Aquifer
Saturated Permeability (m^2)	7.64×10^{-14}[a]	2.00×10^{-15}	2.45×10^{-14}[a]
Storage Coefficient	--	--	1×10^{-4}
Coefficient of Compressibility ($Pascal^{-1}$)	1×10^{-9}	1×10^{-9}	--
Porosity	0.15	0.01	0.01
Residual Saturation	0.20	0.20	--

[a]Based on Tipton and Kalmbach, Inc. (1977).

tivity at a water content for which the pore classes with radii r_i, $r_{i+1}, \ldots, r_n$ are water filled. The Millington-Quirk formula is derived from Poiseuille's equation for flow through a narrow tube of radius r. Using the capillary equation corresponding the pressure head to the pore radius,

$$r = \frac{2\gamma_w}{\rho_w g \psi} \tag{8}$$

the Millington-Quirk formula can be written as:

$$K(\theta)_i = \frac{\gamma_w^2}{2\rho_w g \mu} \frac{\theta^p}{n^2} \sum_{j=1}^{2} (2j + 1 - 2i)/\psi j \tag{9}$$

Using the saturation-pressure head relation given in Figure 22, the unsaturated hydraulic conductivity is computed from the above equation and shown in terms of intrinsic permeability in Figure 23.

To avoid boundary effects, the modeled zone extends radially to a distance of 25 km (16 mi) from the center of the tracts. It is assumed that no other sink exists in the modeled zone. The rates of expansion of the mines are given in Figures 7 and 8 for the C-a and the C-b tracts, respectively. In this analysis, recharge is based on the values and the pattern given by Weeks et al (1974) as shown in Figure 24.

In the present investigation, the actual modeling of the interaction of Yellow Creek and Piceance Creek with ground water has not been carried out. Instead we have analyzed the cone of pressure depression caused by the process of dewatering indicating possible hydrologic consequences to the surrounding surface water bodies.

The C-a Tract

In the dewatering simulations of the C-a tract for the Commercial Phase of the project, it is assumed that the thickness of the retort interval is 229 m (750 ft) extending from the top of the Mahogany Zone to

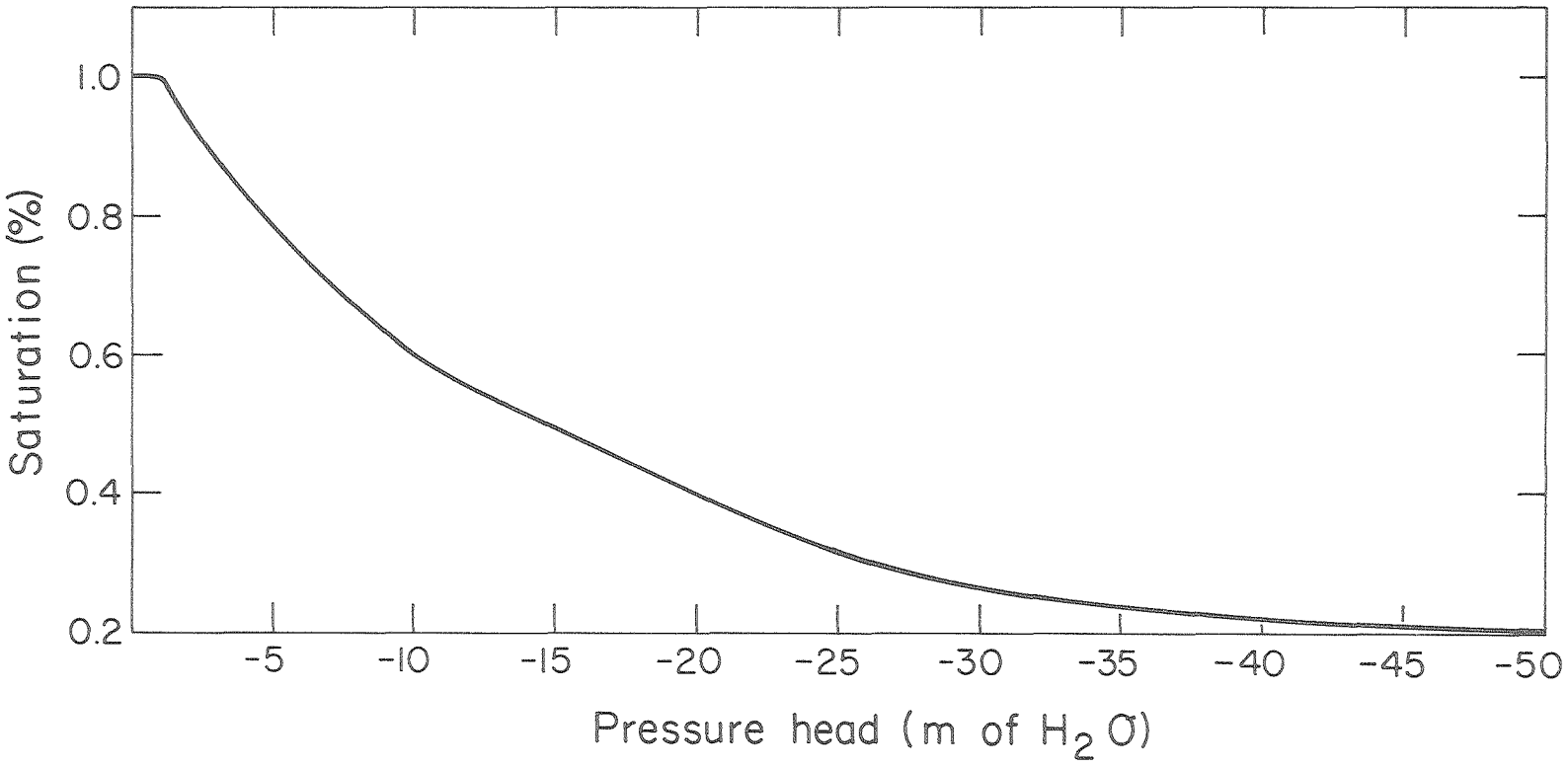

Figure 22. Saturation-pressure head relationship for the unsaturated zone used for long-term simulations of dewatering and reinvasion.

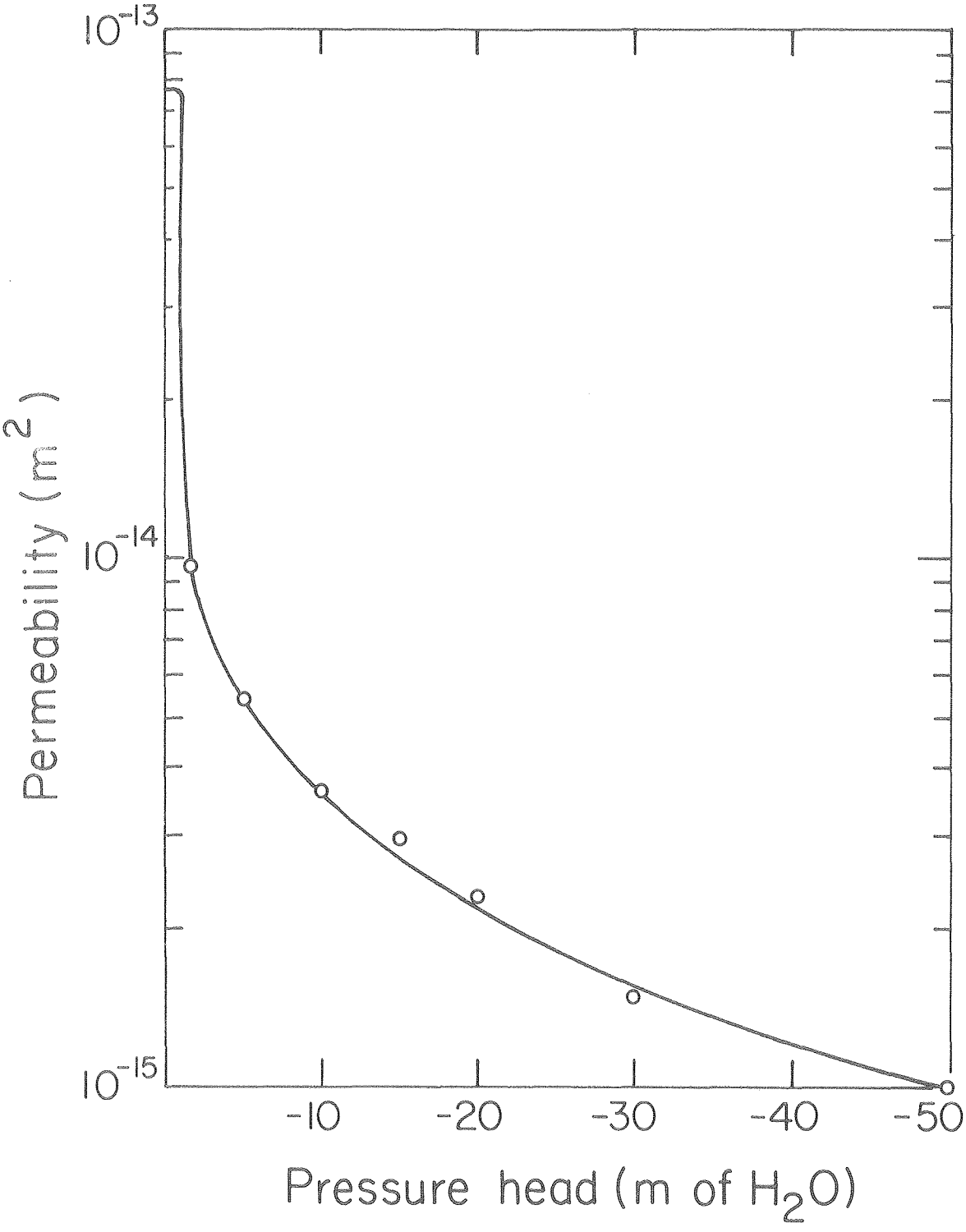

FXBL8011 - 2313

Figure 23. Variation of intrinsic permeability with pressure head computed from Millington-Quirk formula.

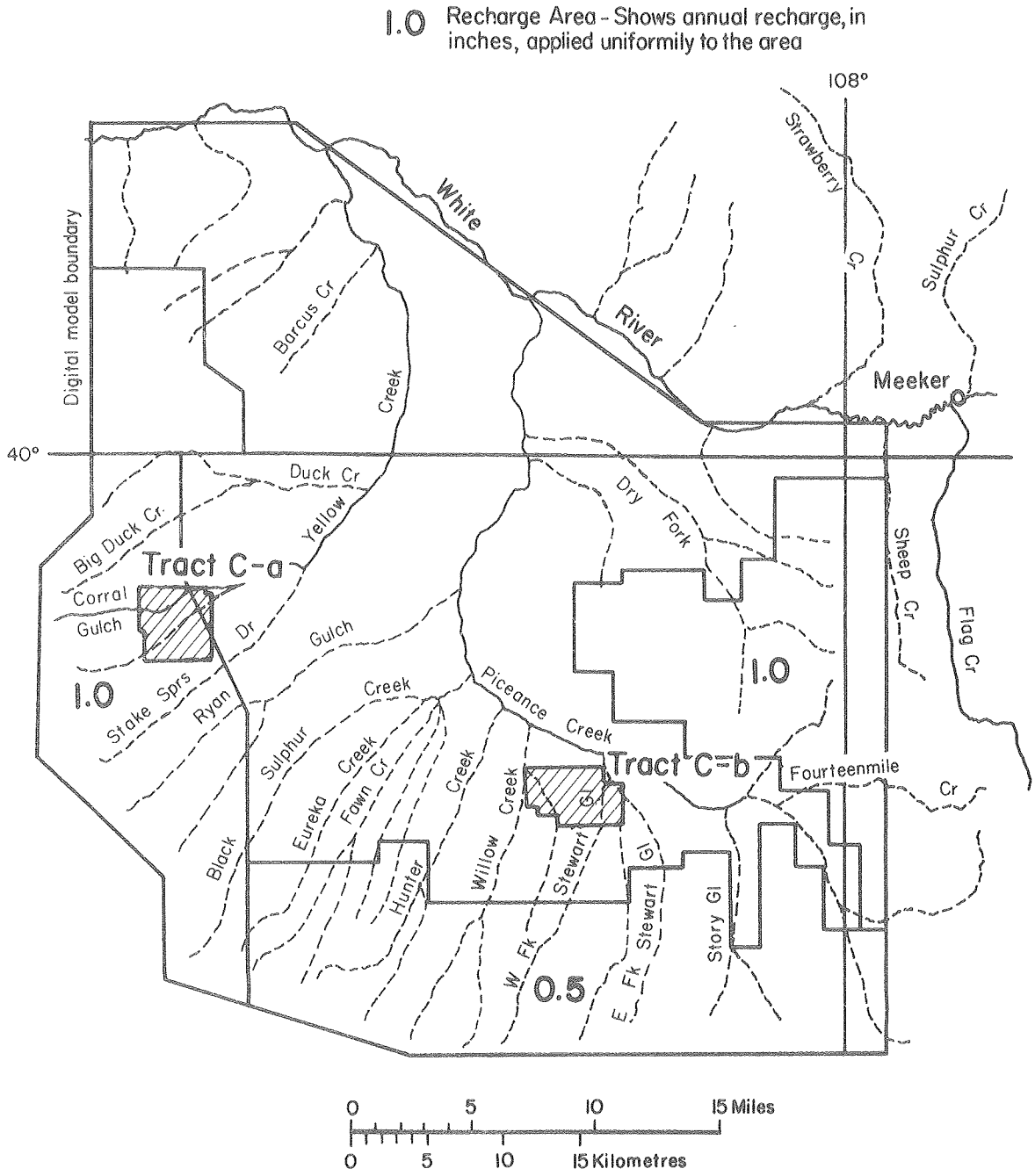

Figure 24. The pattern and intensity of recharge in the Piceance Basin (after Weeks et al., 1974).

the bottom of the R-4 layer as shown in Figure 4. The variation of inflow rates for a 30-year simulation of dewatering is shown in Figure 25 using two different saturated permeabilities for the lower aquifer. The smaller inflow rate, which corresponds to hydraulic properties given in Table 7, reaches a value of 0.15 m^3/sec (2300 gpm) at the end of 30 years. The transmissivity of the lower aquifer is 1.23 m^2/d (99 gpd/ft). The larger inflow rate (1.38 m^3/sec or 21,800 gpm) corresponds to the case where the transmissivity of the lower aquifer is assumed to be 87 m^2/day (7000 gpd/ft) (Rio Blanco, 1977). The inflow rate in this case is about 10 times the previous case, indicating that the lower aquifer plays a significant role in the dewatering operation at the C-a tract. This behavior is expected because the thickness of the upper aquifer is very small, and the aquitard constitutes a large portion of the overall aquifer system. It is clear that since the contribution of the upper aquifer to the total inflow into the mine is small, the effect of porosity and unsaturated properties of the upper aquifer on flow rates would also be less significant. At the C-b tract, on the other hand, the situation will be different due to the larger thickness of the upper aquifer.

According to Rio Blanco (1977), water use on the C-a tract during the commercial phase will be 0.0875 m^3/sec (1400 gpm). The results of this study show that even the lowest estimates of lower aquifer permeability can furnish more than the required water for consumption.

The position of the phreatic surface at various times along with the advancement of the retorted area are shown in Figure 26. It is evident that, due to the small thickness of the upper aquifer, the water table profiles move with a rate at which the upper aquifer above the

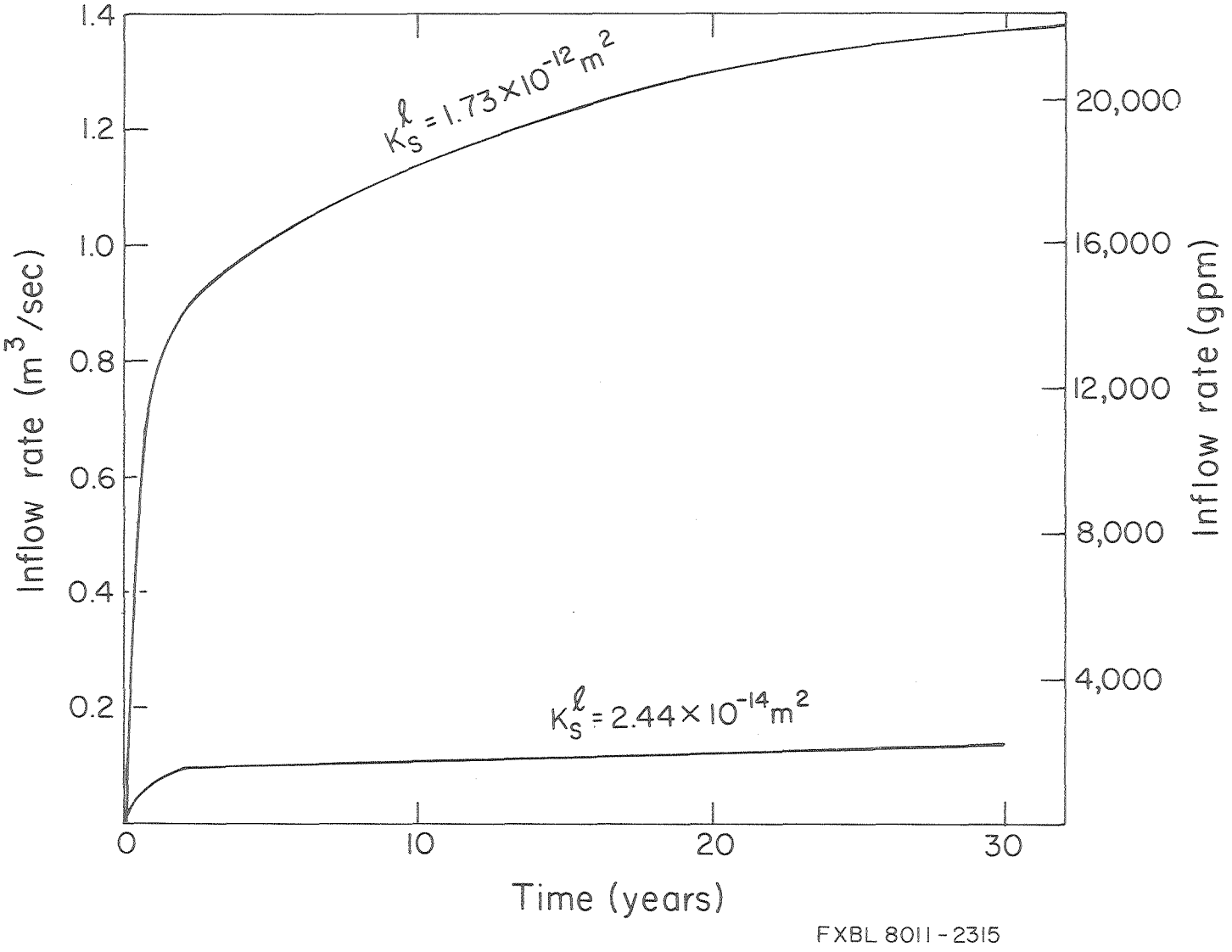

Figure 25. Variations of inflow rates with time over the C-a tract for two permeabilities for the lower aquifer.

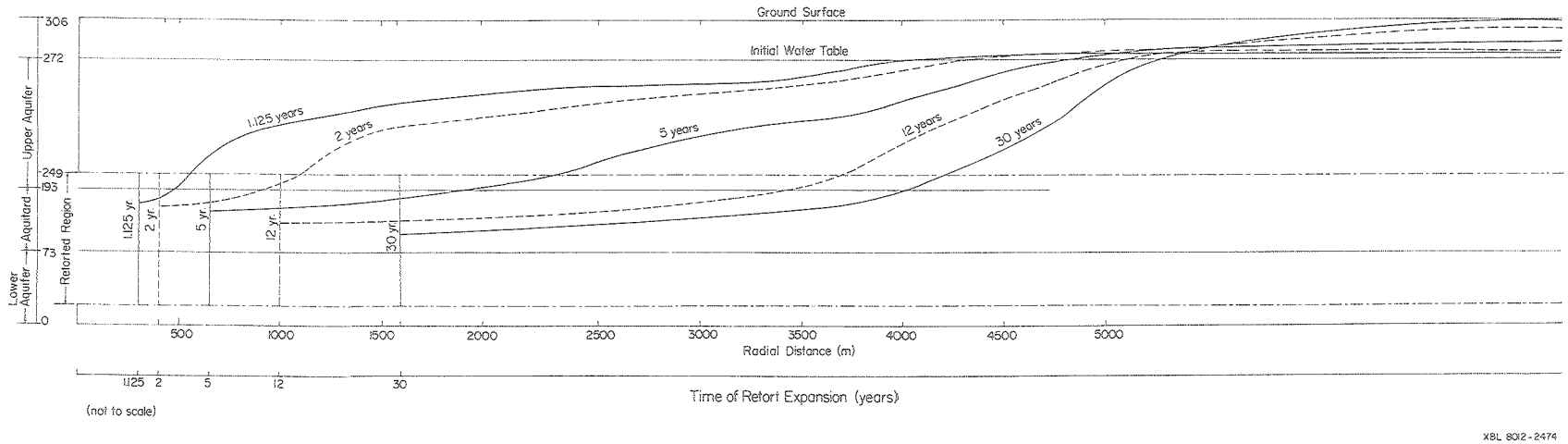

Figure 26. The position of the phreatic surface for dewatering the C-a tract in an expanding retort scenario. (Note: Figure not to scale.)

caved region becomes unsaturated. This implies that inflow from the upper aquifer into the mine may be reduced sufficiently to allow the retorting process to take place probably at higher efficiencies.

The fluctuation of the water table at a radial distance of 5 km (3.1 mi) from the center of the tract (approximate location of waters tributary to Yellow Creek) for the high permeability case is shown in Figure 27. The water table initially rises because of the effect of recharge up to about 15 months after which the influence of dewatering becomes dominant. The maximum drawdown of the phreatic surface after 30 years of dewatering is estimated to be 31 m (100 ft).

The C-b Tract

The variation of inflow rate for the 60-year life of the project at the C-b tract is shown in Figure 28. The expansion of the mine is the primary reason for continuous but gradual increase in mine inflow rate which peaks at 0.9 m^3/sec (about 14,200 gpm). Assuming a production level of 50,000 barrels per day and a maximum water consumption of 6.6 barrels per barrel of oil (Fox, 1981), 0.62 m^3/sec (9800 gpm) of pumped water will be used. Therefore, the balance is excess water at the site and could either be reinjected into the ground, used for stream flow augmentation, used by another oil shale mine or disposed of as waste. Considering the large drawdowns of the water table in the vicinity of the Piceance Creek, the options of reinjection or stream flow augmentation appear most likely. In our analysis, it is assumed that there is no interference from any other mining activity causing dewatering of the modeled area.

The results show that large quantities of water must be pumped to the surface which will require large quantities of energy. Assuming an

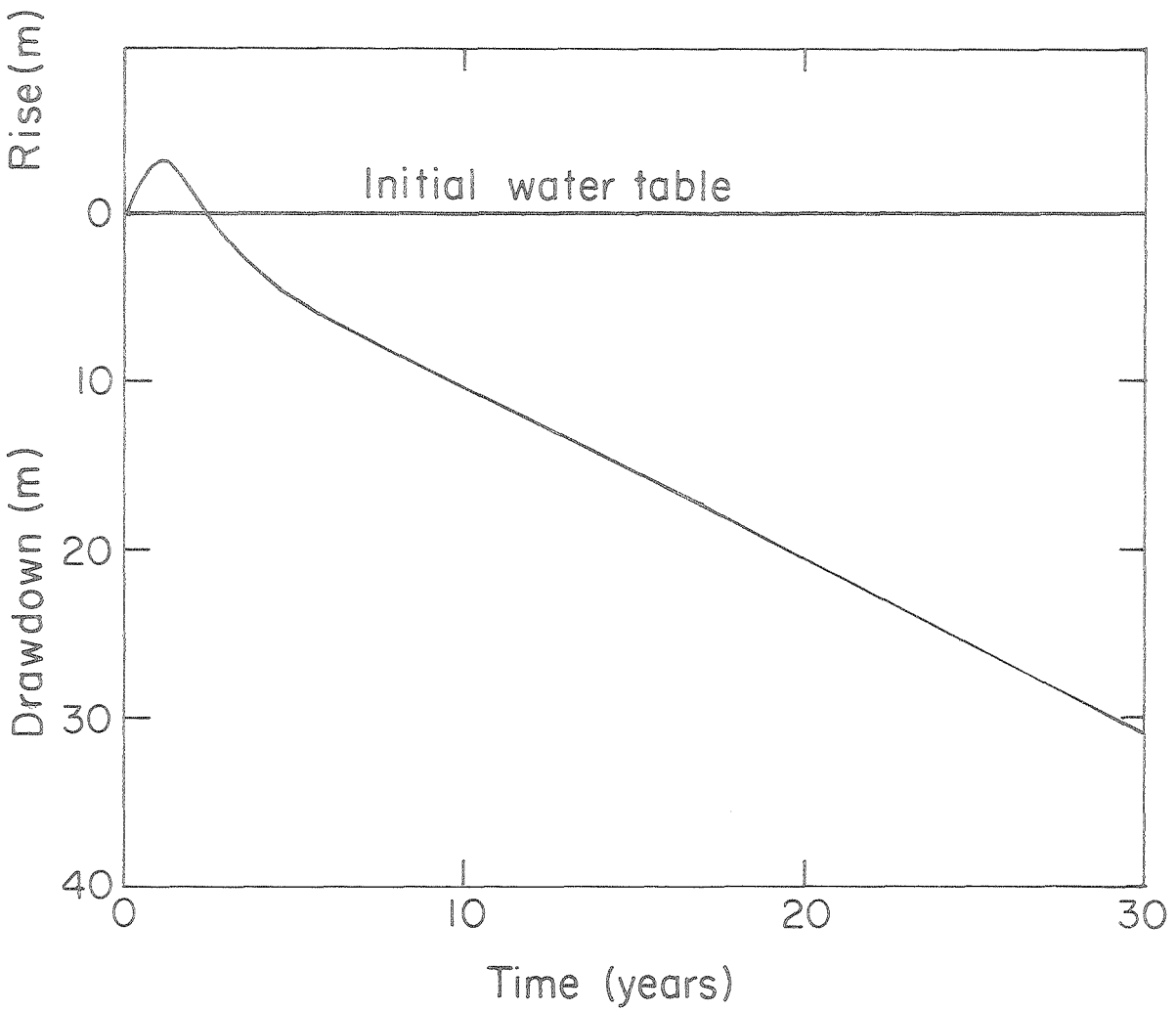

Figure 27. Water table fluctuations at a radial distance of 5 km from the center of the C-a tract.

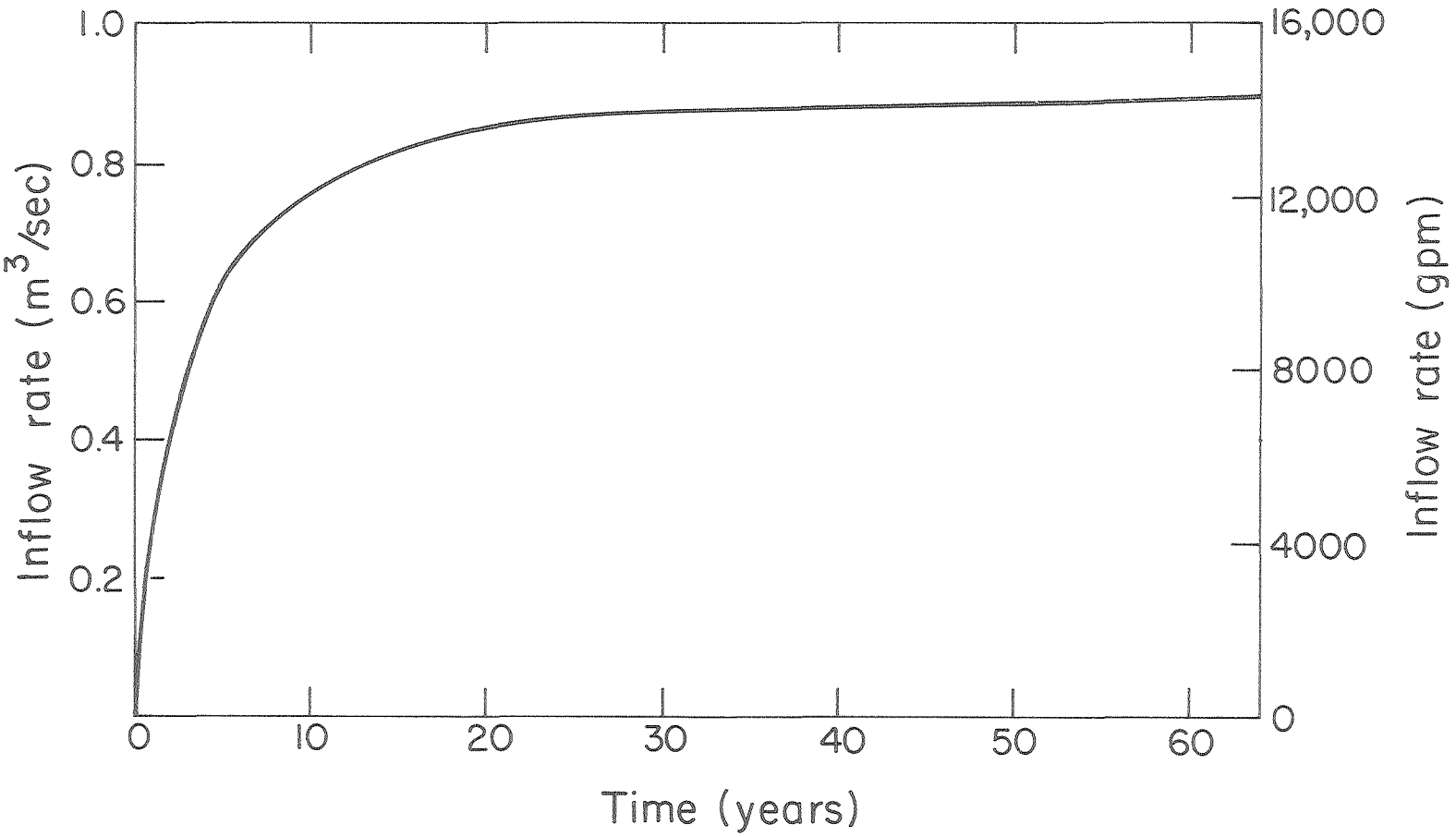

FXBL 8011-2319

Figure 28. The 60-year simulation of dewatering for the C-b tract.

approximate pumping rate of 1 m^3/sec (15,800 gpm) from a depth of 400 m (1300 ft), the power requirements at 50% efficiency will be about 8 MW.

As desaturation proceeds, the phreatic surface becomes dynamic and moves downward as shown in Figure 29. The position of the periphery of the retorted region and corresponding position of the phreatic surface are shown in this figure as a function of time. This figure demonstrates that at the C-b tract, the tail of the phreatic surface intersecting the roof of the retort lags the front of the mined region. This perhaps can give an indication of the proper timing for the retorting process. This means that the actual retorting process can be delayed until the phreatic surface reaches the expected periphery of the caved region causing a considerable reduction in retort inflow rate. The primary reason for the difference between the location of the phreatic surface relative to the position of the front of the caved region for the C-a and C-b tracts is the thickness of the overburden above the excavated region which is about 10 times greater at the C-b tract.

The model results show that the contribution of the unsaturated region of the upper aquifer to the overall inflow into the mine is substantial at the C-b tract primarily because of the large thickness of the upper aquifer.

Figure 29 also demonstrates the effect of dewatering at distances away from the center of the tract. The drawdown of the phreatic surface at 3.5 km (2.2 mi) from the center of the tract which is the approximate location of the Piceance Creek, is shown in Figure 30. Our computations indicate that the phreatic surface could be lowered by as much as 100 m (330 ft) or more after 60 years of dewatering. This suggests that water may be lost from the Piceance Creek and its tributaries and that flow

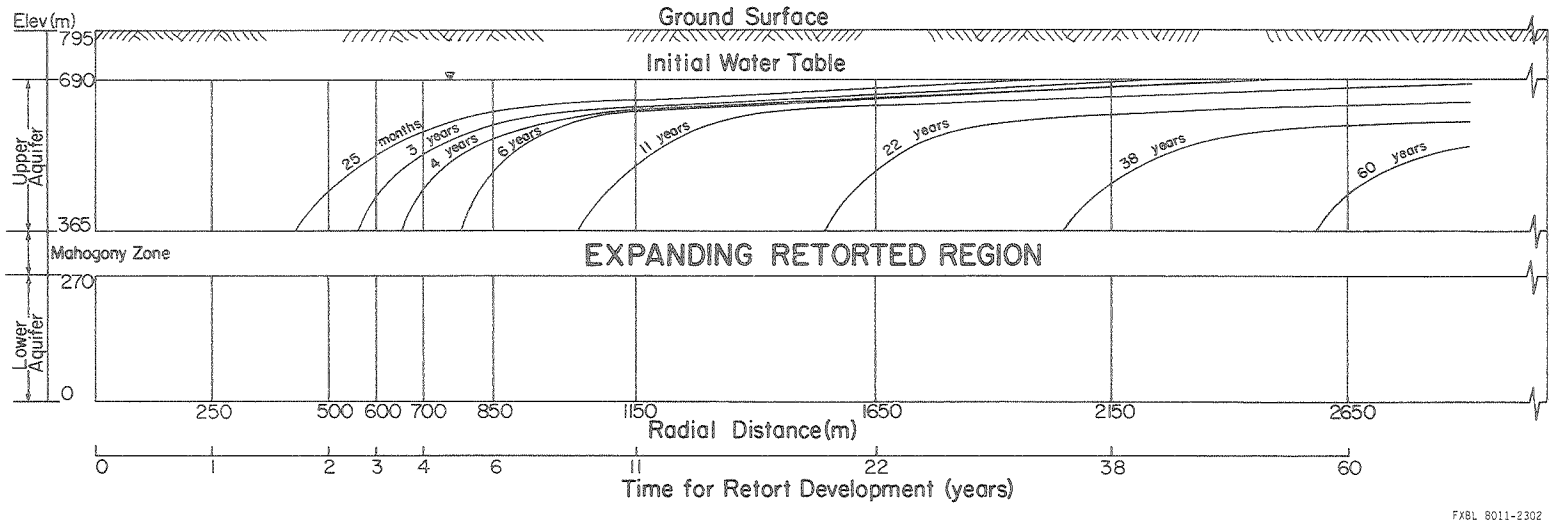

Figure 29. The position of the phreatic surface for dewatering the C-b tract in an expanding retort scenario.

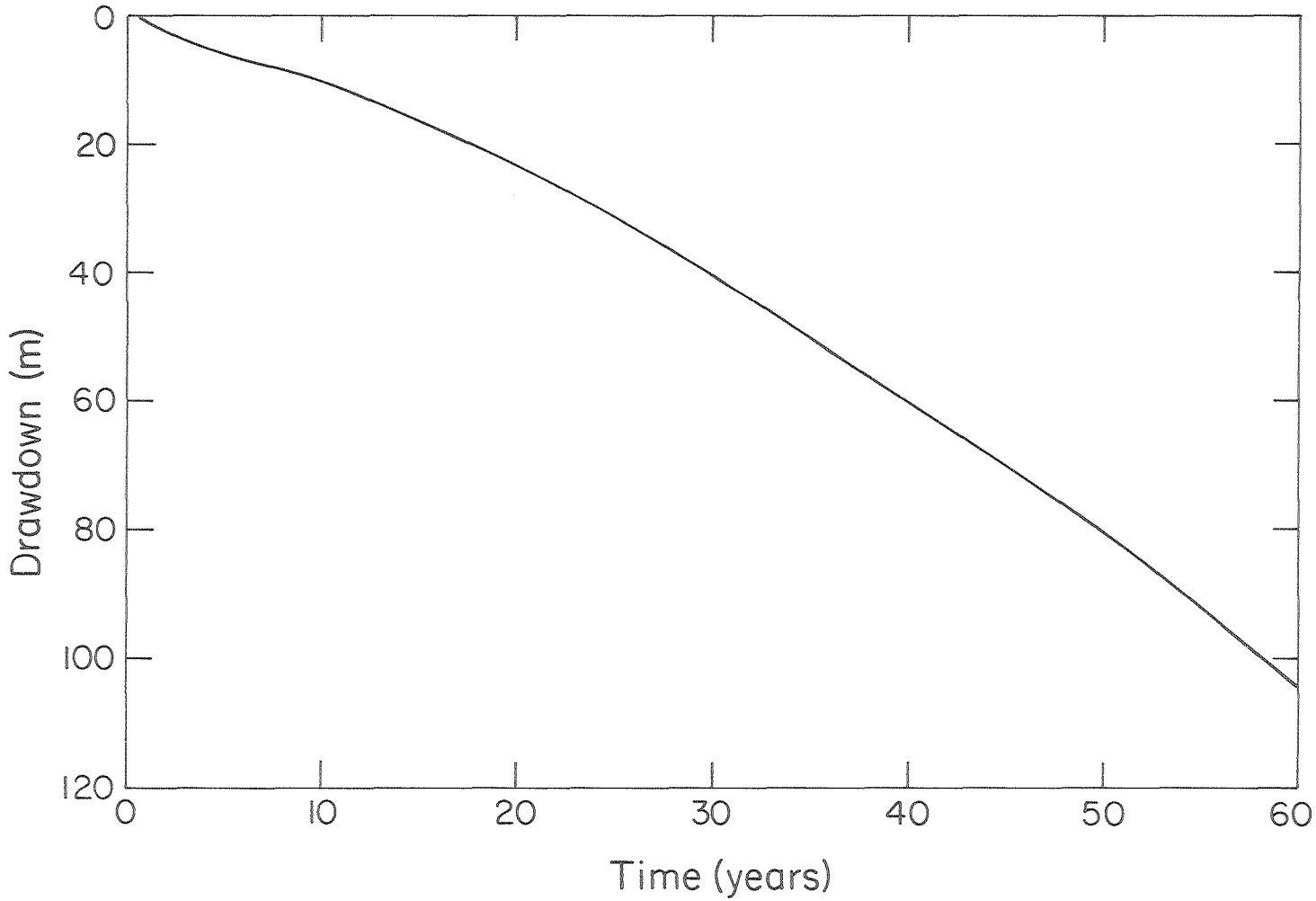

FXBL 8011—2314

Figure 30. Drawdown of the phreatic surface for the 60-year simulation of dewatering at a radial distance of 3.5 (2.2 mi) km from the center of the C-b tract.

from local wells may be reduced. Additional work is required to quantify the effect of drawdown on stream and well flow. The estimates of drawdown by Tipton and Kalmbach, Inc. (1977) at the end of 60 years is less than 60 m (200 ft) at a distance of 3 km (2.2 mi) from the center of the tract.

Estimation of Inflow into Retorts and Implications for Combustion

The model results of the 60-year simulation of dewatering at the C-b tract indicate that about 44% of total inflow into the mine passes through the roof of the excavated region and 53% through the floor. The remaining 3%, the inflow which intersects the periphery of the retorted region, is governed by low permeability of the confining layer. The results also demonstrate that as we approach the center of the retorted area, the inflow rate into the mine decreases at a rapid rate. The distribution of total head in the upper most layer of the lower aquifer and lower most layer of the upper aquifer surrounding the retorted region is shown in Figure 31. It is evident that in the vicinity of the newly retorted region, the induced gradients are very high, causing large contributions of flow into the mine. The distribution of the total head in the system (Figure 32) also indicates that most inflow takes place in the vicinity of the periphery of the retorted region through the top and the bottom of the upper and lower aquifers. In other words, in an expanding mine, inflow gets concentrated in the newly excavated region where potential gradients are highest. Thus, after 60 years, two regions of near stagnation exist away from the periphery towards the axis, one above the roof and the other below the floor of the mine as shown in Figure 33.

For mining and retorting purposes, it would be useful to know ap-

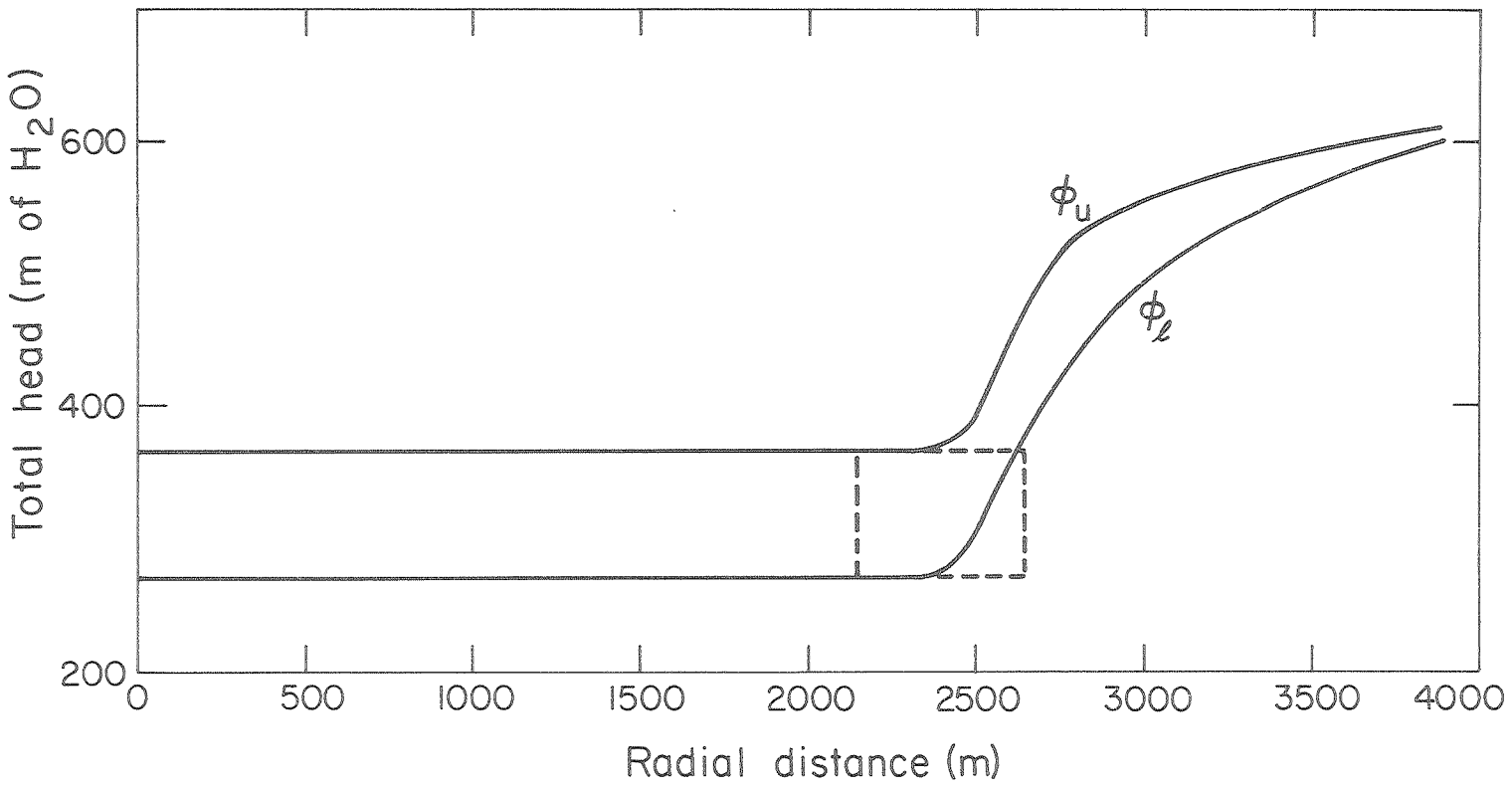

FXBL 8011-2317

Figure 31. Variation of total head with radial distance from the center of the retort in the uppermost layer of the lower aquifer (ϕ_ℓ) and the lower most layer of the upper aquifer (ϕ_u) surrounding the retorted region after 60 years.

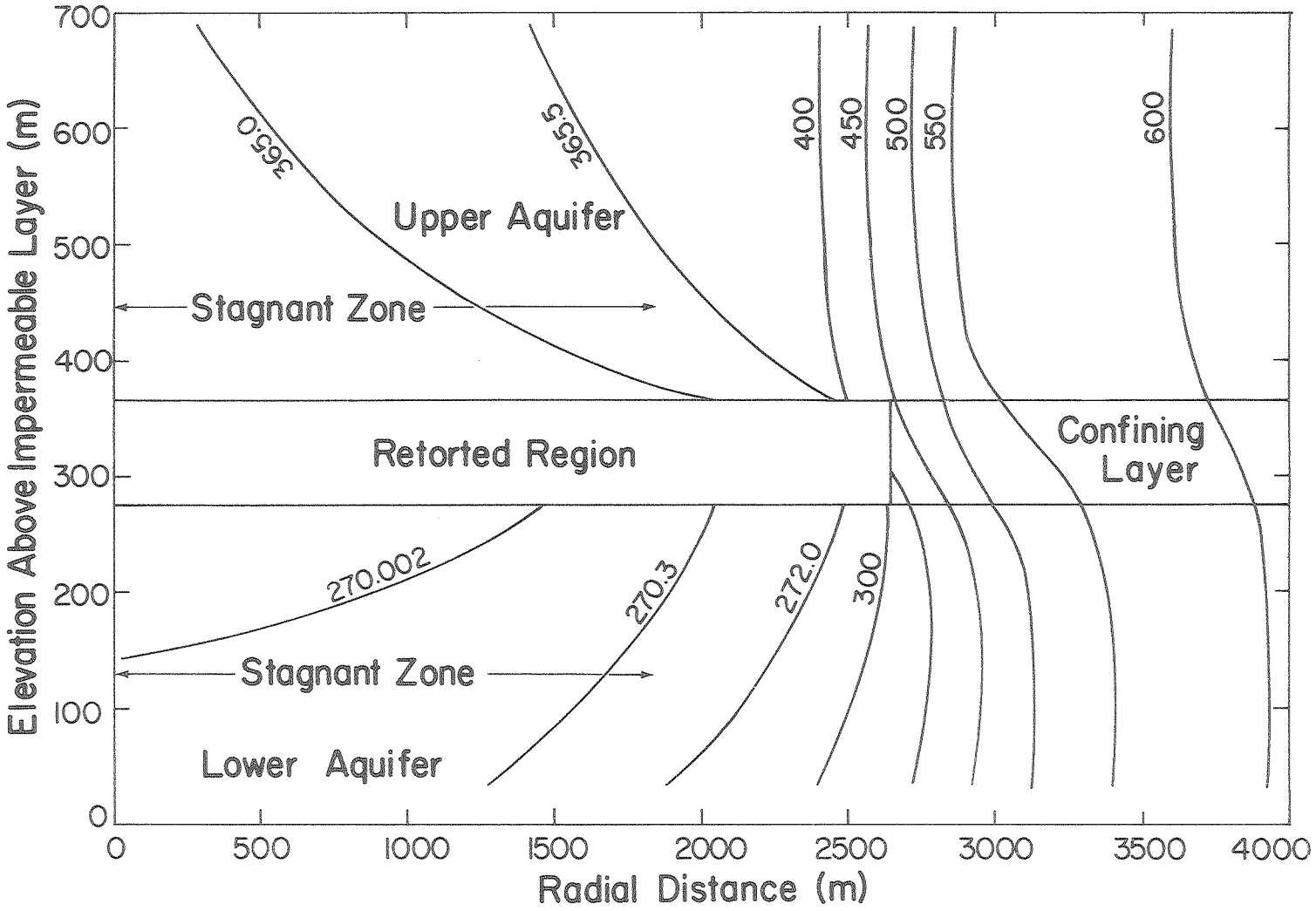

Figure 32. Distribution of total potential in the C-b tract after 60 years of dewatering. Contour interval is not uniform.

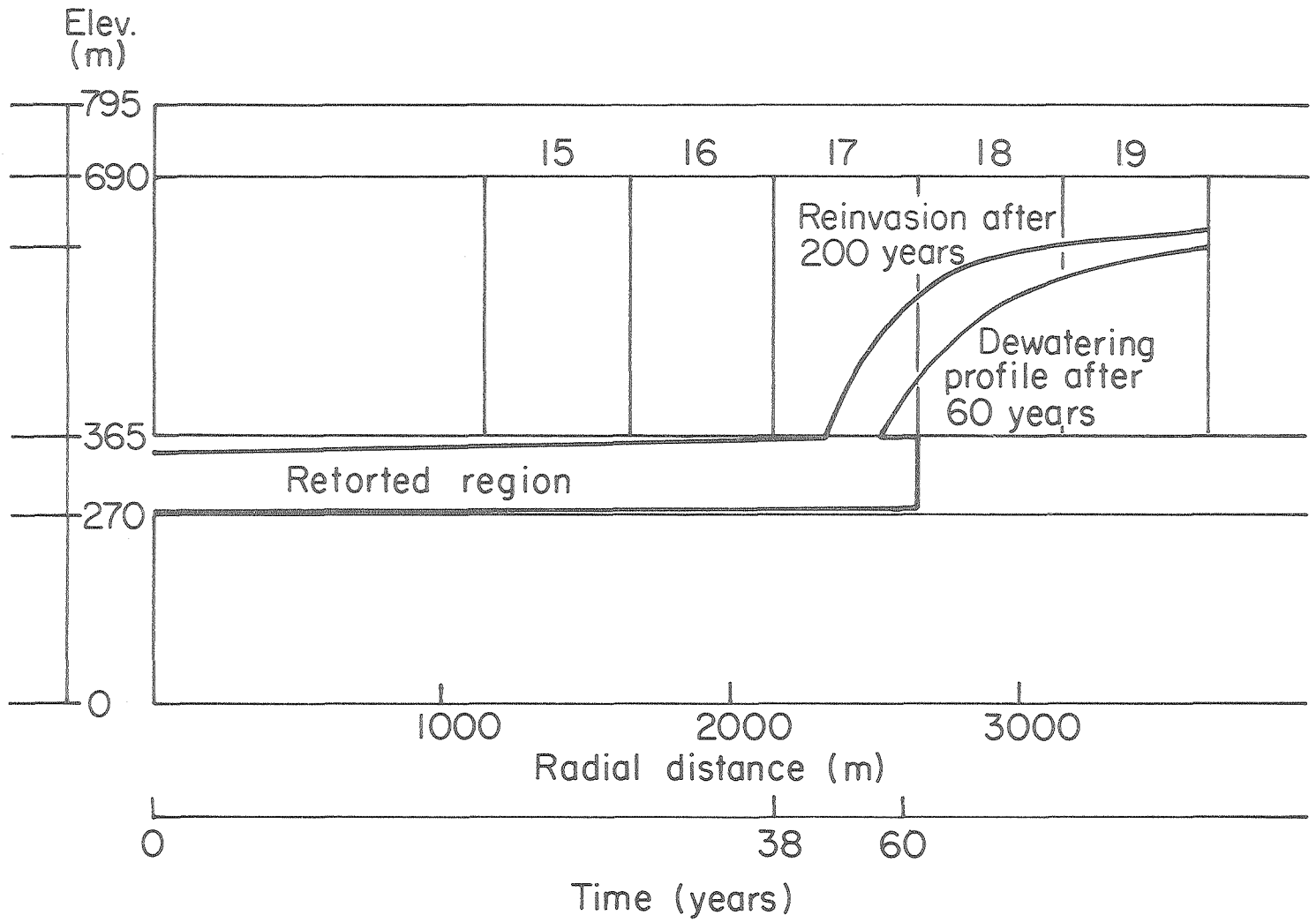

FXBL 8011 – 2320

Figure 33. The profile of phreatic surface after 200 yeras of reinvasion in the C-b tract.

proximately what fluxes (inflow rate per unit cross-sectional area of flow) exist at the surfaces of the newly excavated regions. This would provide some insight with regard to the expected combustion efficiency as a result of mine inflow.

The results obtained for the C-a and C-b tracts show that although the inflow rate increases with time as the retorted region expands, the flux decreases, since in an axisymmetric system, areas expand geometrically with increasing radius. Knowing the inflow rate into the newly excavated region, the flux has been computed and shown in Table 8 for certain selected times at the C-a and C-b tracts.

Recent work by Braun et al. (1980) indicates that the acceptable inflow rate into a retort to sustain combustion efficiency varies depending on the uniformity of flow, richness of the oil shale, steam-air mixture, and other factors. Assuming a uniform water flow into the Zero Retort currently being studied at the C-a tract and assuming a steam-air mixture of 30% and 70%, respectively, a total inflow rate of 1.9×10^{-4} m^3/sec (3 gpm) over the entire retort having plan dimensions of 9.1 m x 9.1 m (30 ft x 30 ft) appears to be acceptable. According to Table 8, during the early periods of the project, one might expect total inflows of 0.47×10^{-4} m^3/sec (0.75 gpm). The inflow rate will decrease with time toward the end of the project as fluxes gradually decrease. The flow rate for the commercial-size retorts in the early stages of dewatering will be higher since the plan area is larger.

At the C-b tract, the flux into an individual retort with plan area of 61 m x 61 m (200 ft x 200 ft) varies from more than 0.946×10^{-3} m^3/sec (15 gpm) in the first 10 years of dewatering to less than 0.126×10^{-3} (2 gpm) at the end of the project. More detailed simula-

Table 8. Flux into the newly excavated regions at the C-a and C-b tracts.

C-a Tract		C-b Tract	
Time after Dewatering (year)	Flux ($m^3 \cdot s^{-1} \cdot m^{-2}$)	Time after Dewatering (year)	Flux ($m^3 \cdot s^{-1} \cdot m^{-2}$)
1.125	0.573×10^{-6}	6	0.125×10^{-6}
2	0.239×10^{-6}	11	0.057×10^{-6}
5	0.177×10^{-6}	22	0.028×10^{-6}
12	0.104×10^{-6}	38	0.0196×10^{-6}
30	0.030×10^{-6}	60	0.0146×10^{-6}

tion of individual retorts is required for better estimates.

Comparison with Other Studies

To compare the results of this study with those of previous workers, we must choose studies that are similar in both geometrical considerations and dewatering procedure. For this reason, these results can only be compared with those obtained by Tipton and Kalmbach, Inc. and Golder Associates.

The inflow rates estimated by Tipton and Kalmbach at the end of 60 years of dewatering range from 0.25 to 0.63 m^3/sec (4000 to 10,000 gpm) depending on the value of storage coefficients (10^{-3} to 5 x 10^{-2}). They also estimated drawdowns of less than 60 m (200 ft) at distances of 3 km (9800 ft) from the center of the C-b tract. In comparison, the estimates of inflow rates in our analysis, depending on the assumed porosity of the upper aquifer, range from 0.48 m^3/sec (7600 gpm) to more than 2 m^3/sec (32,000 gpm) at the end of 60 years for porosities of 1% and 15%, respectively. Considering the preliminary nature of the simulations, the broad agreement between the estimates, particularly for the low porosity case, is worth noticing. Our estimates of drawdown of the phreatic surface are also higher than those of Tipton and Kalmbach. In our work, drawdowns reach about 102 m (330 ft) after 60 years of dewatering at 3.5 km (11,000 ft) from the center of the retort. The lower estimates of inflow rates and drawdowns by Tipton and Kalmbach could perhaps be attributed to: a) their neglecting vertical infiltration from the region above the mine roof and b) their ignoring drainage contribution from desaturation.

Golder Associates have estimated that for a 30,000 barrels per day industry with an expansion rate of 0.246 km^2/year (0.096 mi^2/year) for

the C-b tract, the inflow rates after 30 years of development will be 0.41 m^3/sec (6500 gpm). Extrapolating this inflow rate to a 50,000 barrels per day industry with an expansion of 0.394 km^2/year (0.154 mi^2/year), the inflow rate will be 0.66 m^3/sec (10,400 gpm). This is in close agreement with that of Tipton and Kalmbach, Inc.

REINVASION

Due to its environmental implications, the reinvasion of water subsequent to retort abandonment is one of the crucial aspects of the MIS process. Reinvasion of water into the retorts could result in leaching of soluble chemical species from the spent shale and their transport to surrounding groundwater and surface water supplies. The hydrology of the aquifer system at the time of retort abandonment is complicated by the thermal regime of the spent shale. Since water is the prime agent of chemical transport, it is essential that the hydrogeologic regime at retort abandonment be known before solute transport is studied. Therefore, understanding the flow behavior at retort abandonment is necessary before one can proceed with the analysis of reinvasion.

For the analysis of the reinvasion, we are confronted with a few uncertainties. The thermal regime of the spent shale at the time of abandonment is an unknown which can have a substantial influence on the flow of water. Secondly, the state of saturation of the retorted region, which is influenced by retort abandonment control technologies, is not known. Thirdly, the hysteresis behavior of the entire aquifer system during the wetting process is unknown.

In the reinvasion analysis at the C-b tract, we have assumed no change (relative to the dewatering analysis) in hydraulic properties of the upper and lower aquifers even though this is a gross simplification

of the actural field conditions. Because of rubblization and oil recovery, it is assumed that the retorted region has a porosity of 30% to a radial distance of 2650 m (8690 ft) while the remaining part of the confining layer maintains its original properties (Table 6). Porosity increase due to mining and rubblization will undoubtedly increase the hydraulic conductivity of the medium by many orders of magnitude. In our analysis, we have assumed that hydraulic conductivity of the retorted region is 10,000 times greater than that of the confining layer. Furthermore, the retorted region is assumed to be near residual saturation.

The results indicate that initial reinvasion takes place primarily in the vicinity of the periphery of the retorted region because of the high conductivity of that region. The water table gradually rises along the bottom length of the retorted region, starting with the upper surface of the lower aquifer. This behavior prevents the invasion of water into the upper aquifer for decades and perhaps centuries which is possibly in the same order of magnitude as the time of resource exploitation in the Piceance Creek Basin. Obviously, the reinvasion rate varies from place to place depending on the nature of saturation and other hydraulic properties of the medium such as averaging of hydraulic conductivity across interfaces with various material properties. The results show that the average rise of the phreatic surface along the vertical section of the periphery of the retorted region is approximately 0.54 m/year (1.77 ft/year).

The profiles of the phreatic surface after 200 years show that the upper aquifer remains essentially unaffected by the invading waters (Figure 33). This could have favorable environmental consequences by

allowing sufficient time for control technologies to be implemented. Due to its high porosity and high hydraulic conductivity, the spent retorted region will act as a powerful sink to concentrate flow paths. Therefore, one should expect the reinvasion process to be extremely slow due to the large volume of void spaces that have to be filled and the extremely low hydraulic conductivity due to very low saturation and hysteresis effect. These conclusions are based on the assumptions made about hydraulic properties of the confining layer and also assuming isotropy in the reinvasion process. Considering the uncertainties existing in these assumptions, further work is required to arrive at realistic field data before we can draw any conclusions with regard to the environmental impacts of reinvasion.

The transport of chemical species during the reinvasion process is governed by the diffusion-convection phenomena in the unsaturated state and, therefore, it is an extremely complex problem which needs to be investigated.

SUMMARY AND CONCLUSIONS

The major conclusions from this work are summarized below:

1. The proposed oil-shale development strategies at the C-a and C-b tracts of the Piceance Creek Basin in Colorado will disturb the subsurface hydrogeologic regime on an unprecedented scale. For example, each retort at the C-b tract is expected to have a volume of approximately 0.35×10^6 m^3. Over a 60-year period, nearly 3840 such retorts are proposed, for a total volume of about 1.4×10^9 m^3, of which roughly 20% will be removed prior to rubblization.

2. An immediate effect of this activity is that enormous quantities of groundwater will drain into the mines. For safe and efficient operations as well as efficient underground combustion in the MIS process, this water needs to be pumped out of the mines. The magnitude of this dewatering process will likely have considerable influence on the operational as well as the economic aspects of the MIS technology. Long-term dewatering will also tend to deplete shallow groundwater and surface water supplies. Thus, the dewatering problem needs attention from the technological as well as the environmental and perhaps legal viewpoints.

3. Subsequent to retort abandonment, water will reinvade the retorts, leach soluble chemical species from the spent shale, and transport them to the hydrosphere and biosphere, contaminating shallow groundwater and surface water supplies. The post-abandonment hydrology will be further complicated by the thermal regime of the spent retorts. Since water is the prime agent of solute transport, it is essential that the hydrogeologic regime at retort abandonment be known before one can model solute transport. It is therefore necessary that the dewatering problem be investigated before one takes up solute transport modeling.

4. The present work is an attempt to study the dewatering problem in as comprehensive a manner as currently available data permit. The principal thrust of this study has been to use the same conceptualization of the physical system as previous workers. However, we have incorporated greater physical detail in the form of unsaturated flow effects and complete interaction between various model layers. The results provide insight into the relative importance of key hydrogeologic parameters.

5. Just as previous workers, we have been handicapped by lack of suffi-

cient field data. As a result, a highly idealized analog of the field problem has been used. Thus, our results are quasi site specific in nature and will have to be treated as rough estimates subject to uncertainty. A chief merit of a study such as this is the insight it provides for the magnitudes and sensitivities of critical parameters. This type of information provides guidance for field data collection. Since oil shale is presently a marginally economic natural resource, a careful evaluation of the hydrogeologic consequences will have a strong influence on the economics, and ultimate success, of the resource development.

6. In the present study, we have spent a maximum amount of effort studying the dewatering scenarios, including a sensitivity analysis for the C-b tract. We have used an idealized disc-shaped retorted region expanding with time in a multi-layered system. We have used material properties such as hydraulic conductivity similar to those used by earlier workers. We have considered the reinvasion problem at the C-b tract in a preliminary fashion. We have restricted the study to isothermal, saturated-unsaturated fluid flow. Heat flow and chemical transport have not been considered.

7. The multilayered, axisymmetric system has been analyzed using the computer program TRUST, a numerical, integrated finite difference model. The model takes into account the variability of fluid saturation and hydraulic conductivity with fluid pressure/suction.

8. The calculations indicate that it is more realistic to treat the retorted region with time-dependent geometry rather than with fixed geometry. It is shown that inflow rates could be unrealistically high

in the fixed geometry case, particularly in the initial stages of dewatering. The calculations also show that hydraulic conductivity, anisotropy, porosity, nature of desaturation, and residual saturation are key parameters that govern inflow into the mines. The sensitivity analysis carried out with different magnitudes for various parameters suggests that, in general, higher porosities, lower residual saturations, higher hydraulic conductivities, and isotropy will tend to increase inflows. It seems reasonable to infer from the studies that long-term inflow rates of 0.48 to 0.9 m^3/sec (7600 to 14,200 gpm) could be expected at the C-b tract. Although the C-a tract envisages exploitation at a shallower depth, the size of the proposed retorts is considerably larger and hence one may expect inflows comparable to that of the C-b tract. Our computations show that, depending on the extreme values of the permeability of the lower aquifer, the inflow rates after 30 years of dewatering may vary from 0.15 to 1.38 m^3/sec (2300 to 21,800 gpm).

The dewatering results obtained at the C-b tract show that, although inflow rate is high and increases in time, the flux (inflow rate per unit area) is relaively low and decreases as retort development proceeds, reaching values of less than 2 gpm for each individual retort after 60 years of dewatering. The accepable inflow rate into a retort in order to sustain efficient combustion varies depending on factors such as uniformity of flow, richness of the oil shale, and steam-air ratio. Thus, computed fluxes must be interpreted with caution. Due to the difference in thickness of the overburden above the excavated region, the position of the phreatic surface relative to the front of the retorted region is different at the two tracts. At the C-a tract, the upper aquifer above the excavated region becomes unsaturated while at

the C-b tract, the phreatic surface lags behind the front of the excavated region. The results suggest that inflows into individual retorts may not be high enough to significantly affect combustion efficiency.

9. The actual modeling of the interaction between a stream and a groundwater body is a very complex task requiring a knowledge of river inflows, outflows, and river stage. Considering the uncertainties of the hydraulic properties of the aquifer system and the level of simplification used in the present study, we have considered it unnecessary to embark on such an approach to investigate the influence of dewatering on the Piceance Creek. Instead, we have analyzed the cone of pressure depression caused by the dewatering process. Our computation indicates that in the presence of recharge, the phreatic surface at the C-b tract could be lowered by as much as 100 m (330 ft) or more at a distance of 3.5 km (2.2 mi) from the center of the disc-shaped retorted region after 60 years of dewatering. This is roughly the distance from the center of the tract to the approximate location of the Piceance Creek. Over the C-a tract, the drawdown of the phreatic surface after 30 years of dewatering at 5 km (3.1 mi) from the center of the tract is estimated to be 31 m (100 ft). This suggests that water may be lost from local streams and wells, changing the hydrologic conditions in the vicinity of the tracts.

10. It has been estimated by Weeks et al. (1974) and others that over the entire Piceance Creek Basin the annual recharge is of the order of 1 m^3/sec (15,800 gpm). The present work indicates that the annual recharge plays a more significant role at the C-a tract than at the C-b tract. For instance, the phreatic surface in the initial stages of dewatering

at a radial distance of 5 km (3.1 miles) from the center of the tract rises before it can be affected by the dewatering operation (Figure 31).

11. A comparison of our results with those of other physically similar studies, those by Tipton-Kalmbach Inc. and Golder Associates, indicates some differences due primarily to our inclusion of desaturation. We will not compare our results with those of the USGS since they modeled inflow into a trench rather than internal drainage to an expanding mine. The range of inflows estimated by T-K at the end of 60 years varies from 0.25 to 0.63 m^3 sec (4000 to 10,000 gpm). They also estimated drawdowns of less than 60 m (200 ft) within distances of 3 km (1.6 mi) from the center of the retorted region. In comparison, our estimates of inflows range from 0.48 to 2 m^3/sec (8000 to 32,000 gpm). We believe that the lower estimates of the T-K study are attributable to: (a) their neglecting vertical infiltration from the region above the mine roof and (b) their ignoring the contribution to mine inflow from desaturation. It also seems probable that their estimates of the drawdown away from the retorted region may be too low since their estimate of 0.05 for the storage coefficient for both aquifers may be too high. Still, considering the preliminary nature of the simulations, the broad agreement between the estimates within a factor of two to three is to be particularly noticed.

Golder Associates estimated that for a 30,000 barrel per day mine (expansion rate of 0.096 mi^2/year), the inflow rate after 30 years of development would be 0.41 m^3/sec (6500 gpm). Extrapolating this inflow rate to a 50,000 barrel per day industry (expansion of 0.154 mi^2/year) yields an inflow rate of 0.66 m^3/sec (10400 gpm). This estimate is very

similar to that obtained by T-K, Inc. Here, too, we feel that the Golder Associates estimate is on the low side.

12. The reinvasion calculation is complicated by: (a) the strong influence of the thermal regime, (b) a lack of knowledge of the state of saturation at the time of abandonment which is influenced by retort abandonment control strategies, and (c) the effect of hysteresis which causes imbibition hydraulic conductivitis to be smaller than drainage hydraulic conductivities. We considered a scenario in which the retorted region had a porosity of 30% at the time of abandonment. The properties of the upper aquifer, the confining layer, and the lower aquifer were assumed to remain unchanged relative to the dewatering case. It was also assumed that due to rubblization and oil recovery the high porosity would conduct about 10,000 times more water than during dewatering. The results show reinvasion will be an extremely slow process due to the large void volume in the retorted region and the very low hydraulic conductivity of the upper aquifer. The average rise in phreatic surface along the periphery of the retorted region is approximately 0.54 m/year (1.77 ft/year).

13. Overall, the study indicates that the nature of the desaturation process and the associated permeability variations have important effects on the dewatering and the reinvasion processes. In addition to controlling inflow into the mine, in-situ water saturations might have a strong influence on the effectiveness of retort combustion, depending on the saturation characteristics of the oil-shale and the inflow of water into individual retorts. Drainage of the individual retorts and the effect of in-situ saturation on combustion efficiency fall outside of the

scope of the present investigation. Furthermore, we have very limited knowledge on how to handle unsaturated flow on such a large scale.

14. At this juncture, it is pertinent to point out some of the limitations of a study like this. We are basically embarking on disturbing a natural system on an unprecedented scale. Yet our knowledge of the system is extremely limited. We are thus forced to consider a highly idealized model of the system in order to make long-term predictions. Obviously, our predictions have large uncertainties associated with them. Our studies show that mine inflow rates could reach 16,000 to 20,000 gpm which would require extensive pumping and disposal techniques at a significant cost. Some investigators involved in oil-shale development, based on experience and intuition, feel that these flow rates are extremely high. For example, Smith (1980) indicates that oil shale is essentially impermeable and continuous over the entire region and that, due to special geological conditions, it may be relatively more fractured and permeable at the C-b tract than some other areas in the basin. Thus, he suggests that by shifting the site away from the C-b tract, one could attain good aquitard containment above and below the retorts reducing mine inflows. We studied this case using a five-layer scenario in which the permeability of the region surrounding the retort was as low as the blanketing aquitard. This scenario indicates inflows of less than 0.7 m^3/sec (about 11,000 gpm) would occur.

15. The question raised by Smith (1980) does bring up a very important issue relative to modeling and prediction. The credibility of predictive models is greatly dependent on their conceptual soundness. This, in turn, depends on the manner in which: a) the system is geometrically

idealized, b) the distributed material properties are generalized, and c) the completeness with which the physical phenomena are considered. It is very desirable that field geologists, hydrologists, and mining engineers play an active role in formulating the conceptual model. If this phase is carried out in a rational fashion, the subsequent computational results will be of great help in the design and the execution of the project. In view of the uncertainties in the field data and the simplifying assumptions made in the physical conceptualization of the system, the conclusions drawn from this study should be viewed with caution.

16. Under the circumstances, it will be worthwhile to have a carefully planned workshop in which field scientists and computationalists bring together their expertise to assemble a conceptual model. In the process, they should also be able to identify the areas in which critical data are lacking and field work needs to be initiated. Without this type of integrated effort, any further computational effort will continue to lack credibility.

17. From a purely computational point of view, the critical parameters required include: system geometry, layering and material properties, geometry of underground openings and their variation with time; boundary conditions; and initial conditions.

ACKNOWLEDGEMENTS

This work was funded by the Assistant Secretary for Environment, Office of Environmental Compliance and Overview, Environmental Control Technology Division and the Assistant Secretary for Fossil Energy, Of-

fice of Oil Shale of the U.S. Department of Energy under Contract No. W-7405-ENG-48. Prior to the finalization of this report, we had the benefit of constructive criticisms from outside agencies. We wish to thank Mr. James O. Taylor and Mr. Glenn A. Miller of the U.S. Geological Survey for their critical comments. The cooperation of Cathedral Bluffs Shale Oil Company and Rio Blanco Oil Shale Company for furnishing their recent hydrogeologic information as well as their suggestions for improvement are very much appreciated.

REFERENCES

Ashland Oil, Inc. and Shell Oil Co., "Oil Shale Tract C-b--Detailed Development Plan and Related Materials," Vols. 1 and 2, 1976.

Banks, C. E., W. S. Bradley, B. C. Franciscotti, and J. L. Huckelbury, "Simulated Dewatering Requirements at an Oil Shale Surface Mine, Piceance Creek Basin, Colorado," Mineral Industries Bulletin, Colorado School of Mines, Vol. 21, No. 2, 11 p, 1978.

Braun, R. L. et al., "Proposed Operating Strategy for a Field MIS Oil Shale Retorting Experiment (RBOSP Retort Zero)," UCID Report 18524, Lawrence Livermore Laboratory, Livermore, California, 1980.

Bredenhoeft, J. D. and G. E. Pinder, "Digital Analysis of Areal Flow in Multi-Aquifer Systems: A Quasi Three-Dimensional Model," Water Resources Research, Vol. 6, No. 3, 883-888, 1970.

Cashion, W. B. and J. R. Donnell, "Revision of Nomenclature of the Upper Part of the Green River Formation, Piceance Creek Basin, Colorado, and Eastern Unita Basin, Utah," U.S. Geol. Survey Bull. 1394-G, 9 p, 1974.

Coffin, D. L., F. A. Welder, and R. K. Glanzman, "Geohydrology of the Piceance Creek Structural Basin Between the White and Colorado Rivers, Northwestern Colorado," U.S. Geol. Survey Hydrol. Inv. Atlas HA-370, 1971.

Coffin, D. L., F. A. Welder, R. K. Glanzman, and X. W. Dutton, "Geohydrologic Data from Piceance Creek Basin Between the White and Colorado Rivers, Northwestern Colorado," Colorado Water Conserv. Board, Water Resources Circ. 12, 38 p, 1968.

Donnell, J. R., "Tertiary Geology and Oil-Shale Resources of the Piceance Creek Basin Between the Colorado and White Rivers, Northwestern Colorado," U.S. Geol. Survey Bull. 1082-L, 835-891, 1961.

Edwards, A. L., "Trump: A Comforter Program for Transient and Steady State Temperature Distributions in Multidimensional Systems," National Technical Information Service, Springfield, Virginia, and Lawrence Livermore Laboratory, University of California, UCRL-14754, Rev. 3, 258 p, 1972.

Energy Development Consultants, Inc., "Technology Characterization Task, C-b Tract," 1980.

Fox, J. P., "The Partitioning of Major, Minor, and Trace Elements During Simulaed In-Situ Oil Shale Retorting," Ph.D. Thesis, University of Caifornia, Berkeley, California, 1980.

Fox, J. P., Water-Related Impacts of In-Situ Oil Shale Processing, Lawrence Berkeley Laboratory Report No. LBL-6300, 1981.

Fox, J. P., "Water Quality Effects of Leachates from an In-Situ Oil

Shale Industry," LBL Report No. 8997, 37 p, Lawrence Berkeley Laboratory, University of Caifornia, Berkeley, California, 1979.

Golder Associates, "Water Management in Oil Shale Mining," Volume I and II, Final Report prepared for U.S. Dept. of Interior, Bureau of Mines, 436 p and 354 p, 1977.

INTERCOMP Resource Development and Engineering, Inc., "A Model for Calculating Effects of Liquid Waste Disposal in Deep Saline Aquifers," Part I--Development, Part II--Documentation: U.S. Geological Survey Water Resources Investigations, 76-61, 253 p, 1976.

Jacob, C. E. and S. W. Lohman, "Nonsteady Flow to a Well of Constant Drawdown in an Extensive Aquifer," Trans. Amer. Geophys. Union, Vol. 33, No. 4, 1952.

Liakopoulos, A. C., "Transient Flow Through Unsaturated Porous Media," Dept. of Eng. Dissertation, University of California, Berkeley, California, 1965.

Millington, J. R. and J. P. Quirk, "Permeability of Porous Media," Nature, 183:387-388, 1959.

Millington, R. J. and J. P. Quirk, "Permeability of Porous Solids," Trans. Faraday Soc., Vol. 57, 1200-1207, 1961.

Narasimhan, T. N. and P. A. Witherspoon, "Numerical Model for Saturated-Unsaturated Flow in Deformable Porous Media: 1. Theory," Water Resources Research, Vol. 13, No. 3, 657-664, 1977.

Narasimhan, T. N., P. A. Witherspoon, and A. L. Edwards, "Numerical Model for Saturated-Unsaturated Flow in Deformable Porous Media: 2. the Algorithm," Water Resources Research, Vol. 14, No. 2, 255-261, 1978.

National Academy of Sciences, "Report of Panel on Accessory Elements," Chapter 2, Oil Shale (in press 1978).

Ranney, M. W., "Oil Shale and Tar Sands Technology," Noyes Data Corporation, Park Ridge, New Jersey, 1979.

Rio Blanco Oil Shale Project, "Revised Detailed Development Plan, Tract C-a," Mining, Processing and Support Facilities, Vol. 2, Gulf Oil Corp., Standard Oil Co. (Indiana), 1977.

Robson, S. G. and G. J. Saulnier, Jr., "Hydrogeochemistry and Simulated Solute Transport, Piceance Basin, Northwestern Colorado," U.S. Geological Survey, Open-File Report 80-72, 89 p, 1980.

Sass, Allan, "Commercially Producing Oil Shale: In-Situ is the Answer," World Oil, Vol. 190, No. 7, 165-169, 1980.

Sladek, T. A., P. L. Poulton, W. E. Davis, and P. A. Robinson, "A Technology Assessment of Oil Shale Development," 13th Oil Shale Symposium Proceedings, Colorado School of Mines, 1-25, Golden, Colorado, 1980.

Smith, J. W., Personal Communication, 1980.

Smith, J. W., T. N. Beard, and L. G. Trudell, "Oil Shale Resuces of the Naval Oil Shale Reserve No. 1, Colorado," Laramie Energy Technology Center, RI-79/2, Laramie, Wyoming, 1979.

Stephens, D. B. and S. P. Neuman, "Analysis of Borehole Infiltration Tests Above the Water Table," Tech. Report No. 35, The University of Arizona, Tucson, 1980.

Tipton and Kalmbach, Inc., "Hydrology, Mine Dewatering and Water Use and Augmentation, C-b Tract, Piceance Creek Basin, Colorado," Report to Occidental Oil Shale Inc., 64 p, 1977.

Weeks, J. B., G. H. Leavesley, F. A. Welder, and G. J. Saulnier, "Simulated Effects of Oil Shale Development on the Hydrology of Piceance Basin, Colorado," U.S. Geol. Survey Prof. Paper 908, 84 p, 1974.

Wymore, I. F., "Estimated Average Annual Water Balance for Piceance and Yellow Creek Watersheds," Environmental Resources Center, Tech. Report No. 2, 60 p, Colorado State University, Ft. Collins, 1974.

Yen, T. F., "Science and Technology of Oil Shale," Ann Arbor Science Publishers Inc., Ann Arbor, Michigan, 1976.